

CONTRIBUTIONS TO THE GEOLOGY  
OF THE  
TABLE MOUNTAIN GROUP

BY

A.G. THAMM

A thesis submitted in fulfilment of the degree  
of Master of Science at the  
University of Cape Town  
July, 1988.

SUPERVISOR:

Professor A.O. Fuller

DECLARATION: This thesis represents the original work by  
the author and has not been submitted, in part or in  
whole, to any other university. Where reference has been  
made to the work of others it has been duly acknowledged  
in the text.

A.G. Thamm  
July, 1988.

The University of Cape Town has been given  
the right to reproduce this thesis in whole  
or in part. Copyright is held by the author.

The copyright of this thesis vests in the author. No quotation from it or information derived from it is to be published without full acknowledgement of the source. The thesis is to be used for private study or non-commercial research purposes only.

Published by the University of Cape Town (UCT) in terms of the non-exclusive license granted to UCT by the author.

## FOREWORD

Modern analysis of Table Mountain Group sediments began with I. C. Rust's D.Sc. thesis "On the sedimentation of the Table Mountain Group in the western Cape Province" in 1967. Rust defined the stratigraphy of the Table Mountain Group, produced computer generated isopach and palaeocurrent maps for each formation and attempted palaeoenvironmental analyses based on what data he had available. For work dated prior to 1967 the reader is directed to Rust's excellent review in Chapter 2 of his thesis. The thesis served as a basis for Rust's later published work on the Cape Supergroup.

Current published palaeoenvironmental models of the lower Table Mountain Group (the Piekenierskloof, Graafwater and Peninsula Formations) are based on a transgressive fluvial - littoral - shallow shelf model (Tankard *et al.*, 1982) following earlier facies and palaeoenvironmental analyses (Tankard and Hobday, 1977; Rust, 1977; Hobday and Tankard, 1978; Vos and Tankard, 1981). The validity of this model has recently been questioned (Turner, 1986; 1987) although no comprehensive alternative has been proposed to date.

The sedimentology of the upper Table Mountain Group i.e. the Pakhuis, Cedarberg, Rietvlei, Skurweberg and Goudini Formations (the latter three the newly named Nardouw **Subgroup**) has not been studied systematically. Good progress has recently been made on the fossil content of the Cedarberg Formation (Gray *et al.*, 1986; Cocks and Fortey, 1986) and palaeoenvironmental analyses initiated in the Nardouw Formation.

This thesis documents contributions to the geology of the Table Mountain Group. It is not the intention of the author to present an extensive overview and treatise on the lower Table Mountain Group, but rather to concentrate on three topics that can provide some insight into Table Mountain Group geology. The following three topics were selected :

- 1) Petrology and Diagenesis of lower Palaeozoic sandstones in the S.W. Cape Sandveldt (Clanwilliam and Piketberg Districts).
- 2) Palaeoenvironmental indicators in the Faroo Member, (Graafwater Formation) at Carstensberg Pass, R364.
- 3) Facies analysis of conglomerates and sandstones in the Piekenierskloof Formation: Processes and implications for pre-Devonian braid-plain sedimentology.

These topics form the basis of the thesis.

## ACKNOWLEDGEMENTS

I am deeply indebted to many individuals and institutions for support, guidance and advice during the tenure of this thesis. Firstly Arthur Fuller, my supervisor is thanked for the encouragement and advice so freely given for the last three years. Peter Chadwick is thanked for fruitful discussion and making available unpublished data, and analyzing samples for the author. Dr. Hannes Theron is thanked for showing the author Isopodichnus and for constructive discussion of lower Palaeozoic palaeoenvironmental problems. Dr Anton Le Roux, and Messrs Otter and Ricard are thanked for instruction on the use of the Electron Microprobe, Klaus Schultes for the same on the Electron Microscope Unit S200 machine, Rob Harris for revealing the Pandora's Box of text editing and computing generally. Financial support from the CSIR (FRD) in the form of a Masters Degree scholarship and well as a Harry Crossley Memorial Trust scholarship, awarded by the University of Cape Town, are gratefully acknowledged. The Director, the South African Geological Survey is thanked for the wherewithal to complete this thesis as well as the opportunity to present the results at various national symposia. Mike Bremner (MGU/Geological Survey) is thanked for allowing the author to use the Geological Survey computer and associated software. Charles Basson is thanked for producing the plates and many helpful hints relating to the figures. Finally, my long suffering wife, Kathy, is thanked for patience and understanding during the production of this thesis.

## CONTENTS

### 1. PETROLOGY AND DIAGENESIS OF LOWER PALEOZOIC SANDSTONES IN THE S.W. CAPE (CLANWILLIAM AND PIKETBERG DISTRICTS)

1.1 ABSTRACT.....	1
1.2 INTRODUCTION.....	2
1.3 GENERAL GEOLOGY.....	3
1.3.1. Stratigraphy.....	3
1.3.2. Sedimentology.....	4
1.3.3. Palaeogeography.....	5
1.4 METHODOLOGY.....	6
1.4.1. Sandstone Petrography.....	6
1.4.2. Clay Mineralogy.....	6
1.5 AUTHIGENIC MINERALOGY.....	10
1.5.1. Introduction.....	10
1.5.2. Mineralogy and optical properties.....	10
1.5.3. Textural relationships and mineralogy.....	13
1.6 DETAILED PETROGRAPHY.....	17
1.6.1. Klipheuwel Formation Arenites.....	17
1.6.2. Piekenierskloof Formation Arenites.....	19
1.6.3. Graafwater Formation Arenites.....	20
1.7 TECTONIC PROVENANCE.....	21
1.8 DISCUSSION.....	25
1.8.1. Summation of diagenetic features.....	25
1.8.2. Solvent transfer.....	26
1.8.3. Solute origin.....	27
1.9 CONCLUSIONS.....	31
1.10 REFERENCES.....	34

### 2. PALAEOENVIRONMENTAL INDICATORS IN THE FAROO MEMBER (GRAAFWATER FORMATION) AT CARSTENBERG PASS, R364 : IMPLICATIONS.

2.1 ABSTRACT.....	41
2.2 INTRODUCTION.....	42
2.3 PREVIOUS WORK AND INTERPRETATIONS.....	42
2.4 FACIES DEFINITIONS AND INTERPRETATIONS .....	45
2.4.1. Facies definitions.....	45

2.4.2. Facies descriptions.....	45
A. Facies 1.....	45
B. Facies 2.....	46
C. Facies 3.....	46
D. Facies 4.....	46
E. Facies 5.....	46
2.4.3. Facies interpretations.....	47
2.5 SANDSTONE PETROLOGY.....	49
2.6 ICHNOLOGY.....	50
2.6.1. Classification.....	50
2.6.2. Previous ichnogenera documented.....	51
2.6.3. Systematic ichnology.....	52
2.7 PALAEOENVIRONMENTAL INDICATORS : DISCUSSION.....	57
2.8 CONCLUSIONS.....	58
2.9 REFERENCES.....	58

**3. FACIES ANALYSIS OF CONGLOMERATES AND SANDSTONES IN THE  
PIEKENIERSKLOOF FORMATION : PROCESSES AND IMPLICATIONS FOR  
PRE-DEVONIAN BRAID PLAIN SEDIMENTOLOGY.**

3.1 ABSTRACT.....	63
3.2 INTRODUCTION.....	64
3.3 STRATIGRAPHIC SETTING.....	67
3.4 NEW APPROACH TO FLUVIAL SEDIMENTOLOGY: A SUMMATION....	67
3.5 FACIES DEFINITIONS.....	69
3.5.1. Conglomerates.....	69
A. Clast type and conglomerate classification.....	69
B. Inversely graded to ungraded matrix supported, disorganized conglomerate.....	70
C. Clast supported normally graded to ungraded conglomerate.....	71
D. Conglomerate lag.....	71
E. Low-angle cross-stratified conglomerate (and pebbly sandstone).....	71
F. Planar cross-stratified conglomerate (and pebbly sandstone).....	72
3.5.2. Sandstones.....	72

A. Planar cross-bedded sandstones.....	72
B. Trough cross-bedded sandstone (and pebbly granule conglomerate).....	73
C. Low-angle cross-stratified medium- to coarse-grained sandstone, may be pebbly.....	73
D. Horizontally plane bedded sandstone.....	74
E. Horizontally laminated sandstone.....	74
F. Mudrock.....	74
3.6 FACIES INTERPRETATIONS.....	75
3.6.1. Conglomerates.....	75
A. Gm(d) and Gm facies.....	75
B. G1, Gi and Gp facies.....	80
3.6.2. Sandstones.....	81
A. St facies.....	81
B. Sp facies.....	82
C. Sl facies.....	83
D. Sh(a) and Sh(b) facies.....	84
E. Facies M.....	84
3.7 VERTICAL PROFILES.....	84
3.7.1. Elands Bay.....	86
3.7.2. Lambert's Bay.....	89
3.7.3. Piekenierskloof Pass.....	95
3.8 DISCUSSION.....	96
3.9 CONCLUSIONS.....	98
3.10 REFERENCES.....	98
4. PUBLISHED WORK.....	103

**ACKNOWLEDGEMENTS**

**PLATES**

**TABLES**

**APPENDICES**

1. **THE PETROLOGY AND DIAGENESIS  
OF LOWER PALAEOZOIC SANDSTONES  
IN THE S.W. CAPE SANDVELDT  
(CLANWILLIAM AND PIKETBERG DISTRICTS)**

## 1.1

**Abstract**

Fifty seven samples of Klipheuwel, Piekenierskloof and Graafwater Formation arenites were sampled at outcrop to the north - west of the Cape fold belt in the Sandveldt. These arenites are relatively tectonically undisturbed and are gently folded and locally faulted. The Piekenierskloof and Graafwater Formation arenites are classified as sublitharenites to quartzarenites. Klipheuwel Formation arenites are feldspathic, and are best classified as lithic subarkoses. The feldspar present is either orthoclase or microcline. No calcic or sodic feldspars are present.

These Ordovician arenites contain small, but significant amounts of authigenic phyllosilicates. Illite and kaolinite, identified by X-ray diffraction and wavelength dispersive microprobe techniques, occur as pore fills, framework grain replacements and more rarely as secondary pore fills. Kaolinite occurs as both vermiform (> 20µm diameter) and blocky (< 10µm diameter) aggregates. It is replaced by illite in some rocks, while in rocks which have been more deeply buried or those near major fault zones it is succeeded by the low grade metamorphic mineral pyrophyllite.

Modelling the diagenesis of thick sequences of quartz-arenites is an unresolved problem in sedimentology and sedimentary geochemistry. The lack of, or relative rarity of, shale, necessary as source for authigenic cement solutes and solvent expulsion (on burial and compaction), remains a major conceptual obstacle. These arenites, with pervasive silica cement, are most plausibly modified by groundwater (and attendant solute) flux and labile grain leaching. The presence of feldspar in poorly sorted sandstones sampled from between permeability barriers (where groundwater flux would be reduced) supports this hypothesis. It can be further demonstrated that the abundance of authigenic clays infilling primary and secondary porosity increases in samples collected towards the basin margin, features highly suggestive of groundwater influx beneath an unconformity.

The major causal factor determining framework composition is tectonic setting. The quartz-rich framework modes of Table Mountain Group sandstones are the result of derivation from older, late Precambrian and Proterozoic, deformed supracrustal and basement sequences to the north and northwest of the Table Mountain Group basin. Diagenetic processes, which have dissolved feldspar and other rock fragments have emphasised the quartz rich nature of these sandstones. The need for sustained shallow marine feldspar and rock fragment attrition suggested by previous authors is obviated. Winnowing of the fine-grained fraction may have occurred as a result of pre-Devonian unvegetated landscapes and aeolian action.

## 1.2

### INTRODUCTION

The origin and sedimentology of quartzarenites has long been a contentious topic. Recent treatises on the subject have produced two schools of thought on their origin.

Firstly, quartzarenites are held to be the result of prolonged terrigenous sediment influx balancing sea level rise during periods of tectonic quiescence (Hobday and Tankard, 1978; Soegaard and Eriksson, 1985). These successions are transgressive overall and are coeval with first order sea level rise. Arenites in these sequences are typically compositionally (lack labile rock fragments and feldspar) and texturally (lack silt and clay-sized detrital matrix) mature.

Secondly, the sheet-like bedding geometry of many quartzarenites is believed to be incompatible with modern transgressive, marine processes, given the slight or minor reworking of substrate sediment as a result of the post-glacial Holocene transgression (Dott et al., 1986). The sedimentology of many of these successions is complicated in that few reliable palaeoenvironmental indicators exist (Long, 1978).

The plate tectonic setting has been shown to be the major determinant of sandstone composition (Dickenson et al., 1983; Potter, 1984; Suttner and Dutta, 1986). Sands derived from older orogenic and cratonic terrains are typically quartz rich. Compositional and textural maturity can be enhanced by prolonged transport and sorting in both non-marine and nearshore sedimentary environments (Mack, 1978; Suttner et

al., 1981).

Compositional maturity can be enhanced by post depositional, diagenetic dissolution of unstable framework grains (Wilson and Pittman, 1977; Boles and Franks, 1979; Pye and Krinsley, 1985; Shanmugan, 1985; Dutta and Suttner, 1986; McBride, 1987). Climatic control of pedogenesis (weathering and rock fragment production) is a further contributing factor. Not only does climate affect the way parental crystalline rocks are weathered but it controls pore water chemistry in early diagenesis (Suttner and Dutta, 1986). Early diagenesis (Schmidt and McDonald's, 1979 **EOGENETIC** regime) includes processes that occur to depths where significant framework grain dissolution occurs (usually ~ 3000m). Where this process is initiated the climatic signature of the framework is lost (Suttner and Dutta, 1986). Meteoric circulation has been reported up to depths of 1.5 km (Galloway, 1984) and as far as 100km offshore at several 100's of metres depth in shallow marine sandbodies connected to onshore aquifers (Bjørlykke, 1984). It is thus possible that shallow marine sediments as well as non-marine sediment can undergo early diagenesis in contact with meteoric, fresh pore water from burial depths of less than 100m to several 100's of metres. Climate would be a major factor controlling pore water chemistry, which in turn controls which framework grains are stable or not.

This work evaluates the petrology and diagenesis of arenites sampled from the Klipheuwel, Piekenierskloof and Graafwater Formations given published palaeoenvironmental interpretations of these formations and recent advances in sandstone petrology. No data exist on Table Mountain Group sandstone classification and petrogenesis (Potgieter and Oelofsen, 1984): this is the first such study on this topic.

### 1.3

### GENERAL GEOLOGY

#### 1.3.1. Stratigraphy

The Piekenierskloof and Graafwater Formations are the lowermost two formations of the Table Mountain Group (Table 1). The age of these two formations is not well constrained. The topmost formation of the Table Mountain Group (hereafter abbreviated to TMG), the Nardouw Formation, is believed to be late Emsian (Devonian) in age (Cooper, 1986) at the contact between it and the overlying Bokkeveld Group. The TMG unconformably overlies Pan - African metasediment (the

Malmesbury Group) that was intruded by granitoids at around 500-610 My. (Tankard et al., 1982; Gray et al., 1986). The contact relationships of the TMG Formations are conformable, other than the Peninsula Formation/ Winterhoek Subgroup contact where a slight unconformity exists (Rust, 1967). Isopachs of each formation show a progressive northward thinning, where each formation successively onlaps onto basement (Rust and Theron, 1964; Rust, 1967).

The best age estimates come from the Cedarberg Formation in the Winterhoek Subgroup. This formation, which interfingers with, and overlies, the Pakhuis Formation diamictites contains a well documented trilobite /brachiopod /chitinozoa and plant spore assemblage (Cramer et al., 1974; Cocks and Fortey, 1986; Gray et al., 1986) dated as of probable uppermost Ordovician (Ashgill) age. The uppermost parts of the Klipheuwel Formation underlie the Piekenierskloof Formation in the study area and have been interpreted as distal facies equivalents of the latter (Vos and Tankard, 1981). The lowermost divisions of the Klipheuwel Formation are demonstrably deformed by the Pan African Orogeny (Hartnady, 1969). The above data constrain the upper Klipheuwel, Piekenierskloof and Graafwater Formations to a latest Cambrian to middle Ordovician age. Rust (1967) suggested an age of 505 My for the base of the Piekenierskloof Formation, i.e. at the base of the Ordovician.

### 1.3.2. Sedimentology

The sedimentology of the Klipheuwel, Piekenierskloof and Graafwater Formations has been interpreted as a coarsening upward marine to fluvial progradational sequence (Vos and Tankard, 1981). A distal interfingering of the Piekenierskloof Formation with the Graafwater Formation sediments has been inferred (Tankard and Hobday, 1977). The Graafwater Formation conformably overlies the Piekenierskloof Formation, a stratigraphic relationship resulting from the transgression of distal facies (Graafwater Formation) over more proximal facies (Piekenierskloof Formation). The Peninsula Formation is in turn interpreted as marine shelf deposits transgressed over nearshore marine sediment (Hobday and Tankard, 1978; Tankard et al., 1982). The stratigraphic relationship between the Peninsula and the Graafwater Formations is currently under investigation (Turner, 1987) and the sedimentological relationship appears to be a regressive (progradational) rather than a transgressive one (Turner, 1986).

An Ordovician age is accepted for these formations (Tankard et al., 1982). The Graafwater Formation contains a diverse assemblage of shallow marine trace fossils. If the Graafwater seaway is assumed to have been connected to the world ocean then eustatic sea level changes might explain the stratigraphic relationship between the alluvial, Piekenierskloof Formation and the nearshore marine Graafwater Formation above it. Three large eustatic transgressions occur in the Ordovician (Hallam, 1984): in the Tremadoc, the Caradoc and in the Llandeilo. Given sparse age constraints (an uppermost Ordovician age for the Cedarberg Formation and an upper Cambrian age for the Klipheuwel Formation) the Caradoc or Llandeilo transgressions are the most likely cause of this stratigraphic relationship. The Tremadoc transgression may be too early in the Ordovician, given the age (~500-600 My.) and depth of intrusion (~14km) of granitoids beneath the Palaeozoic cover sequence.

### 1.3.3. Palaeogeography

While no palaeogeographical evidence is directly available from data derived from the TMG, good data constrain the palaeoposition of the lower TMG given its position in a reconstructed West Gondwana (as part of a larger continent, Pangea). In the latest Precambrian and Cambrian the palaeoposition of what is now the southern margin of Africa occupied a near-equatorial palaeoposition (Zonneshein et al., 1985; Donovan, 1987). This position changed through the Ordovician, resulting in what appears to be (on a Lambert equal area projection, centred at 0<sup>0</sup>, 90<sup>0</sup>) a clockwise rotation to the South Pole, which it reached in the earliest Silurian (Hargraves, pers. comm., 1986).

This inferred movement is supported by the progressive change in age of glacial centres across Gondwana (Caputo and Crowell, 1986). The earliest glaciation is in the Caradoc in Morocco (Cocks and Fortey, 1986). The glacial centres young southwards across Africa into South America, resulting in the appearance of diamictites in the Hangklip Member of the Peninsula Formation (Sohngé, 1985) and in the Pakhuis Formation above it in the late Ordovician. The global palaeoclimate is believed to have been warm in the Cambrian and early Ordovician, (Fisher, 1984). The appearance of West Gondwana tillites attests to climatic deterioration towards the end of that period.

## 1.4

## METHODOLOGY

## 1.4.1. Sandstone Petrography

Fifty seven samples were thin sectioned, examined petrographically and point counted on a Swift Model F automatic point counter. The roundness and sorting of the framework constituents of each thin section were estimated using the visual comparator of Powers (1953). The following components were identified in each analysis: monocrystalline quartz, polycrystalline quartz, feldspar, rock fragments (non-quartzose lithic fragments), matrix (that component not optically resolvable), silica cement and heavy minerals.

The point count was based on a rectangular grid that varied with grain size. The sandstones sampled are mostly in the medium to coarse sand-size range, thus the grid interval varied from 0,25 to 0,5mm. Point count methods where individual sand sized crystals within each grain are used to classify the point under the microscope cross hairs (the Gazzi-Dickenson method) were not employed. Instead each point under the microscope cross hairs was assigned to one of the components given above. Each analysis was recalculated on a matrix and cement free basis. A listing of the samples and their location can be found in Appendix 1; Appendix 2 is a presentation of the raw and recalculated analyses.

Two standard deviation confidence intervals were calculated for the raw and recalculated data using the method outlined by Van der Plas and Tobi (1965). The sandstones were classified using McBride's scheme (McBride, 1963). In this classification all quartzose framework grains (including quartzite, chert and sandstone) are grouped at the same pole (quartz), granite and gneiss are grouped with other rock fragments at the lithic pole. The latter does not affect the classification of these sandstones: no discrete sand sized granite and gneiss framework fragments were encountered in this study and the samples plot along the quartz-feldspar line. The recalculated analyses were then used to identify the tectonic provenance of these sandstones, using the method outlined by Dickenson et al. (1983).

## 1.4.2. Clay Mineralogy

Traditional analysis of clay mineralogy has been the X-ray diffraction of a cation spiked 2 $\mu$ m size fraction. This size fraction is extracted by crushing the sample, sieving out the coarse unbroken fraction, and settling the > 2 $\mu$ m size

fraction out of suspension. The suspended < 2 $\mu$ m size fraction is poured off, washed in distilled water, centrifuged and smeared onto a glass slide for diffraction. Different pre-diffraction treatments such as baking at 500°C and exposing the sample to ethylene glycol add refinements to the technique. Diffraction in this study was accomplished on a Phillips PW2273/20 machine under the following analytical conditions: Cu K-alpha radiation, 40kV and 30mA power settings, divergence and receiving slits of 1/2°, scan ranges from 2 to 35° two theta, at scan speeds of 1° two theta per minute, chart drive speed of 4 cm/minute and maximum count ranges of 4 x 10<sup>3</sup> c/s. Cation spiking, ethylene glycolation and baking techniques are described in Chadwick (1987), for a similar suite of samples of Table Mountain Group arenites.

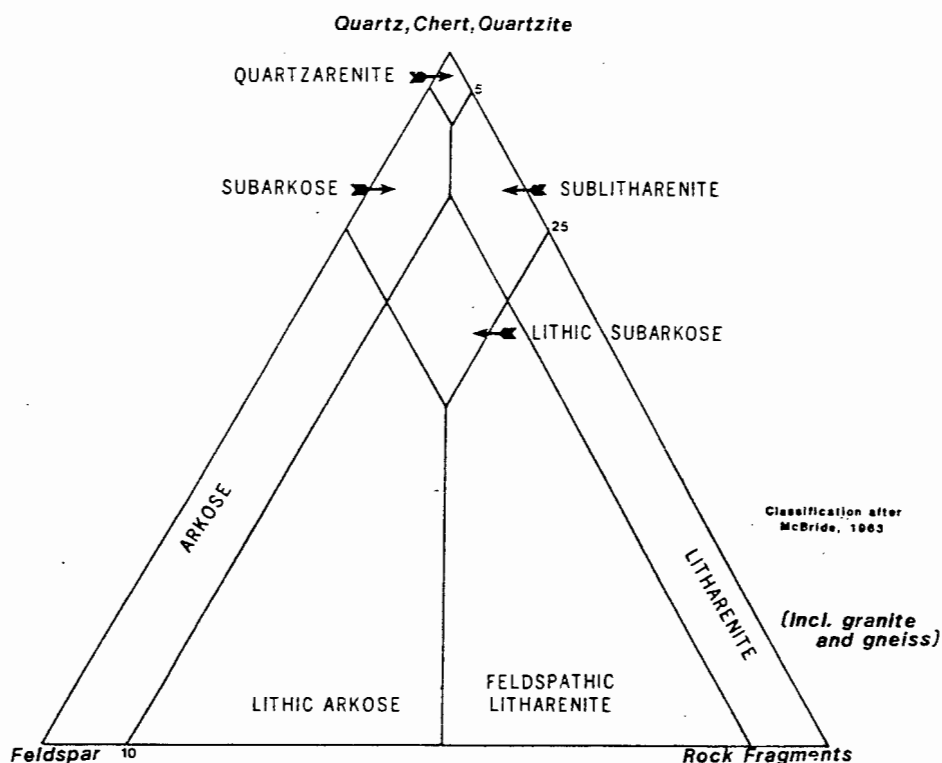


Figure 1.1. Sandstone classification scheme.

Where clay minerals occur as matrix in a sandstone it is highly desirable to analyse clay mineralogy in situ, while simultaneously observing matrix-framework textural relationships. The diffraction technique outlined above is by process destructive and textural relationships are lost. The most common analytical techniques used to determine in situ clay mineralogy are 1) energy dispersive (EDS) analytical methods, with or without backscattered electron image detectors on

Fig 1.2. Tectonic provenance scheme devised by Dickenson et al. (1983)

Q: quartzose components, F: feldspar & granite, L: non quartzose lithic fragments.

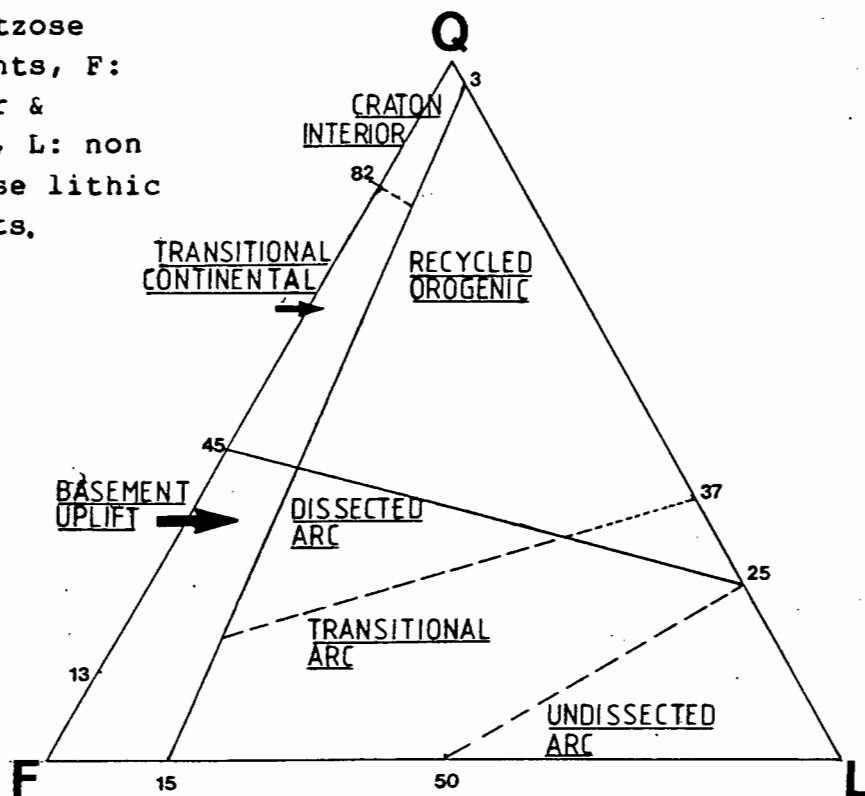
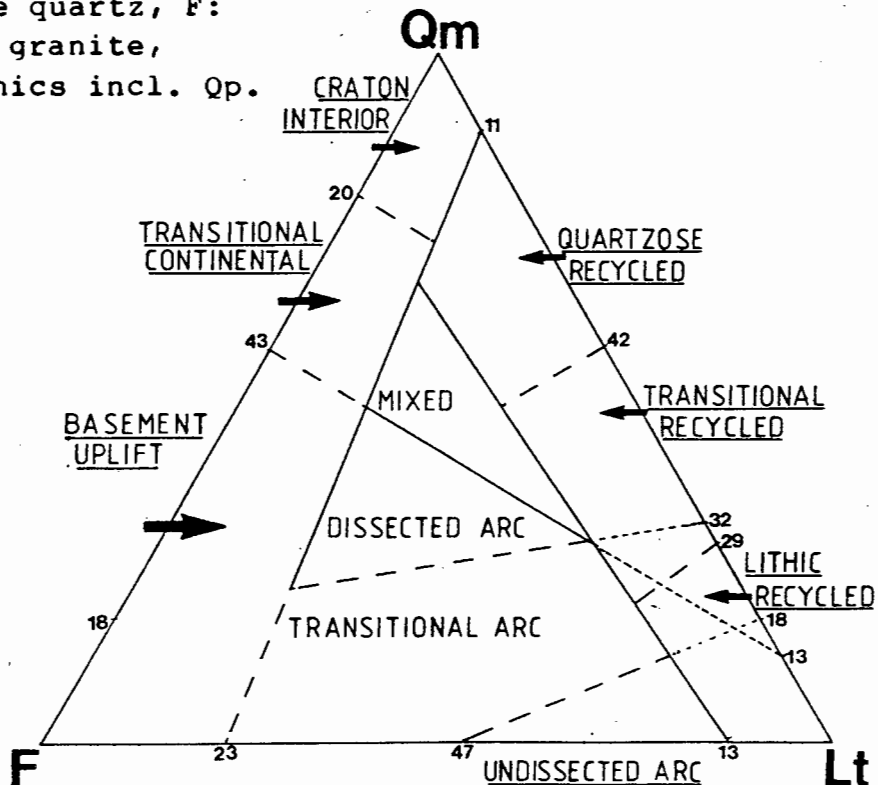


Fig 1.3. Tectonic provenance scheme devised by Dickenson et al. (1983).

Qm: mono-crystalline quartz, F: feldspar & granite, L: All lithics incl. Qp.



scanning electron microscopes or 2) wavelength dispersive (WDS) analytical methods installed on electron microprobes.

The analysis of polished sandstone thin sections using the latter method is a proven (Velde, 1984) but little used method in sandstone diagenetic studies. Not only can the clay mineral(s) textural relationships be observed but reliable chemical data are produced. The microprobe analyses listed hereunder were produced on a CAMECA MICROPROBE, with analytical techniques normally used in the **Department of Geochemistry, The University of Cape Town** where a MICA standard is used to analyse micas and clay minerals (15kV accelerating potential and beam currents of 17.8 - 18.9 nA). Counting times were kept to less than 200s (for a full 12 element analysis) to prevent alkali loss. Backgrounds of intensities were calculated in each analysis. Potassium and sodium were amongst the first elements analysed. Beam width was 10-15  $\mu\text{m}$ . This system is configured with four spectrometers, making simultaneous, multiple element analyses possible. Clay morphologies were imaged on the CAMBRIDGE INSTRUMENTS S200 SEM housed in the **Electron Microscope Unit** of the University of Cape Town.

Interpretive problems arise when different clay minerals are interlayered on a scale smaller than the probe beam diameter. Such chemical data are of a composite nature (reflecting the chemistry of the interlayered minerals) and are difficult to compare with data for pure end members. A reconnaissance diffraction study showed that such interlayered minerals were not present in the samples selected. Where two clay minerals were detected, subsequent microprobe analysis showed that these phases were present as discrete, distinct monomineralic entities.

Most of the clay minerals present are sufficiently coarse grained to be analysed by microprobe. The mole ratios of  $\text{SiO}_2/\text{Al}_2\text{O}_3$  and that of  $\text{K}_2\text{O}/\text{Al}_2\text{O}_3$  are useful in determining the reliability of chemical analyses. Many clay minerals have distinctive ratios (Garrels, 1984 Fig.2). These ratios aid not only identification in conjunction with X-ray diffraction but allow discrimination of acceptable chemical analyses. Further, the clay minerals possess sufficiently distinctive optical properties so that their abundances can be estimated in routine point count analyses. The composition of the clay minerals in 10 samples was determined using this technique of preliminary X-ray diffraction followed by WDS analysis. The clay mineralogy of the remaining 47 samples was determined by comparing optical properties.

## 1.5

## AUTHIGENIC MINERALOGY

## 1.5.1 Introduction

The authigenic origin of a matrix can be established using acknowledged petrographic and mineralogical criteria. Amongst these are 1) clay composition and structure, 2) clay morphology and distribution and 3) sandstone/matrix textural relationships (Wilson and Pittman, 1977). The most reliable criteria are: delicacy of clay morphology (precluding sedimentary transport), occurrence of clay as pore linings and fillings absent at grain contacts and chemical compositions radically different from allogenic clays. The former two criteria were found most useful in this study. Allogenic (depositional) clay in the samples studied usually occurs as blebs of diagenetically oxidised (reddened) matrix that have been deformed by compaction and are distinctive in both hand specimen and thin section.

## 1.5.2. Mineralogy and optical properties

Preliminary X-ray diffraction studies determined that illite (*senso lato*), kaolinite and pyrophyllite were present as "matrix" in these samples, on the basis of the 10,1, 7,18 and 9,2 angstrom reflections. Kaolinite and illite, as well as illite and pyrophyllite, were rarely detected in each sample; most samples are monominerallic.

Kaolinite was identified during microprobe analysis. Kaolinite chemical data (TABLE 2) have  $\text{SiO}_2/\text{Al}_2\text{O}_3 = \sim 2$  and  $\text{K}_2\text{O}/\text{Al}_2\text{O}_3 = 0$ . Optically (using a petrological microscope) kaolinite is identifiable by its low relief, low,  $1^\circ$  interference colours and moderate to poor cleavage. Pyrophyllite is most distinctive in thin section. It occurs as globular or vermiform (plates stacked in the  $\langle 001 \rangle$  axis direction) aggregates exhibiting low relief,  $2^\circ$  blue, green yellow and red interference colours and good cleavage. Pyrophyllite chemical analyses have  $\text{SiO}_2/\text{Al}_2\text{O}_3 = 4$  and  $\text{K}_2\text{O}/\text{Al}_2\text{O}_3 = 0$ . Representative pyrophyllite analyses are presented in TABLE 3. Illite occurs as low relief aggregates that show no cleavage in thin section and exhibit low  $1^\circ$  interference colours (grey and yellow-white). Representative illite analyses are presented in Table 4.

Kaolinite analyses were reduced from raw oxide chemical

data (using ZAF correction factors) to atomic proportions based on a 14 oxygen unit cell. Ideally kaolinite should have 8 cations for a 14 O cell: the sum of cations in these analyses ranges from 7.999 to 8.028 and thus shows good correspondence with theoretical values. Pyrophyllite and illite raw oxide data were reduced using ZAF correction factors and recalculated to atomic proportions based on a 22 oxygen formula unit. Pyrophyllite should ideally have 12 cations per formula unit: these analyses have sums of cations in the range 12.023 - 12.123. Illite data were reduced to a 22 oxygen formula unit, and cations assigned to octahedral, tetrahedral and interlayer sites (Table 8). Analyses with  $>6.1$  octahedral ions,  $>8.1$  tetrahedral ions and  $>2.2$  interlayer ions were disqualified from use (these are suggested values for microprobe analysis, by Velde, 1985). For each illite analysis the following were calculated (Table 5):

- 1) K/A, the mole ratio of  $K_2O/Al_2O_3$ ;
- 2) S/A, the mole ratio of  $SiO_2/Al_2O_3$ ;
- 3) T\*, the tetrahedral charge: all Si and Ti are assigned to this site, plus enough Al to make up 8 cations per formula unit in the tetrahedral site, the figure tabulated being the charge deficiency due to the  $Si^{4+} \rightarrow Al^{3+}$  substitution;
- 4) O\*, the octahedral site charge if the remaining  $Al^{3+}$ , and the  $Cr^{3+}$ ,  $Mn^{2+}$ ,  $Mg^{2+}$  and  $Fe^{2+}$  are assigned to this site;
- 5) Il\*, the interlayer charge if  $K^+$ ,  $Na^+$  and  $Ca^{2+}$  are assigned to this site;
- 6) A%, B% and the C% are co-ordinates of a triangular plot where A is the  $MR^3$  component, B is the  $2R^3$  component and C is the  $3R^2$  component. These components are calculated and defined as follows (Velde, 1985a, p.39):
  - a) raw oxide microprobe data are converted to relative atomic proportions based on the elements present and 22 oxygens (for illite),
  - b) The  $M^+R^3$  component is equal to the sum of the atomic proportions of K, Na and 2Ca,
  - c) The  $R^3$  component is the sum of Al and  $Fe^{3+}$ . Since  $R^3$  is included in  $MR^3$  (in 6b above, by definition) one subtracts the value of  $MR^3$  from  $R^3$ , the remainder halved to give  $2R^3$ ,

d) Mg and  $\text{Fe}^{2+}$  are summed and divided by three to give  $3R^2$ , e) the values of each component are summed, and each component is divided by the total to give the percentage of A, B and C as defined above.

The allocation of Fe in the reduction of microprobe data is problematical: Fe occurs both as  $\text{Fe}^{2+}$  and  $\text{Fe}^{3+}$  in diagenetic illites, usually in the proportion of 13.5 : 86.5  $\text{Fe}^{2+}:\text{Fe}^{3+}$  (Weaver and Pollard, 1973 ; Yau *et al.*, 1987). However as the proportion of Fe is usually small (in all cases < 6 %, and in 17 out of the 21 representative analyses it is present in amounts < 2,5%) the distortion of the  $\text{MR}^3 - 2R^3 - 3R^2$  diagram is minimal and no recalculation was thus deemed necessary.

The calculated components (A%, B% and C%) for the 21 representative illite analyses are given in TABLE 9 and presented in Fig 1.4 (below).

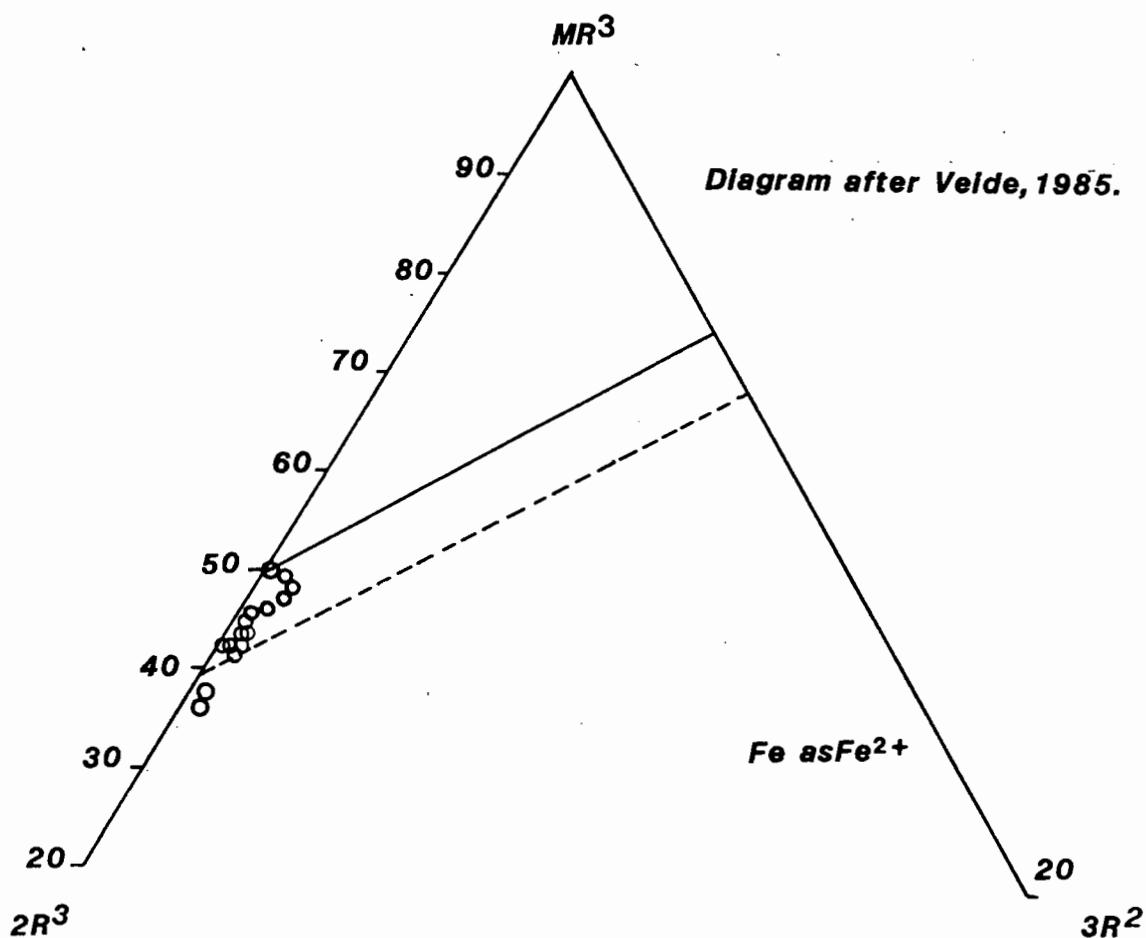


Fig 1.4. Klipheuwel Formation Microprobe data (Table 9) reduced after the method of Velde, (1985). Data plot within the field of diagenetic illite. Muscovite plots at 50%  $2R^3 - \text{MR}^3$ .

---

Potassium is the most abundant interlayer ion (by several orders of magnitude) in these illites. Those with greater than 1.5 K ions per 22(O) formula unit are considered to be the illite end member of the diagenetic illite-illite/smectite series where the illite has been produced by the illitisation of smectite (Srodon et al., 1986). The chemistry of neoformed illites precipitated in sandstone pores, and illites resulting from the illitisation of kaolinite and feldspar are known to have different chemistry (Srodon et al., 1986). Further, neoformed illite resulting from the evolution of smectite to illite in shale differs in chemistry from neoformed illite precipitated in sandstone pores (Nadeau et al., 1985).

The K<sub>2</sub>O content of illites in shale is known to increase with increasing diagenesis (Hunziker et al., 1986) from 6-8% in the diagenetic zone to 8.5- 10 % in the anchizone and to 10,5 - 11% in the epizone (Hunziker et al., 1986).

Illite analyses presented here have K<sub>2</sub>O contents ranging from 6,5 to 10,6 %, most analyses (16 out of 21) having K<sub>2</sub>O contents >8.5%. Most illites (16 out of 21 analyses) have potassium (and negligible sodium and calcium) present in quantities greater than 1.5 interlayer atoms per 22(O) formula unit. Ideal (2M) muscovite has 2 interlayer ions per formula unit.

Indirect evidence indicate that these illites were neoformed at high grades of diagenesis. It is ordered and non-expandable (contains no smectite) i.e. is illite senso stricto. Illites extracted from sandstones in stratigraphically higher Formations in the study area (Peninsula and Nardouw Formations) contain ISII ordered illite (with minor expandable smectite component) as well ordered, non-expandable (2M) illite (Chadwick pers. comm., 1987).

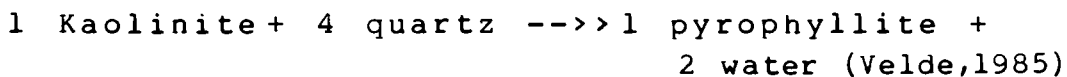
### 1.5.3. Textural relationships and morphology

Authigenic illite and kaolinite occur as secondary (diagenetically enhanced), and less commonly as primary pore fills that occlude porosity and must have reduced permeability. Syntaxial quartz overgrowths occlude porosity around framework nuclei: authigenic clays fill-in the remnant porosity. Syntaxial overgrowths (Plate 1a) and framework nuclei commonly show features indicative of chemical corrosion (Plate 1 f&g). In thin section, kaolinite and

illite are often observed infilling embayments and notches in both framework and silica cement (Fig 1.5c & d, Fig. 1.6b).

Illite commonly occurs as pore fills or as framework grain (feldspar) replacements (Fig. 1.6a&b). Kaolinite occurs as primary pore fills (Fig. 1.5c) and as secondary pore fills (Fig. 1.5a). In samples where no kaolinite fills in the remnant pore space the quartz overgrowth faces are uncorroded. The significance of this observation and that of the corroded overgrowth and framework is discussed below. Secondary porosity has resulted from the dissolution of the quartz framework, framework feldspar and quartz overgrowths. In thin section corroded grains, elongate pore fill, oversize pore fill (pore fill of similar size to grain size) and the inhomogeneity of packing are the textural attributes of secondary porosity (Schmidt and McDonald, 1979a). These features are present in varying degree in Klipheuwel, Piekenierskloof and Graafwater sandstones containing illite and or kaolinite.

Where pyrophyllite occurs in Piekenierskloof sandstones it can be observed to fill embayments in both quartz framework and overgrowth (Plate 1.6 c&d). This textural relationship is best explained by examining the relationship between pyrophyllite and its precursor:



This reaction consumes kaolinite and quartz (presumed to be present in excess). Textural evidence (kaolinite and pyrophyllite **never** occur in the same sample) supports this relationship. The Piekenierskloof Formation sandstones are thus considered to have contained precursor kaolinite.

The morphology of each clay mineral phase is quite distinctive. Illite occurs as thin, < 5µm, laths (Plate 1g&h). Such authigenic illite laths have been reported growing in pore space in sandstones (Nadeau et al., 1985) and in shales (Yau et al., 1987) and may be characteristic of precipitation in permeable (chemically) open systems with high fluid/rock ratios.

Kaolinite occurs as stacked vermiform aggregates (> 10µm diameter pseudo-hexagonal plates) as well as smaller (5µm diameter) blocky aggregates (Plate 1c). Euhedral kaolinites (Plate 1d) such as these are believed to have precipitated from solution (Hurst and Urwin, 1979). Pyrophyllite occurs as

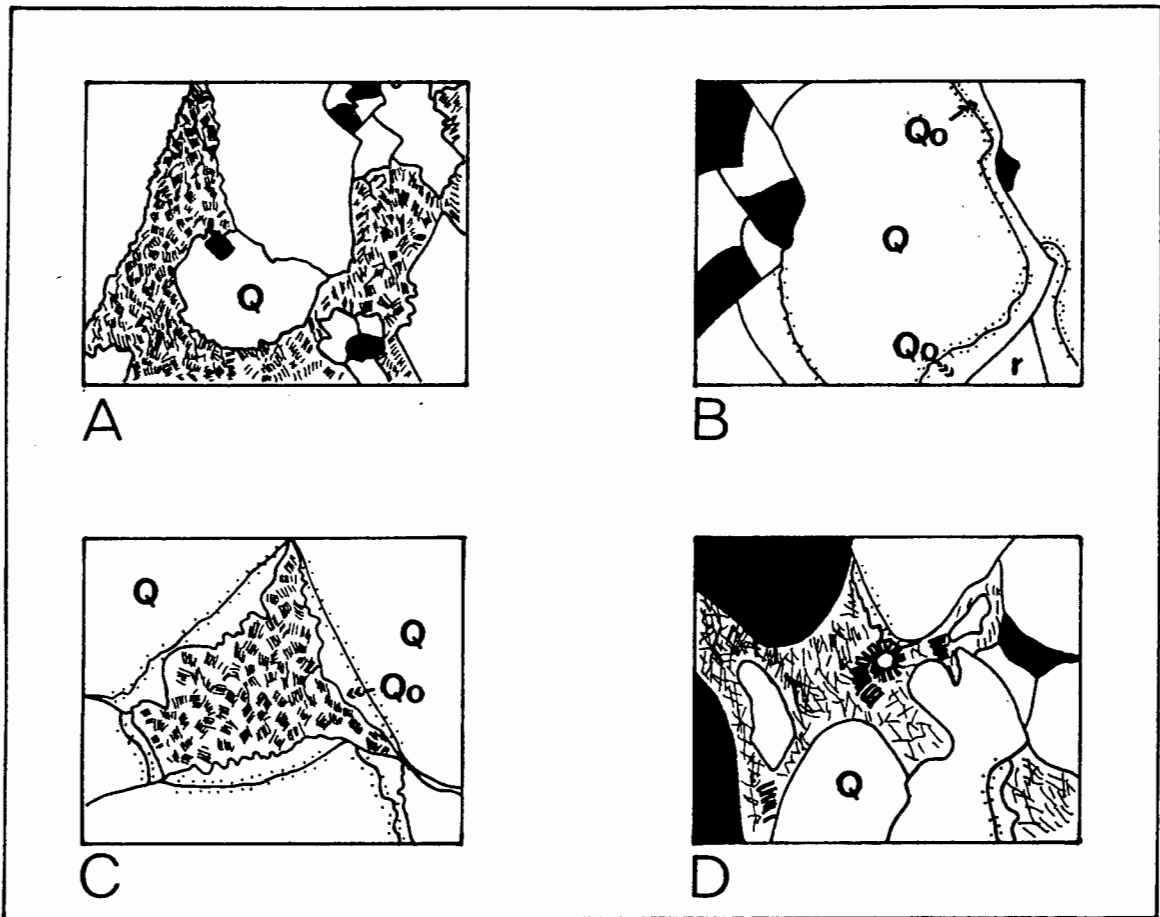


**Figure 1.5.**

A) Arenite G 303, x 225 magnification, field of view (length) = 0,56mm. Vermiform kaolinite occludes secondary porosity after quartz cementation and later cement and framework dissolution.

B) Arenite P 107, x 225 magnification, field of view = 0,56 mm. Remnant unfilled porosity (r) after quartz cementation. Note unresorbed syntaxial overgrowths on quartz framework nuclei.

C) Arenite P 107, x 225 magnification, field of view = 0,56mm. Vermiform kaolinite occludes secondary porosity after syntaxial quartz cementation and subsequent resorbition.

D) Arenite G 305, x 450 magnification, field of view 0,28mm. Illite and vermicular kaolinite occlude secondary porosity. (Q): quartz framework, (Qo): quartz overgrowths.

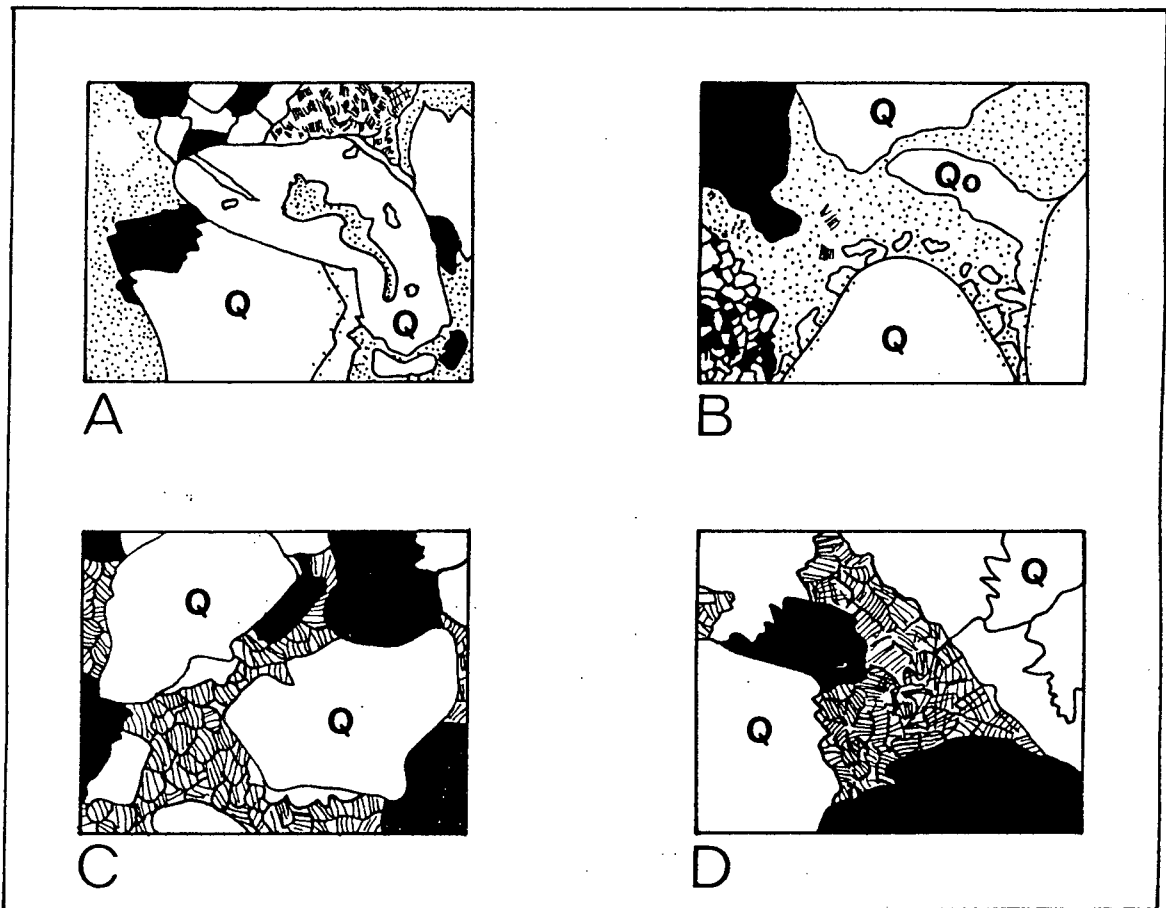


Figure 1.6.

A) Arenite K 105, x 225 magnification, field of view (length) = 0,28mm. Illite (dots) replaces feldspar. Illite and kaolinite (vermiform booklets) occlude porosity.

B) Arenite K 204, x 40 magnification, field of view 1,5mm. Illite occludes secondary porosity after quartz (Q) cementation and resorption.

C) Arenite P 1883, x 225 magnification, field of view = 0,56mm. Pyrophyllite resorbs quartz.

D) Arenite P 6112, x 90 magnification, field of view = 1,5 mm. Pyrophyllite occurs in former pore space, replacing kaolinite.

(Sample codes are given in Appendix 1).

crinkly flakes that commonly interlock and radiate from a common point (Plate 1,i).

## 1.6

## DETAILED PETROGRAPHY

## 1.6.1. Klipheuwel Formation Arenites

Klipheuwel Formation sandstones are poorly to well sorted feldspathic arenites. Framework grains are angular to sub-angular. Of ten samples five are classified as lithic subarkoses, two as feldspathic litharenites and one each as arkose, litharenite and lithic arkose respectively (Fig. 1.6). The more poorly sorted sandstones are feldspar rich. Sandstones with grain sizes in the fine sand size range are quartz rich.

The poorly sorted sandstones contain minor amounts of detrital clay. The poor sorting and allogenic clay content may have resulted in lower initial permeability. Sandstones rich in detrital clay have lower depositional permeability (Hazeldine et al., 1984); reduced flux of "corrosive" groundwater would result in a relative preservation of feldspar. Feldspar contents range from 3,6 to 33,2 % in raw (prior to recalculation without matrix and cement) point count analyses.

Feldspars were analysed on a CAMECA CAMEBAX microprobe against the FELDSPAR standard of the Department of Geochemistry, University of Cape Town. A defocussed beam (20 um) was used and the analytical conditions were those normally extant in the Department of Geochemistry as reported in Duncan et al., (1984). Sixty four analyses were obtained. The feldspars examined showed no significant zoning. Twenty five representative analyses are presented in TABLE 6. Data are reduced using Bence-Albee correction factors and atomic proportions calculated on the basis of 8 (oxygen) anions.

Klipheuwel feldspars are potassic. The mean orthoclase content of Klipheuwel Formation feldspars is 92,0% (standard deviation [abbrev. = s hereafter] = 2,47%; n=64) the mean albite content 7,3% (s=2,4%; n=64) and the mean anorthite content 0,06% (s=0,14% ; n=64). The ranges of orthoclase and albite contents are 80,9 - 97,9 and 2,1-19 % respectively. No albite or anorthite rich feldspars were encountered during the microprobe analysis nor seen in thin section. The potassic feldspars are usually microcline or untwinned orthoclase. Lithic fragments are commonly aphanitic

and intraformational sedimentary or schistose metamorphic types.

These sandstones contain small amounts of authigenic clay minerals. The range of authigenic clay contents (identified as such using the criteria listed above) is 5,0 - 14,8 % (mean = 9,7% ; n=9 samples). The clay minerals present are kaolinite and illite. This illite may show the straw yellow birefringence normally indicative of "sericite" (a sack term used by petrographers for micaceous matrix) The  $K_2O$  contents of illites ranges from 6.5-10.6 %. Values greater than 8.5% are common. These percentages are normally indicative of the highest grade of diagenesis (Hunziker et al., 1986).

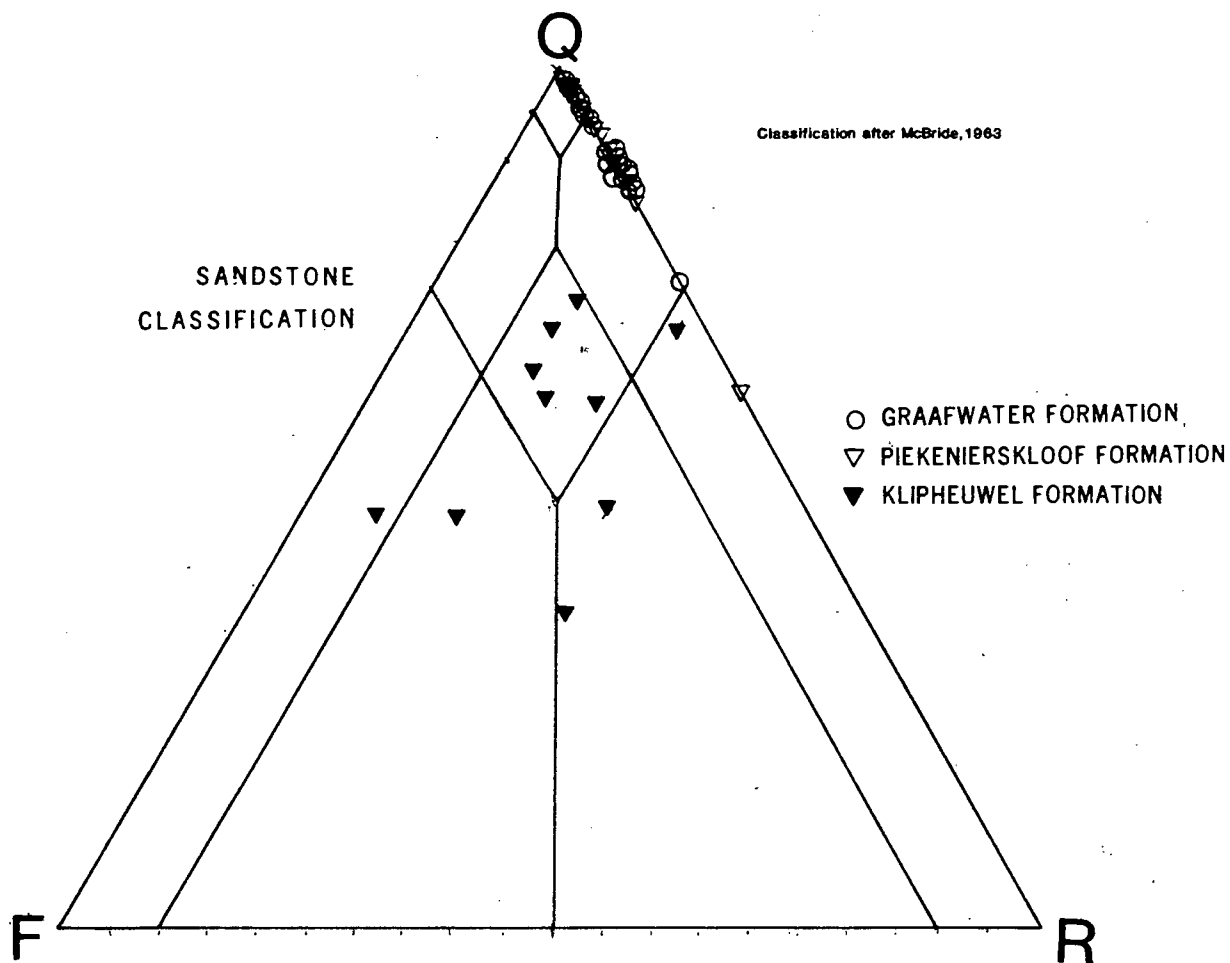


Fig 1.7. Sandstone classification.

The authigenic minerals commonly occlude a secondary porosity: both major components of the framework (quartz and feldspar) show dissolution features (seen as embayments in thin section at clay/framework and clay/cement contacts and etch pits seen using a Scanning Electron Microscope [SEM]). Feldspars are commonly replaced by illite and quartz. Quartz occurs as blebs within patches of illite as well as within partially dissolved feldspars. Similar features are reported from dissolved feldspars in Proterozoic arenites in Norway (Morad and Aldahan, 1987). A summary of Klipheuwel Formation petrographic data is presented in TABLE 7.

### 1.6.2. Piekenierskloof Formation Arenites

Piekenierskloof Formation sandstones are poorly to well sorted quartzarenites and sublitharenites (Fig. 1.7). Framework grains are angular to rounded. Of 23 samples examined 6 are classified as sublitharenites, the remainder as quartzarenites. These sandstones are cemented by syntaxial quartz overgrowths. Two different phyllosilicates were identified in these arenites: kaolinite and pyrophyllite.

Statistical summaries of kaolinite and pyrophyllite bearing sandstones are presented separately (TABLES 8 & 9). Clay mineral extracts from a similar suite of rocks sampled in the same study area contain illite (sensu stricto) and interlayered illite/smectite (ISII variety) (Chadwick, pers. comm., 1987; Chadwick, 1987).

Kaolinite is present in a range from 5,0 to 14,8 % (11 samples). The kaolinite occurs as primary pore fills that post-date (Fig.1.5g), or which co-precipitate silica cement. The different types of Piekenierskloof Formation arenite pore fills are presented in Appendix 3.

Twelve of the Piekenierskloof Formation sandstones contain pyrophyllite. The presence of this mineral is indicative of the onset of low grade metamorphism (Hunziker et al., 1986). It should be noted that where pyrophyllite occurs it is the sole phyllosilicate mineral in the sample. Kaolinite reacts to produce pyrophyllite at temperatures greater than 300° C (Velde, 1977). The development of pyrophyllite is on a regional scale and is related to the development of the Clanwilliam - Citrusdal - Porterville monocline (Söhngé, 1983, Fig 1.). If a "normal" geothermal gradient of approximately 30° C per km is assumed, depths of burial near 10km are indicated. It should further be noted that no sample of Piekenierskloof Formation sandstone contained

feldspar.

### 1.6.3. Graafwater Formation Arenites

Graafwater Formation arenites are well sorted quartz- and sublitharenites (Fig 1.7.) that are rarely feldspathic (Table 10). Framework grains are well rounded. Of 24 samples one is classified as a litharenite, six as quartzarenites and the remainder as sublitharenites. These arenites are cemented by quartz. Overgrowths are present in a range from 1,7 to 26,5 volume percent (mean = 7,6% for 24 samples). Feldspar is rare but can occur in amounts up to 6%. Lithic fragments are mainly intraformational shale and siltstone reworked from finer grained facies into the arenites. These lithic fragments are characteristically red in colour. Some hematized biotite fragments are present. Authigenic matrix occurs in amounts from 1,1 to 20,3% (with a mean of 8,7% and standard deviation of 6,9% for 24 samples).

Most Graafwater arenites are better sorted and contain more well rounded to very well rounded framework grains, relative to Piekenierskloof and Klipheuwel Formation arenites. Six Graafwater Formation arenites contain poly- or bi-modal size distributions (Appendix 2). These arenites are thinly laminated on a scale smaller than the thin section diameter, hence the apparent bi/poly-modality. The arenites contain a very well rounded coarse fraction and an angular finer (fine sand or finer) fraction.

The increased roundness of Graafwater Formation arenites can be reconciled with the nearshore marine palaeoenvironmental models proposed for this formation (Rust, 1967, 1977), the angular finer fraction resulting from the breakage of sediment in the nearshore and the increased roundness from abrasion of sediment. Subsequent sorting (into laminae with distinct grain size) may be the result of sedimentary processes such as swash and backwash on beaches. However if a transgressive model for the Graafwater Formation is accepted it is equally likely that these size characteristics may be inherited from older reworked sediment: extreme rounding is achieved in subaerial dunefields, which have poor preservation potential in such transgressive situations. Such sediment may however be subsequently reworked by nearshore sedimentary processes.

Clay minerals fill and occlude pore space not filled by syntaxial quartz overgrowths, i.e. are primary pore fills. Authigenic fills of secondary pores are rarer. Some

quartzarenites contain a secondary porosity generated by quartz framework and cement dissolution, which has been infilled by kaolinite. Kaolinite is present as both large, vermiform ( $> 20\mu\text{m}$ ) and smaller ( $< 10\mu\text{m}$ ) blocky aggregates. The former occurs as one or two aggregates per pore, the latter as many thousands of aggregates per pore. The former morphology is characteristic of precipitation from meteoric water, the latter precipitation from saline water (Hurst and Urwin, 1982; Hazeldine, et al., 1984). Some kaolinite is of the ragged edge variety. Kaolinite is rarely replaced by filamentous illite (Plate 1h).

## 1.7

## TECTONIC PROVENANCE

Quartzarenites are usually assumed to be the product of multicycle processes (Dutta, 1987). Tectonic classification of sandstone provenance is based on the good correlation between framework mineralogy and the tectonic setting of provenance areas (Dickenson et al., 1983; Potter, 1984). The Q-F-L and Qm-F-Lt diagrams (Figs 1.2 & 1.3) of Dickenson and his co-workers at the University of Arizona, are used to determine the tectonic provenance of sandstone on the basis of matrix, cement and carbonate-free point count analyses.

The poles on the Q-F-L diagram are 1) total quartzose grains (Q) including polycrystalline lithic fragments such as chert and quartzite; 2) monocrystalline feldspar grains (F); and 3) unstable polycrystalline lithic fragments (L) of either igneous or sedimentary parentage, including metamorphic types. The tectonic classification so defined is compatible with McBride's sandstone classification. The poles on the Qm-F-Lt diagrams are 1) Qm, quartz framework grains that are exclusively monocrystalline; 2) monocrystalline feldspar (F) and 3) total polycrystalline lithic fragments (Lt) including quartzose varieties (Dickenson et al., 1983, p.222).

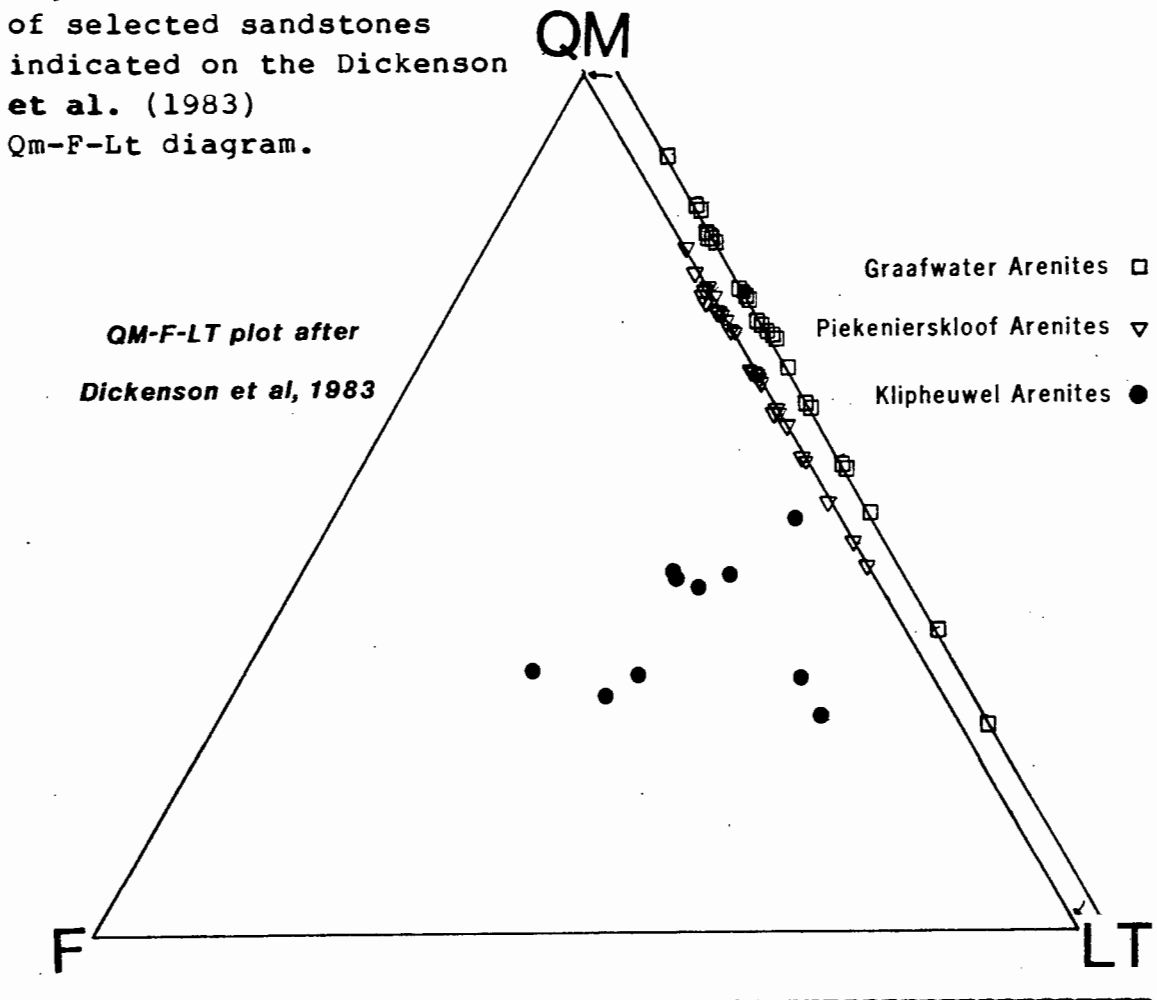
Sandstones originating from older orogenic terrains are typically quartz rich. These quartz rich provenance terrains plot on the Qm-Lt join of the Qm-F-Lt diagram; sediments from these source areas are usually feldspar poor, having less than 13-18% feldspar present.

The value of such petrographic data can be seriously degraded where diagenesis dissolves and or replaces one or more of the framework modes (Dickenson et al., 1983;

Shanmugan, 1985). Diagenetic modification of feldspar and rock fragments are reported in early diagenesis (the eogenetic regime where sediment is in contact with pore water of similar chemistry to depositional water) as well as at greater depths when in contact with more evolved, saline groundwater (Wilson and Pittman, 1977; Schmidt and McDonald, 1979; Suttner and Dutta, 1986)

Data from the Piekenierskloof and Graafwater Formation arenites plot within the quartzose recycled and transitional recycled fields of the Qm-F-Lt diagram (Fig 1.8). Data from Klipheuwel Formation arenites sampled from immediately below the Piekenierskloof / Klipheuwel contact plot within the transitional recycled (2 samples), lithic recycled (2 samples), mixed (3 samples) and dissected arc (3 samples) fields. Given that the Klipheuwel is a distal facies equivalent of the Piekenierskloof Formation in the sample area (Vos and Tankard, 1981), the relative position (on Fig. 1.8) of sandstones from these two formations is taken to indicate a loss of both feldspar and lithic fragments during diagenesis.

Fig 1.8. Tectonic provenance of selected sandstones indicated on the Dickenson et al. (1983) Qm-F-Lt diagram.



The Klipheuvel Formation samples are more poorly sorted than the other samples (Appendix 2). Porosity and permeability are a function of both grain size and sorting (Leder and Park, 1986, Fig. 3, p.1718). As grain sizes are comparable, porosity reduction due to poor-sorting coupled with reduced permeability due to deposition between impermeable shales (which occur in the Klipheuvel Formation in the sample area and are absent in the Piekenierskloof Formation), may account for the relative preservation of Klipheuvel feldspars and rock fragments. Reduced permeability would result in reduced fluxes of solvents and solutes.

The deleterious effect that solution of framework constituents has on provenance data can be illustrated assuming the following reactions are pertinent:

- 1)  $2KAl_3O_8 + 2H_2O + 2H^+ \rightarrow Al_2Si_2O_5(OH)_4 + SiO_2 + 2K^+$   
i.e. feldspar, water and acid react to produce kaolinite, silica and  $K^+$  in solution. One  $cm^3$  of feldspar produces  $0,46 cm^3$  of kaolinite and  $0,43 cm^3$  of silica (Leder and Park, 1986) and
- 2) 1 Kaolinite + 4 quartz  $\rightarrow$  1 Pyrophyllite + 2 water  
(Velde, 1985a), where  $0,74 cm^3$  of kaolinite reacts with  $0,34 cm^3$  of quartz to produce  $1 cm^3$  of pyrophyllite and  $0,14 cm^3$  of water.

Assuming mass balance is conserved on the scale of the thin section, then of 24 Graafwater Formation samples, 16 have authigenic matrix (kaolinite) contents  $> 5\%$ . If a simple premise is held that feldspar alone contributed the necessary solutes for authigenic cement formation then a rock with  $5\%$  kaolinite would have had approximately  $10\%$  feldspar originally. The mean kaolinite content of these 16 samples is  $11,9\%$ : the approximate original feldspar content, modelled conceptually using the above premises (and using eqn. 1 above), would have been in the region of  $20\%$ .

Eight out of eleven Piekenierskloof Formation samples contain authigenic kaolinite in abundances  $> 5\%$ . The mean kaolinite content of these eight samples is  $9,4\%$ , indicating an approximate original feldspar content of  $20\%$ . The amount of precursor kaolinite in Piekenierskloof Formation sandstones containing pyrophyllite can be estimated using eqn. 2 above. Ten out of 12 Piekenierskloof Formation samples contain pyrophyllite in abundances greater than  $5\%$ . The mean pyrophyllite content of these samples is  $16,8\%$ , indicating an

approximate kaolinite abundance of 12% using eqn. 2. If the kaolinite in turn was derived from feldspar breakdown, 20 - 25% feldspar would originally have been present.

The above arguments illustrate that the diagenetic dissolution of the framework mineralogy can change the tectonic provenance as inferred by the Q-F-L and Qm-F-Lt diagrams, as well as the sandstone classification. The premises above, namely that (1) mass balance is conserved on the scale of a thin section and (2) that feldspar alone is the source of ions, are extreme simplifications of what are known to be geochemically complex reactions. Solutes and solvents are known to migrate some distance (m to km) and other framework components (cherts, limestones, dolomites, volcanoclastic fragments amongst others) apart from feldspar dissolve as readily. Petrographic and SEM evidence indicates that even quartz, normally insoluble (under geochemically normal physio-chemical conditions) (Williams et al., 1985) was dissolved (Fig. 1.5 c&d, Plate 1 f&g).

Previous work (Rust, 1967) indicated that the source areas of Graafwater and Piekenierskloof Formation arenites were to the NE and the SW of the Table Mountain Group Basin (Rust, 1967, Fig. 85 & 88). Provenance areas to the NW of the basin are now submerged on the West Coast continental shelf and are thus unexposed and unsampled. The basement to the SW is buried under Palaeozoic cover, except where erosional windows and late Gondwana age (rift) faults have exposed it: Cape Granite Suite and late Proterozoic supracrustal sequences (Malmesbury and Kango Groups) are inferred to underlie this area.

Geochemical analyses, including trace element data, of Graafwater shales (Marchant and Moore, 1978) indicate provenance from parental material of chemical composition similar to the Cape Granite Suite and Namaqualand granites and gneisses. Klipheuwel Formation petrography and palaeocurrent data (this work) indicate derivation from a granitic/ supracrustal terrain. If sediment was derived from the late Proterozoic Malmesbury/Nama terrain then the following lithologies were available to release sediment : quartzite, conglomerate, sandstone, marble, limestone, phyllite, pelitic wackes, greywacke, slate, and metadolerite (Hartnady, 1969; SACS, 1980) (Fig. 1.9).

Pebble counts of Piekenierskloof Formation clasts (this study, Table 11) indicate a supracrustal provenance. The above sediment provenance areas were subjected to orogeny in

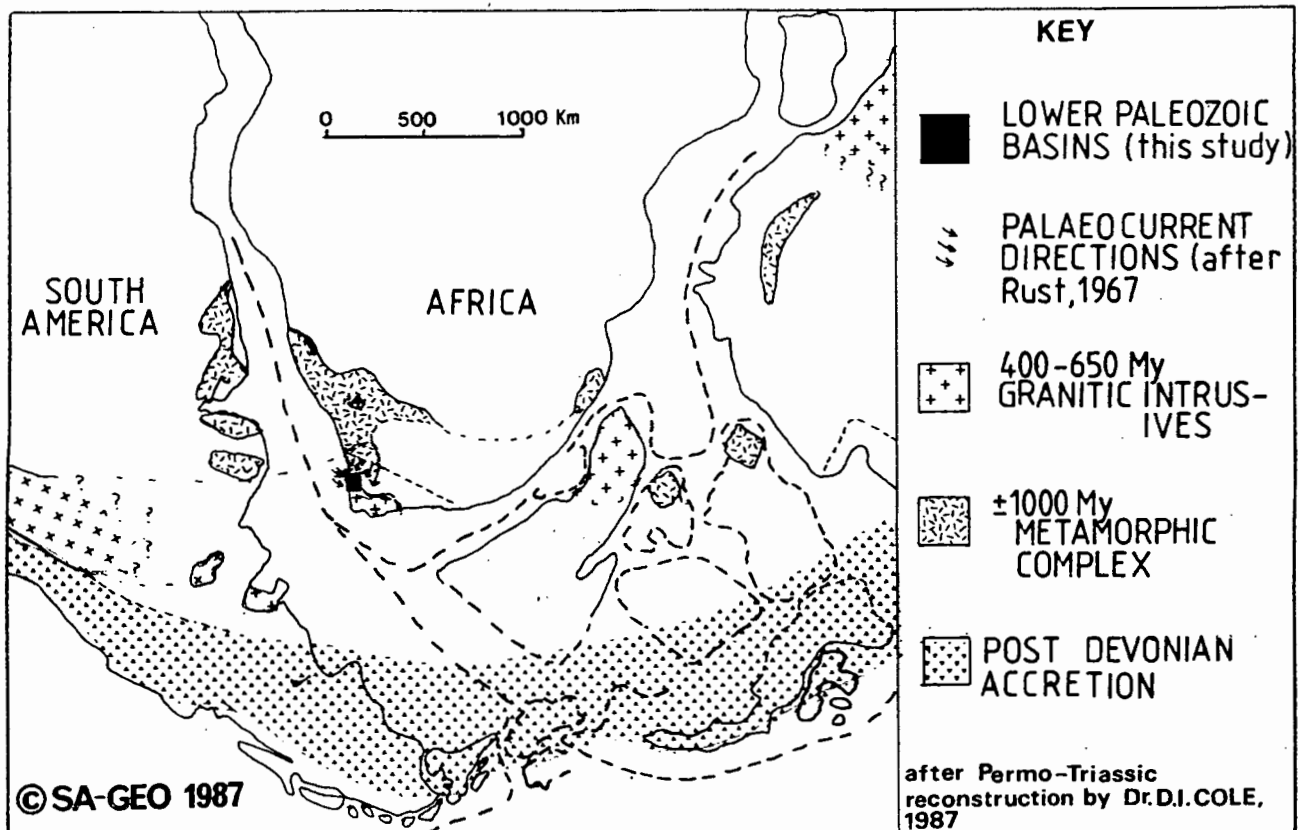


Fig. 1.9. Location of lower Palaeozoic strata within Gondwana: Likely sources of sediment are 1000 My metamorphic complexes and orogens as well as late Precambrian - Cambrian intrusives.

the late Proterozoic (the "Pan-African" event or Saldanian Orogeny of Tankard *et al.*, 1982). Areas to the N and NW had been subjected to earlier orogeny in the Mid-Proterozoic (the Namaqua Orogeny, dated at ~ 1900 - 1100 My SACS, 1980. McStay, pers. comm., 1987).

## 1.8

## DISCUSSION

### 1.8.1 Summation of diagenetic features

Two distinct diagenetic trends and two separate phases of diagenetic mineral production have been discerned in Klipheuwel, Piekenierskloof and Graafwater Formation arenites. The poor sorting of the framework and the presence of detrital clay results in Klipheuwel Formation arenites with preserved feldspar, less authigenic silica cement and only late stage framework breakdown. Detrital feldspar and quartz as well as silica cement dissolution resulted in the formation of secondary porosity, which has subsequently been occluded by illite (and minor kaolinite) precipitation.

Graafwater and Piekenierskloof arenites contain negligible or no feldspar, show improved sorting and greater roundness up stratigraphic section and contain significant volumes of syntaxial silica overgrowths (as cement) and kaolinite as primary and secondary pore fills. Kaolinite occludes porosity subsequent to the creation of secondary porosity by the dissolution of detrital quartz grains and silica cement, with simultaneous precipitation of small quartz euhedra. Kaolinite is subsequently dissolved and illite precipitated or (with increasing temperature) reacts with silica to produce pyrophyllite. The general diagenetic sequence is 1) silica precipitation as syntaxial overgrowths, 2) silica dissolution and the creation of secondary porosity, 3) precipitation of kaolinite in pore space and 4) reaction of kaolinite to produce illite or pyrophyllite.

Any discussion of these diagenetic features must address the following concepts: 1) the origin and mechanism of movement of solvent (water) 2) the origin, solubility, mechanism of transport and precipitation of solutes (i.e. Si, Al and K mainly) and 3) diagenetic reactions that produce illite or pyrophyllite from kaolinite.

Given the low solubility of Si and Al in groundwater (Williams et al, 1986; Bjørlykke, 1984) attention must be given to diagenetic models that do not require unrealistic amounts of solvent (pore volumes) and to the mechanism of solvent movement. Further, central to the premise that Piekenierskloof and Graafwater lithologies were subarkosic prior to diagenetic alteration, is the question of Al mobility. The origin of the secondary porosity whether it be the result of framework dissolution or, alternatively, the dissolution of an earlier cement (carbonate) is critical to the premise that Graafwater and Piekenierskloof Formation arenites had subarkosic mineralogy (+ labile lithic fragments) prior to the onset of diagenesis.

### 1.8.2. Solvent transfer

Mechanisms of solvent transfer are fundamental to diagenetic studies: solutes that precipitate as neoformed minerals and as overgrowths on detrital minerals are transported in solution by a combination of four recognised processes. These are (a) meteoric water, driven by hydrostatic head; (b) solvent recycling driven by convection; (c) compactional pore water, driven out of sediment by the weight of sediment above and porosity

occlusion due to cementation and (d) clay mineral reactions that liberate water, such as smectite or kaolinite reacting to produce illite i.e. clay dehydration reactions (Boles and Franks, 1979; Bjorlykke, 1984; Galloway, 1984).

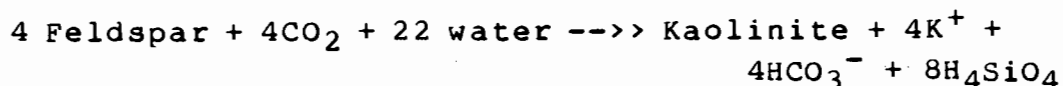
Several of these possibilities can be eliminated on examination: the Piekenierskloof Formation in the study area contains negligible siltstone and shale. The Graafwater Formation has a shale:sandstone ratio of 1:20 (Rust, 1967): the Klipheuwel Formation contains in this author's estimate no more than 20% shale. Volumetrically the succession contains too little shale to account for the volumes of silica cement and neofomed clay present, given clay mineral dehydration, the volumes of solvent expelled and the solubility of solutes contained therein. Hazeldine et al. (1984) calculated that  $1.2 \times 10^6$  volumes of pore water was required to precipitate 15% silica cement in an arenite given the decrease of silica solubility change from 100°C to 80°C. (Worked examples are presented in Leder and Park, 1986 p.1714-1715 and Hazeldine et al., 1984 p.397).

Estimates of 50000 pore volumes (Bjorlykke, 1984) to cement an arenite with 25% porosity further illustrate that large volumes of solvent are required. Most authors (Wood and Hewett, 1982; Bjorlykke, 1984; Hazeldine et al., 1984; Leder and Park, 1986) would agree that sufficient volumes of water cannot be supplied by mechanical compaction and dewatering to precipitate significant volumes of cement given the low solubility of silica and alumina.

Convection cells will arise in porous, fluid saturated, sandbodies of geologic dimensions (Wood and Hewett, 1982), with fluid velocities of  $\sim 1 \text{ m.y}^{-1}$  at geothermal gradients of 25° C per km. These convection cells provide a realistic mechanism of solvent flux and recycling in terms of the volume necessitated by low Al and Si solubility.

### 1.8.3. Solute origin

The major species present in cement and clay mineral species are  $\text{K}^+$ ,  $\text{Al}^{3+}$  and Si. These species are derived from the breakdown of feldspar ,



or



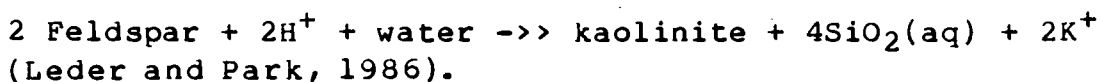
illitised in the rocks studied. The occurrence of kaolinite in oversized and elongate pores that are sometimes associated with what appears to be corrosion of quartz framework and cement is highly suggestive of kaolinite infill of a cement (carbonate) dissolution secondary porosity. These textural criteria are suggestive of generation of cement dissolution porosity (Burley and Kantorowicz, 1986) and subsequent infill. However not all oversized and elongate pores are associated with corrosion textures (Appendix 3). The occurrence of these pore fills whose size range is comparable with that of the framework grains is suggestive of in situ dissolution of a framework precursor and subsequent kaolinite precipitation.

The solubility of silica and alumina is known to increase if complexing by organic compounds occurs (Surdam et al., 1984; Bennet and Siegel, 1987) during diagenesis, as in the case of oilfield solvents. The pre-Devonian age and lack of shale makes an organic-complexed Al and Si solubility increase unlikely as the source sediment and organic detritus for this process is lacking in the lower TMG.

Textural evidence exists indicating the occurrence of kaolinite infill of dissolution induced oversized porosity. If the secondary porosity is due either to feldspar replacement or carbonate cement dissolution both these cases require the flushing of sediment by relatively low pH water i.e.

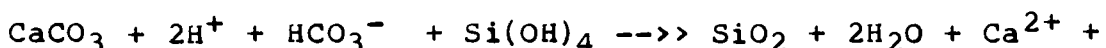


Feldspar dissolution under acidic conditions leads to the precipitation of kaolinite and quartz (Bjorlykke, 1984 p. 27) or



Both these reactions are constrained by the need for acidic conditions and the necessity of potassium removal. Increased activity of potassium will result in illite, rather than kaolinite precipitation (Hurst and Urwin, 1982).

If the secondary porosity is the result of carbonate dissolution then the pertinent reaction is:



$2\text{HCO}_3^-$  (Burley and Kantorowicz, 1986)

which necessitates the influx of acidic water and results in the removal of carbonate, a rise in pH and the precipitation of kaolinite as the solubility product of Al is reached.

The diagenetic assemblage is best understood by considering an ideal activity diagram showing solute activity and clay mineral equilibria at given temperatures and silica saturation (Aagaard and Hegelson, 1983). The kaolinite stability field contains an area of quartz undersaturation. The dissolution of feldspar releases potassium in solution which results in the increase of  $\text{K}^+$  in these pore solutions, resulting in the pore solution equilibrating with illite, mixed layer clay or montmorillonite. Excess potassium results in the following reaction:

$3 \text{ Kaolinite} + 2\text{K}^+ \rightarrow 2 \text{ Illite} + 2\text{H}^+ + \text{H}_2\text{O}$  (Bjorlykke, 1984 p.284) which lowers pH, and may result in further feldspar dissolution:

$3 \text{ K-feldspar} + 2\text{H}^+ \rightarrow \text{Illite} + 6\text{SiO}_2 + 2\text{H}_2\text{O}$  (Bjorlykke, 1984)

These reactions explain the late diagenetic replacement of kaolinite by illite in Graafwater and Piekenierskloof Formation arenites, as well the replacement of feldspar by illite and quartz in Klipheuwel Formation arenites.

Textural evidence (kaolinite fill of oversized porosity) may thus be ambiguous, and may simply be the result of the increased solubility of Si with increasing temperature. Basinal groundwater is known to become more saline with increasing age and depth: as the solubility product of kaolinite is exceeded kaolinite is precipitated. Some minor silica euhedra are precipitated in pores simultaneously. Thus kaolinite precipitation in the field of quartz saturation is inferred. Where flux of  $\text{K}^+$  in solution was low, pore solutions successively equilibrated with illite, resulting in the partial to total replacement of kaolinite. Where temperature was  $> 300^\circ\text{C}$  kaolinite reacted to form pyrophyllite.

The source of the Al-bearing solvent remains ambiguous. The above discussion indicates that the dissolution of either feldspar framework grains or carbonate cements necessitates

flux of relatively low PH solvent water (meteoric water). The diagenesis of these sandstones may thus approximate the diagenesis of many other quartzarenites and subarkoses that show similar trends in quartz and clay authigenesis (Hazeldine et al., 1984; Burley et al., 1985).

## 1.9

## CONCLUSIONS

1) Klipheuwel Formation arenites are classified as feldspathic litharenites or lithic subarkoses. These arenites are cemented by quartz and contain illite as (potassic) feldspar replacements as well as pore fills. The mineralogical assemblage is quartz + feldspar + illite + minor kaolinite. Authigenic clay minerals occlude porosity post to quartz framework and cement dissolution. These arenites are more poorly sorted and contain more polycrystalline quartz than Piekenierskloof or Graafwater Formation arenites. Poor sorting may account for the preservation of feldspar.

2) Piekenierskloof and Graafwater Formation arenites are classified as quartzarenites or sublitharenites. The arenites show improved sorting relative to Klipheuwel Formation arenites. The arenites contain pore filling kaolinite that occludes secondary diagenetically enhanced porosity. As the corrosion of quartz is restricted to the immediate vicinity of the replacive mineral, this relationship is taken to indicate kaolinite replacement of earlier carbonate cement. The embayments, pits and notches in quartz framework and cement are indicative of a quartz - pore filling carbonate reaction. Oversized and elongate blebs of kaolinite indicate the former (rare) presence of feldspar. Some kaolinite occurs in textural relationships where co-precipitation is inferred. Vermiform kaolinites provide evidence of fresh water flushing.

3) The solubility of Al species is low enough to support the simple premise that in the absence of organic complexing Al is conserved on a local scale. Arenites with kaolinite present in significant volume suggest a pre-diagenetic feldspathic (?) mineralogy.

4) The diagenetic assemblage of quartz + kaolinite + illite (sensu lato) indicates that significant chemical species present can be modelled in the system  $K_2O - SiO_2 - Al_2O_3$ : likely precursors are feldspar, detrital mica or detrital clay. As the latter is observed as oxidised, haematitic blebs, and the detrital mica rock fragments are preserved in

a number of samples, feldspar is considered the most likely source.

5) Textural evidence (kaolinite replacement of feldspar, kaolinite replacing carbonate, vermiform kaolinite) indicate authigenic mineral neof ormation as a result of flux of low salinity solvent i.e. meteoric water. Some textural evidence is ambiguous but kaolinite neof ormation by either mechanism outlined above requires flow of low salinity solvent. These arenites are inferred to have been invaded by solvent with bicarbonate alkalinity, resulting in the preservation of Al on a local scale (as in Surdam et al., 1984).

6) Later diagenetic changes appear to be illitisation of kaolinite (as a response to increased salinity and  $K^+$  activity) or reaction of kaolinite and quartz to form pyrophyllite.

7) Klipheuwel Formation arenites point count data plot in the "dissected arc" and "mixed" fields of the Qm-F-Lt diagram. Given the abundant textural evidence indicative of replacement of parts of the framework, tectonic source areas are more likely to have been "basement uplift" or "transitional continental" types, which contain more feldspar. Point count data of Piekenierskloof and Graafwater Formation arenites plot within the "quartzose recycled", "transitional recycled" and "craton interior" fields of this diagram. The relative displacement on a Qm-F-Lt diagram of these arenites, sampled across a distal to proximal facies transition is taken to mean relative preservation of feldspar in Klipheuwel Formation arenites.

8) Likely provenance areas, given trace element composition of shales within the succession, palaeocurrent data and the location of the basin within a reconstructed Gondwana, are Pan-African and Late Proterozoic deformed supracrustal rocks and associated syn- to post-tectonic granitoids. Sediment from such "recycled orogenic" source areas is typically quartz rich. The mineralogic nature of these arenites is thus attributed in part to source area lithology.

9) Abundant textural evidence exists indicating pervasive fluid flux. Diagenetic processes substantially contributed to the enhancement of the quartz rich nature of these rocks.

10) The process of sediment maturity enhancement by attrition and abrasion can only be inferred in the case of some Graafwater Formation arenites where improved rounding and

sorting is evident.

oo00000oo

## References

- Aagaard, P. and Hegelson, H.C. (1983). Activity/Composition relations among silicates and aqueous solutions: II. Chemical and thermodynamic consequences of ideal mixing of atoms on homological sites in montmorillonites, illites, and mixed-layer clays. Clays and Clay Minerals, 31, 207-217.
- Bennet, P. and Siegel, D.I. (1987). Increased solubility of quartz due to complexing by organic compounds. Nature, 326, 684-686.
- Bjørlykke, K. (1984). Formation of secondary porosity ; how important is it ? In: McDonald, D.A. and Surdam, R.C., eds., Clastic diagenesis. American association of Petroleum Geologists, Tulsa, Oklahoma, 277-286.
- Boles, J.R. and Franks, S.G. (1979). Clay diagenesis in Wilcox sandstones of Southwest Texas: implications of smectite diagenesis on sandstone cementation. J. sedim. Petrol., 49, 55-70.
- Bowers, T.S., Jackson, K.J., Helgeson, H.C. (1984). Equilibrium activity diagrams. Springer Verlag, Berlin, 397pp.
- Burley, S.D. , Kantorowicz, J.D. and Waugh, B. (1985). Clastic Diagenesis. In: Brenchley, P.J. and Williams, B.P.J. Eds., Sedimentology. Recent Developments and Applied Aspects. The Geological Society, Blackwell Scientific Publications, Oxford, 189-228.
- Burley, S.D. and Kantorowicz, J.D. (1986). Thin section and S.E.M. textural criteria for the recognition of cement-dissolution porosity in sandstones. Sedimentology, 33, 587-604.
- Caputo, M.V. and Crowell, J.C. (1985). Migration of glacial centres, across Gondwana, during the Paleozoic era. Geol. Soc. Am. Bull., 96, 1020-1036.
- Chadwick, P.J. (1987). A 32° traverse through the Table Mountain group in the Western Cape Province. A stratigraphical, mineralogical and petrographic study. B.Sc.(Hons.) thesis, Univ. Cape Town, 50pp.

Cocks, L.R.M. and Fortey, R.A. (1986). New evidence on the South African Lower Palaeozoic : Age and Fossils Reviewed. Geol. Mag., 123, 437-444.

Cooper, M.R. (1984). Discussion of "Cruziana Acacensis - the first Silurian index-trace fossil from South Africa", by C.D. Potgieter and B.W. Oelofsen. Trans. Geol. Soc. S. Afr., 86, 51-54.

Cooper, M.R. (1986). Facies shifts, sea level changes and event stratigraphy in the Devonian of South Africa. S. Afr. J. of Sci., 82, 255-258.

Cramer, F.H., Rust, I.C. and Cramer, M. (1974). Upper Ordovician Chitinozoans from the Cedarberg Formation of South Africa. Preliminary Note. Geol. Rund., 63, 340-345.

Dickenson, W.R. and Suczek, C.A. (1979). Plate tectonics and sandstone compositions. Amer. Assoc. Petrol. Geol., 63, 2164-2182.

Dickenson, W.R., Beard, L.S., Brakenridge, G.R., Erjavec, J.L., Ferguson, R.C., Inman, K.F., Knepp, R.A., Lindberg, F.A. and Ryberg, P.T. (1983). Provenance of North American Phanerozoic sandstones in relation to tectonic setting. Bull. Geol. Soc. Am., 94, 222-235.

Donovan, S.K. (1987). The fit of the continents in the late Precambrian. Nature, 327, 139-141.

Duncan, A.R., Erlank, A.J. and Betton, P.J. (1984). Appendix 1. Analytical techniques and database descriptions. In: Erlank, A.J., Ed., Petrogenesis of the volcanic rocks of the Karoo Province. Spec. Publ. Geol. Soc. S.Afr., 13, 387-395.

Dutta, P.K. and Suttner, L.J. (1986). Alluvial Sandstone composition and palaeoclimate, II. Authigenic mineralogy. J. sedim. Petrol., 56, 346-358.

Dutta, P.K. (1987). Origin and rarity of first cycle quartz arenite. Abstract: Amer. Assoc. Petrol. Geol. Bull., 71, p.551.

Dott, R.H., Byers, G.W., Fielder, S.R., Stenzel, S.R. and Winfree, K.E. (1986). Aeolian to marine transition in Cambro-Ordovician cratonic sheet sandstones of the northern

Mississippi valley, U.S.A. Sedimentology, 33,345-367.

Fisher, A.G. (1984). The two Phanerozoic supercycles In: Bergerren, W.A. and Van Couvering, J.A., Eds., Catastrophes and Earth History. Princeton Univ. Press, Princeton, New Jersey, 129-150.

Galloway, W.R. (1984). Hydrogeologic regimes of sandstone Diagenesis. In: McDonald, D.A. and Surdam, R.C., Eds., Clastic Diagenesis. American Association of Petroleum Geologists, Tulsa, 3-13.

Garrels, R.M. (1984). Montmorillonite/illite stability diagrams. Clays and Clay Minerals, 32,161-166.

Gray, J., Theron, J.N. and Boucot, A.J. (1986). Age of the Cedarberg Formation, South Africa and early land plant evolution. Geol. Mag., 123,445-454.

Hallam, A. (1984). Pre-Quaternary sea-level changes. Ann. Rev. Earth and Planet. Sci., 12, 205-243.

Hartnady, C.J.H., (1969). Structural analysis of some pre-Cape Formations in the Western Cape Province. Precambrian Research Unit Bulletin No. 6, 70 pp.

Hazeldine, R.S., Samson, I.M. and Cornford, C. (1984). Quartz diagenesis and convective fluid: Beatrice Oilfield, U.K. North Sea. Clay Minerals, 19, 391-402.

Hobday, D.K. and Tankard, A.J. (1978). Transgressive-barrier and shallow shelf interpretation of the lower Palaeozoic Peninsula Formation, South Africa. Geol. Soc. Am. Bull., 89, 1733-1744.

Hunziker, J.C., Frey, M., Clauer, N., Dallmeyer, R.D., Friedrichsen, H., Flehmig, W., Hochstrasser, K., Roggwiler, P. and Schwander, H. (1986). The evolution of illite to muscovite: mineralogical and isotopic data from the Glarus Alps, Switzerland. Contrib. Mineral. Petrol., 92, 157-180.

Hurst, A. and Irwin, H. (1982). Geological Modelling of Clay Diagenesis in sandstones. Clay Minerals, 17, 5-22.

Hurst, A. and Bjorkum, P.A. (1986). Discussion. Thin section and S.E.M. textural criteria for the recognition of cement - dissolution porosity in sandstones. Sedimentology, 33,

605-614.

Land, L.S, Milliken, K.L and McBride, E.F. (1987). Diagenetic evolution of Cenozoic Sandstones, Gulf of Mexico sedimentary basin. Sedim. Geol., 50, 195-225.

Leder, F. and Park, W.C. (1986). Porosity reduction in sandstone by quartz overgrowth. Bull. Amer. Assoc. Petrol. Geol., 70, 1713-1728.

Long, D.G.F. (1978). Proterozoic stream deposits: some problems of recognition and interpretation of ancient sandy fluvial systems. In: Miall, A.D., Ed., Fluvial Sedimentology. Can. Soc. Petrol. Geol., Calgary, 313-342.

Mack, G.H. (1978). The survivability of labile light minerals in fluvial, aeolian and littoral marine deposits : the Permian Cutler and Cedar Mesa Formations, Moab, Utah. Sedimentology, 25, 587-604.

Marchant, J.W. and Moore, A.E. (1978). Geochemistry of Table Mountain Group, II : Analysis of two suites of Western Graafwater Rocks. Trans. Geol. Soc. S. Afr., 81, 353-357.

McBride, E.F. (1963). A classification of common sandstones. J. sedim. Petrol., 33, 664-669.

McBride, E.F. (1987). Diagenesis of the Maxon Sandstone (Early Cretaceous), Marathon Region, Texas: a diagenetic quartzarenite. J. sedim. Petrol., 57, 98-107.

Morad, S. and Aldahan, A.A. (1987). Diagenetic replacement of feldspars by quartz in sandstones. J. sedim. Petrol., 57, 488-493.

Nadeau, P.H., Wilson, M.J. McHardy, W.J. and Tait, J.M. (1985) The conversion of smectite to illite during diagenesis: evidence from some illitic clays from bentonites and sandstones. Min. Mag., 393-400.

Potgieter, C.D. and Oelofsen, B.W. (1983). Cruziana Acacensis - the first Silurian index-trace fossil from southern Africa. Trans. Geol. Soc. S. Afr., 86, 51-54.

Potgieter, C. D. and Oelofsen, B.W. (1984). Authors reply to discussion on "Cruziana Acacensis - the first Silurian index-trace fossil from southern Africa. Trans. Geol. Soc

- S. Afr., 87, 53-54.
- Potter, P.E. (1984). South American beach sand and plate tectonics. Nature, 311, 645-648.
- Powers, M.C. (1953). A new roundness scale for sedimentary particles. J. sedim. Petrol., 23, 117-119.
- Pye, K. and Krinsley, D.H. (1985). Formation of secondary porosity in sandstones by quartz framework dissolution. Nature, 317, 54-56.
- Rust, I.C. and Theron, J.N. (1964). Some aspects of the Table Mountain Series near Vanrhynsdorp. Trans. Geol. Soc. S. Afr., 62, 131-136.
- Rust, I.C. (1967). On the sedimentation of the Table Mountain Group in the western Cape Province. Unpubl. D.Sc. thesis, Univ. Stellenbosch, 110 pp.
- Rust, I.C. (1973). The evolution of the Palaeozoic Cape Basin, Southern Margin of Africa. In: Nairn, A.E.M. and Stehli, F.G., Eds., The ocean basins and margins, vol. 1: The South Atlantic. Plenum Press, London, 247-269.
- Rust, I.C. (1977). Evidence of shallow marine and tidal sedimentation in the Ordovician Graafwater Formation, Cape Province, South Africa. Sed. Geol., 18, 123-133.
- South African Committee for Stratigraphy (SACS), (1980). Stratigraphy of South Africa, Handbook, No. 8. Part 1 : Lithostratigraphy of the Republic of South Africa , South West Africa/Namibia and the Republics of Bophuthatswana, Transkei and Venda. Kent, L.E., Comp., Department of Mineral and Energy Affairs, Pretoria, 690 pp.
- Sohnge, A.P.G. (1983) The Cape Fold Belt - Perspective . In: Sohnge, A.P.G. and Halbach, I.W., Eds., Geodynamics of the Cape Fold Belt. The Geological Society of S.A. Spec. Pub., 12, 1-6.
- Sohnge, A.P.G. (1984). Glacial diamictite in the Peninsula Formation near Cape Hangklip. Trans. Geol. Soc. S. Afr., 87, 199-210.
- Schmidt, V. and McDonald, D.A. (1979). Texture and recognition of secondary porosity in sandstones. In: Aspects of Diagenesis : SEPM Special Publication 26, 209-

225.

Shanmugam, G. (1985). Significance of secondary porosity in interpreting sandstone composition. Bull. Amer. Assoc. Petrol. Geol., 69 378-384.

Srodon, J., Morgan, D.J., Elsinger, E.V., Eberl, D.D. and Karlinger, M.K. (1986). Chemistry of illite/smectite and end-member illite. Clay and Clay Minerals, 34, 368-378.

Surdam, R.C., Boese, S.W. and Crossey, L.J. (1984). The chemistry of secondary porosity. In: McDonald, D.A. and Surdam, R.C., Eds., Clastic Diagenesis. American Association of Petroleum Geologists Memoir, Tulsa, Oklahoma, 127-149.

Suttner, L.J., Basu, A., and Mack, G.H. (1981). Climate and the origin of quartz arenites. J. sedim. Petrol., 51, 1235-1246.

Suttner, L.J. and Basu A. (1985). The effect of grain size on detrital modes : a test of the Gazzi-Dickenson method - Discussion. J. sedim. Petrol., 55, 616-617.

Suttner, L.J. and Dutta, P.K. (1986). Alluvial sandstone composition and palaeoclimate, I. Framework Mineralogy. J. sedim. Petrol., 56, 329-345.

Soegaard, K. and Eriksson, K.A. (1985). Evidence of tide, storm and wave interaction on a Precambrian siliclastic shelf : The 1,700 M.Y. Ortega Group, New Mexico. J. sedim. Petrol., 55, 672-684.

Tankard, A.J. and Hobday, D.K. (1977). Tide dominated back-barrier sedimentation, early Ordovician Cape basin, Cape Peninsula, South Africa. Sed. Geol., 18, 135-159.

Tankard, A.J., Jackson, M.P.A., Eriksson, K.A., Hobday, D.K., Hunter, D.R. and Minter, W.E.L. (1982). Crustal Evolution of Southern Africa. 3.8 million years of Earth history. Springer-Verlag, Berlin, 523pp.

Turner, B.R. (1986). Environmental significance of desiccation cracks in the Early Ordovician Graafwater Formation, Cape Peninsula. Abstract: Geological Society of South Africa Geocongress 86, 433-435.

Turner, B.R. (1987). Research report on the sedimentology and depositional environments of the Graafwater and

Peninsula Formations, in the Cape Peninsula, South Africa. CSIR-FRD Research Report, 19pp.

Van der Plas, L. and Tobi, A.C. (1965). A chart for judging the reliability of point counting results. Amer. J. Sci., 263, 87-90.

Velde, B. (1984). Electron microprobe analysis of clay minerals. Clay Minerals, 19, 243-247.

Velde, B. (1985a). Clay Minerals. A physico-chemical explanation of their occurrence. Developments in sedimentology 40. Elsevier, Amsterdam, 427 pp.

Velde, B. (1985b). Diagenetic mineral composition as a function of pressure, temperature and chemical activity. J. sedim. Petrol. 55, 541-547.

Vos, R.G. and Tankard, A.J. (1981). Braided fluvial sedimentation in the lower Palaeozoic Cape Basin, South Africa. Sed. Geol., 29, 171-193.

Weaver, C.E. and Pollard, L.D. (1973). The chemistry of Clay Minerals. Elsevier, Amsterdam, 213 pp.

Williams, L.A., Parks, G.A. and Crerar, D.A. (1985). Silica Diagenesis, I. Solubility controls. J. sedim. Petrol., 55, 301-311.

Wilson, M.D. and Pittman, E.D. (1977). Authigenic clays in sandstones: recognition and influence of reservoir properties and palaeoenvironmental analysis. J. sedim. Petrol., 47, 3-31.

Wood, J.R. and Hewett, T.A. (1982). Fluid convection and mass transfer in porous sandstones - a theoretical model. Geochim. Cosmochim. Acta, 46, 1707-1713.

Yau, Y., Peacor, D.R. and McDowell, S.D. (1987). Smectite-to-illite reactions in Salton Sea shales: a transmission and analytical electron microscopy study. J. sedim. Petrol., 57, 335-342.

Zonnenshain, L.P., Kuzmin, M.I. and Kononov, M.V. (1985). Absolute reconstructions of Paleozoic oceans. Earth Planet. Sci. Lett., 74, 103-116.

## 2. PALAEOENVIRONMENTAL INDICATORS IN THE FAROO MEMBER (GRAAFWATER FORMATION) AT CARSTENBERG PASS, R364: IMPLICATIONS

### 2.1

#### ABSTRACT

Graafwater Formation (Faroo Member) arenites exposed at Carstensberg Pass contain a number of palaeoenvironmental indicators. Sand filled desiccation cracks, polymodal cross-bedding, sedimentary facies and a diverse trace fossil assemblage indicate deposition on a foreshore/backshore and or washover fan.

Horizontally laminated and thinly bedded quartzarenites contain trace fossils of the *SKOLITHOS* ichnofacies. The ichnogenera *Arenicolites* Hall, 1858; *?Allocotichnus* Osgood, 1970; *Trichichnus* Frey, 1970; *Metaichna* Anderson, 1975; *Planolites* Nicholson, 1873; *Skolithos* Haldeman, 1840; *?Scolicia* De Quatrefages, 1849; *Monocraterion*, Torrel, 1870 and *?Rhizocorallium* Zenker, 1836 are represented here.

Sedimentary facies show strong affinity with shoreline deposits, which are documented in the overlying Peninsula Formation, and contrast strongly with the more heterolithic nature of the Graafwater Formation in the Cape Peninsula, which contains trace fossils *Isopodichnus*, *Rusophycus* and *Diplichnites*. These traces are attributed to trilobites in early Palaeozoic sediment.

A number of palaeoenvironments are represented within the Graafwater Formation, one of which is nearshore marine. Facies models erected locally and proposed as definitive palaeoenvironmental models for the formation as a whole are in need of re-evaluation. Sandstones within the heterolithic portions of the Graafwater Formation as well as foreset stratification in Faroo Member sandstones lack spring-neap cycle foreset thickness variations ("tidal bundles"). Graafwater Formation sandstones in the Cape Peninsula were previously interpreted as shallow subtidal and low tidal terrace deposits: these sandstones

conspicuously lack cyclicity extant in Dutch North sea tidal estuaries to which direct analogy was drawn by previous workers.

## 2.2 INTRODUCTION.

The Graafwater Formation is the second lowermost Formation (Table 1) of the Table Mountain Group. At its maximum this formation is 430m thick. However the greater part of this formation, as at this locality, is less than 250m thick (Rust, 1977, Fig. 1). In the depocentre, four of the five informal members (Middlepos, Loop, Tierhoek and Faroo Members) recognised by Rust (1967) are present, the Faroo member being the uppermost (arrowed, Plate 2a). At Carstensberg Pass (Fig. 2.1) this member is well exposed in an accessible recent road-cutting and is documented here and contrasted with published facies models of the Graafwater Formation in the depocentre (Rust, 1977) and in the Cape Peninsula (Tankard and Hobday, 1977).

No exact ages can be assigned to the Graafwater Formation: it has thus far not yielded any body fossils, dateable or otherwise. Consensus has been reached on the age of the Cedarberg Formation which is the only fossiliferous formation in the lower Table Mountain Group. This formation is of late Ordovician to earliest Silurian age (Gray et al., 1986; Cocks and Fortey, 1986). The basement which the Graafwater and other Formations of the lower Table Mountain Group overlie contain granitoids dated as late Precambrian to early Cambrian in age (Cocks and Fortey, 1986). These two ages constrain the age of the Graafwater Formation. Recent workers have assigned an Ordovician age to the Graafwater Formation (Rust, 1977; Tankard and Hobday, 1977; Hobday and Tankard, 1978) and related its sedimentology to documented Ordovician eustatic transgressions (Tankard et al., 1982).

## 2.3 PREVIOUS WORK AND INTERPRETATIONS.

The Graafwater Formation has been regarded as a transitional (tidal-flat, tide dominated and back-barrier) nearshore marine deposit (Rust, 1977; Tankard and Hobday, 1977; Tankard et al., 1982) between

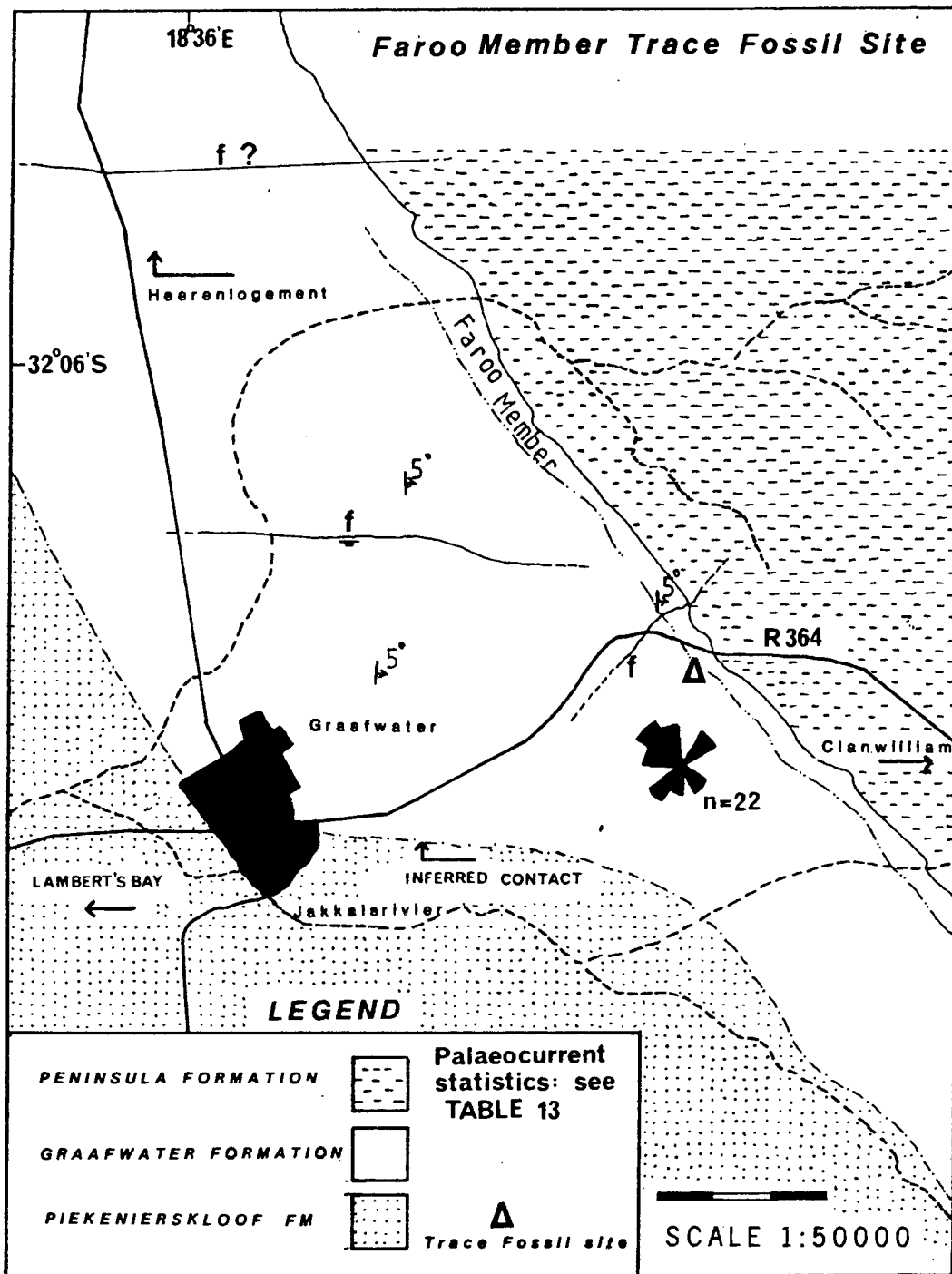


Figure 2.1. Graafwater Village Trace Fossil site. The site documented is to the east of Graafwater village, in the Faroo Member, immediately beneath the Faroo Member-Peninsula Formation contact.

the braided fluvial Piekenierskloof Formation and the shallow marine Peninsula Formation (Tankard *et al.*, 1982).

A variety of structures were attributed to tidal processes in the three facies defined: a subtidal and low tidal quartzarenite, a heterolithic (mixed arenite and mudrock) mid-tidal flat, and a supratidal (mudrock) flat (Tankard and Hobday, 1977). Structures such as herringbone cross-stratification, polymodal foreset orientation, presence of reactivation surfaces and complex sandbody internal architecture led these authors to propose such a palaeoenvironment. In the Northern part of the Graafwater basin (where this formation is more sandy, Rust, 1967) shallow marine and tidal palaeoenvironments have been suggested on the basis of reversed palaeocurrent directions, trace fossil assemblage, presence of reactivation surfaces and supposed fining upward cyclicity (Rust, 1967).

Many of these features are ambiguous and can be found in non-tidal settings. Reactivation surfaces are reported in fluvial settings as is herringbone cross-stratification (Kreisa and Moila, 1985). Further, Tankard and Hobday admit that "within cosets, foresets are strongly unidirectional" as does Rust (1977). Supposed subtidal sandstones lack tidal bundle foreset variations found in North Sea tidal flats and estuaries (Burg Flemming, pers. comm., 1985). Consistent unidirectional current trends away from the source area coupled with the regressive (upward coarsening) nature of the Graafwater-Peninsula Formation contact has led Turner (1986) to question the transgressive, tidal flat and shallow water paradigm erected by Tankard *et al.* (1982).

The depth of desiccation cracks led Turner (1986) to suggest that their depth of penetration was inconsistent (deeper) with desiccation cracks normally associated with a supratidal/mid tidal flats. These cracks occur in a single lithology, have a structureless, homogeneous infill and are infilled from above (Turner, 1987). The depth of these cracks (45 cm) is greater than that recorded on tidal flats (< 10cm) and similar in size to those recorded on modern, semi-arid internal

drainage basins (45cm, Turner, 1987). Rare rain-drop imprints (H. Theron, pers. comm., 1987) support theories of subaerial desiccation and infill rather than syneresis as formative processes for these features. The sedimentology of the Graafwater Formation in the Cape Peninsula is thus not well established. The more northern parts of this formation, which contain diverse trace fossil assemblages, are less controversial.

## 2.4 FACIES DEFINITIONS AND INTERPRETATIONS

### 2.4.1. Facies definitions

Five sedimentary facies are recognised within the outcrop selected. These are: 1) thinly bedded and laminated plane-bedded sandstones; 2) medium to small scale; < 30cm thick, coarse-grained cross-bedded sandstone associated with scour surfaces; 3) sets and cosets of cross-bedded medium to coarse-grained sandstone with polymodal foreset orientations; 4) apparently massive coarse-grained sandstone with mudchip conglomerate within shallow scour channels; 5) laterally discontinuous, thin (< 5mm) patches of mudrock (grain size less than silt size) which may contain sandstone casts of desiccation cracks.

### 2.4.2. Facies descriptions

A. **Facies 1:** Laminated and thinly bedded plane-bedded sandstones can be laterally continuous or discontinuous on the scale of the outcrop. Laminations are a few grain diameters thick and grain size variations are difficult to discern. Laminated plane-bedded sandstone may show low angle lateral truncation against other plane-laminated bedsets. Upper contacts may be eroded or show upward transition into massive, thinly bedded to thick bedded sandstone. Rare small scours (< 1m width) in plane-laminated sandstone are themselves laminated with laminae showing an angular discordance with the lower scour surface which becomes less discordant upward. Plane-laminated sandstones are burrowed and locally bioturbated. Massive, thinly to thickly bedded, sandstone is laterally discontinuous and appears to fill wide shallow scours. The tops of

these beds are normally truncated by plane-bedded laminae overlying a planar erosion surface. This facies is the dominant lithofacies present at this locality.

B. **Facies 2:** Low-angle coarse-grained cross-bedded sandstones are laterally discontinuous and overlie erosion surfaces. They contain abundant, diagenetically reddened mudrock chips. These sandstones are medium to small scale features (< 20cm height) and are volumetrically insignificant relative to other facies.

C. **Facies 3:** Sets and cosets of cross-bedded (> 10° dip) coarse-grained sandstone overlie planar erosion surfaces. No systematic foreset thickness variation is apparent. Foreset azimuths are polymodal (Fig. 2.1, Table 13) with a mean azimuth direction of 117°. When compared to data obtained at outcrop scale for azimuths in the fluvial Piekenierskloof Formation (the underlying stratigraphic unit) the consistency ratio of pooled azimuth data is significantly lower (Table 13). Azimuth data presented in a rose diagram with 30° class intervals (Fig. 2.1) indicate a polymodal distribution with modes directed NW-SE and NE-SW. This facies is the second most prominent lithofacies type present at this outcrop. These sandstones contain very occasional burrows. It is best exposed in the southern wall of the road-cutting at the base of the outcrop at the level of the tarred road.

D. **Facies 4:** Massive coarse-grained sandstone with mudchip granule to small pebble mudchip conglomerate occurs in a single channel in the southern wall of the road-cutting. The channel is 30cm at its thickest, is at least 4 m wide and overlies Facies 3 with a scoured concave-up contact. It is in turn succeeded by an erosion surface and Facies 1.

E. **Facies 5:** Thin (< 5mm thick), laterally discontinuous patches of mudrock are volumetrically insignificant relative to other facies present but contain a significant palaeoenvironmental indicator in the form of desiccation cracks. These (Plate 2h) are preserved as sandstone filled casts with orthogonal, triple junction and angular crack

intersections evident. The crack fill is a homogenous coarse-grained sandstone. Crack depths are less than 5cm. This facies may contain horizontal traces, preserved as grooves and ridges on the upper bedding surface. Mudrock present as granule to small pebble sized oxidized flakes in cross-bedded sandstone was probably derived from the scour of such horizontally bedded, discontinuous fine-grained horizons. The only other occurrence of mudrock is as small scale vertical burrow fills.

#### 2.4.3. Facies interpretations

Horizontally laminated and thinly plane-bedded sandstone with low angle discordance are reported from modern foreshore sediment as "1-15 cm thick beds of evenly laminated sand with low angle discordance" (Reineck and Singh, 1980, p. 301.). Plane-bed lamination is reported from washover fans where it is associated with antidunes and small mudfilled depressions as well as from backshore sediment. Antidunes are absent but small discontinuous beds of mud sized sediment are present. These horizontally laminated and plane-bedded sandstones contain abundant trace fossils.

Structureless units of well sorted clean quartz sand are associated with washover fans as aeolian sediment (Kochel and Dolan, 1986). Horizontal lamination and bedding is reported from aeolian sediment (Dott *et al.*, 1986; Kocurek, 1981; Kocurek and Dott, 1981; Nielson and Kocurek, 1986) but the "single most definitive megascopic criterion of aeolian deposition is the adhesion structure where sand is blown across and adheres to a wet subaerial surface" (Dott *et al.*, 1986, p. 348) is absent from this outcrop. Other diagnostic aeolian palaeoenvironmental criteria such as climbing translant stratification and coarse-grained ripples are absent.

Plane-bedded washover fan sediment is known to evolve distally into low-angle cross-stratified sediment associated with scours: this may account for the origin of Facies 2. The association of trace fossils with these plane-bedded sandstones indicates that not all sediment was deposited on the foreshore: some sedimentation on a washover fan is

indicated. This premise is supported by the occurrence of sand casts of mudcracks in Facies 5. Fine-grained sediment may be deposited in subtidal or supratidal in nearshore settings: its association here with desiccation cracks whose morphology are in accord with described characteristics of subaerial desiccation cracks (as described by Plummer and Gostin, 1981) indicates supratidal deposition of mud-sized sediment.

Evidence for tidal deposition is apparent in Facies 3 palaeocurrent data. The polymodal distribution of palaeocurrent data (Fig. 2.1) indicates tidal reversal. Bedforms that reverse completely during a single tidal cycle are called dunes (Terwindt and Brouwer, 1986) and migration of these bedforms produces high angle cross-stratification. The cross-stratification of sandstone in this facies lacks spring-neap foreset variations reported in subtidal sandstone (Visser, 1980; Terwindt and Brouwer, 1986; Kreisa and Moila, 1986). Cross-bedded sandstone is reported in association with plane-beds in low tidal terraces (Reineck and Singh, 1980) as well as ridge and runnel systems or nearshore bars in the non-barred nearshore.

The origin of channelised massive sandstone with mudchip conglomerate is enigmatic given its rare occurrence and poor exposure. Channelization is documented in tidal, washover and nearshore sandstones (Reineck and Singh, 1980). Mudchip conglomerate clasts indicate scour and erosion of this mudrock facies elsewhere. Combined with the massive nature of the channel fill, rapid deposition is indicated. An origin associated with storm surges or washover events is possible.

Sediment with lithological characteristics similar to those described above is reported from the base of the Peninsula Formation (Hobday and Tankard, 1978, Facies 1) and interpreted as washover fan sedimentation by these authors. Other plane-laminated and bedded sediment (their Facies 3) are interpreted as beach foreshore environments. These environments are here inferred to be extant in the Graafwater Formation at this locality.

## 2.5 SANDSTONE PETROLOGY

Faroo member sandstones are well sorted, rounded medium to coarse-grained quartzarenites that commonly show bimodal size distributions in thin section. (For definitions of rounding and sorting and the arenite classification scheme used please refer to Part 1 of this thesis and to Appendix 2). They are pervasively cemented with syntaxial quartz overgrowths. Porosity remnant after quartz cementation is occluded by 50-100 um booklets of kaolinite sufficiently coarse grained enough to be visible in thin section. Such coarse-grained kaolinite is characteristically precipitated from low pH, meteoric water (Hurst and Urwin, 1982). Coastal nearshore marine sandbodies are known to be good fresh water aquifers. Thus kaolinite morphology is a poor palaeoenvironmental discriminator in nearshore marine/ coastal alluvial plain settings.

In specimens with a bimodal grain size distribution a difference in the degree of rounding of different grain sizes is observed: coarse to very coarse-grained framework grains show improved rounding relative to grains in the finer mode. Detrital clay, where present, occurs as oxidized matrix that has been deformed by compaction. Pores containing detrital clay lack quartz overgrowths and kaolinite cementation.

Extreme rounding is reported from both marine and aeolian sandstones (Ekdale and Picard, 1985; Dott et al., 1986; Mazzullo et al., 1986). Aeolian processes can accomplish rounding more rapidly and preferentially sort spherical grains very rapidly (Mazzullo et al., 1986). Bimodal size distributions with a more angular finer fraction and a coarser, more rounded fraction are reported from aeolian sandstone (Ekdale and Picard, 1985).

Improved rounding may result with closed circuit sediment circulation in shallow marine, tidal settings (Rust, 1977). Such mechanisms have been inferred by previous workers. Modern transitional depositional environments such as the backshore and shoreface may

contain aeolian deposits (Reineck and Singh, 1980). It is thus difficult to assess the relative effect of aeolian and or shallow marine processes on such grains given that framework surface characteristics (upturned cleavage plates, triangular pits, frosting) which are commonly used to discriminate between grains shaped by these processes are comprehensively masked by cementation.

Relative lack of finer grained sediment in early Palaeozoic nearshore, shallow marine sandstones (relative to more modern shelf and nearshore settings) is a consequence of enhanced deflation and erosion of clay sized sediment from non-marine sediment (Fischer, 1985), due to lack of vegetative cover.

## 2.6 ICHNOLOGY

To date eight ichnogenera are documented in the Graafwater Formation (above) of which systematic descriptions are available for only two, the arthropod track *Petalichnus*, and the burrow *Metaichna* Anderson (1975). Systematic descriptions are provided here for four previously documented ichnogenera and five new forms. These ichnogenera are all found in the Faroo Member at the locality given.

### 2.6.1. Classification

Trace fossils are classified by one or more of three proposed schemes (Hallam, 1975; Basan *et al.*, 1978; Mason, 1985). The simplest is a descriptive/morphological approach, where shape, size and change in branching angle are used to determine new species and genera. Other schemes emphasize that trace fossils are sedimentary structures (the toponomic, stratonomic approach of Seilacher, 1964 and Martinsson, 1970) produced at sediment/sediment and sediment/fluid interfaces. The most recent approach is an ethological approach whose premise is that trace fossil morphology reflects a behavioural response (walking, grazing, burrowing, resting and feeding) that produced it (Seilacher, 1978). A useful summary is presented in Basan *et al.* (1975, Table 2).

The latter classification is not attempted here. No body fossils have been documented in the Graafwater Formation. Thus the ecological behavior and aetiology of these specimens is unknown. Comparison could be by established precedent (Hantzschel, 1975) only, knowing that one species can produce several trace fossils and that a single ichnogenera can be produced by many dissimilar fauna.

A simple descriptive approach is adopted here, combined with the schemes of Seilacher (1964) and Martinsson (1970). These two authors use different terminology that is synonymous. Where given below, that of the latter is in parenthesis.

Trace fossils exposed and preserved at the upper sediment (bed, casting medium) contact are called epichnia (epireliefs). Epichnia are further subdivided into grooves and ridges (concave and convex epireliefs). Trace fossils located within the casting medium, i.e. within the bed, are named endichnia (full reliefs) and are not in contact with the upper surface. Traces at the sole of the bed are named hypichnia (hyporeliefs) and can be classified on the basis of positive or negative relief into ridges and grooves respectively. One further class exists: exichnia, where the trace is outside the casting medium and not in direct contact with it.

Once described in terms of the classification scheme above (Seilacher, 1964; Martinsson, 1970) these traces were classified by comparison to examples given and illustrated in Seilacher (1970); Hantzschel (1975); Crimes et al. (1977); Crimes and Harper (1977); Basan et al. (1978) and Hakes (1985).

#### 2.6.2. Previous ichnogenera documented

The Graafwater Formation contains a diverse suite of trace fossils: the ichnogenera *Skolithos*, *Cruziana*, *Helminthoidea*, *Platysolenites* and *Scolicia* are reported in Tankard et al. (1982) and the additional genera *Petalichnus*, *Arthrophyucus* and *Metaichna* are reported from the Loop Member (Rust, 1977).

Trace fossils in the early Palaeozoic are confined to marine and nearshore marine palaeoenvironments (Miller, 1984; Dott, *et al.*, 1986). Workers studying Palaeozoic sandstones elsewhere (Dott *et al.*, 1986) have adopted a convention of accepting the presence of trace fossils as evidence for marine deposition.

Two new ichnogenera have been located within the Graafwater Formation in the Cape Peninsula: an incomplete example of *Diplichnites* Dawson, 1873 (an arthropod walking trace) has been identified from the quarry at Simonstown and *Isopodichnus* Boremann and *Rusophycus* Hall from the outcrop near the naval battery at Simonstown.

The latter sample was identified by and is in the possession of Dr. Hannes Theron (Geological Survey, P.O. Box 572, Bellville, 7530, South Africa). *Isopodichnus* is considered a *Scoyenia* (non-marine, redbed) index trace fossil in post-Palaeozoic sediment (Hakes, 1985). In early Palaeozoic sediment, it may be a smaller form of *Cruziana* or *Rusophycus* (Hakes, 1985). These samples mostly have widths less than 5-6 mm, the lower size limit for *Rusophycus* (Crimes, 1970; Hakes, 1985). The range of widths transcends this boundary, thus both species are inferred to be present.

The presence of these traces is significant in that arthropod tracks previously documented (Anderson, 1975) are inferred *not* to be trilobite traces but those of *Malacostraca* instead (Rust, 1977). *Rusophycus*, *Diplichnites*, and *Isopodichnus* (if it is taken as a dwarf *Rusophycus* as in *Isopodichnus* *eutendorfensis* and *Rusophycus* *eutendorfensis*) are trilobite traces in Cambrian and Ordovician sediment (Crimes, 1970). These traces are thus the earliest traces documented in the South African lower Palaeozoic. Other trilobite traces (*Cruziana* and *Diplichnites*) have been documented previously in the Peninsula Formation (Potgieter and Oelofsen, 1983; Cocks and Fortey, 1986; Hunter, 1987).

### 2.6.3. Systematic ichnology.

**Trace A: Plate 2(f)**

Description: Simple, vertical to subvertical, unbranched unornamented cylindrical burrows. These burrows are filled with medium to coarse sand which is the same grain size as the surrounding sediment. The width of these burrows varies from 13-25mm ( $n=26$ , mean ( $x^*$ ) = 16,9mm, standard deviation ( $s$ ) = 3,0mm) and their length ranges from 35-174mm ( $n=26$ ,  $x^*=102,3$ mm,  $s=41,0$ mm). Some tubes may be clay lined. The tops of this trace are commonly truncated by the succeeding bed. A rare downward deflection of adjacent sedimentary lamination is observed. The trace is preserved as full reliefs (truncated hypichnia). These traces occur gregariously with lateral extent of several metres and are common in the outcrop studied.

Classification: Ichnogenus *Skolithos* Haldemann, 1840, ichnospecies *Skolithos* sp.

**Trace B: Plate 2(e)**

Description: These are simple, small, unbranched vertical tubes, 0,45-3,5mm in diameter ( $n=30$ ,  $x^*=2,2$ mm,  $s=0,7$ mm), 15,7-69,7mm long ( $n=30$ ,  $x^*=30,8$ ,  $s=14,1$ ). This trace is usually upright and straight, curved to slightly sinuous and subhorizontal forms are rare. Each trace is solitary. The traces crowd both laminated and massive sandstone and may be found in association with *Skolithos*. The trace is filled with darker, finer matrix than the surrounding sediment, which may be oxidized clay. These traces are common throughout the outcrop and are preserved as full reliefs (exichnia) which compare well with specimens illustrated in Basan et al. (1978, p.162, Fig. 128).

Classification: Ichnogenus *Trichichnus* Frey, 1970. Ichnospecies *Trichichnus linearis*. This ichnospecies has not previously been documented in the Graafwater Formation.

**Trace C: Plate 2(g)**

Description: This trace is a simple U-shaped tube, which is slightly asymmetrical, without spreite (internal ornamentation). The sediment filling in the trace is of the same grain size as the surrounding sediment but is slightly paler in colour. Tube diameter varies from 15 to 19mm, the trace is 45mm high. It is preserved as a full relief (endichnia). A solitary specimen was located at this outcrop.

Classification: Ichnogenus *Arenicolites* Salter, 1857. Ichnospecies *Arenicolites* sp. (unnamed). This is a newly documented trace.

#### Trace D: Unfigured.

Description: A solitary funnel shaped, horizontal tube that deflects and passes upward into a vertical funnel was located at this outcrop. The funnel diameter is > 50mm with slightly raised rims and steep sides. The sediment within the trace is a bioturbated medium to coarse sand with abundant red clay chips. The specimen is preserved as a full relief (endichnia). This trace may have some relationship with circular burrows (below) exposed on bedding planes.

Classification: Problematic. This specimen may be classified in the ichnogenus *Monocraterion* Torrel, 1870, but lacks downward deflection of surrounding matrix laminae associated with M. Torrel. This ichnospecies has not been previously documented.

#### Trace E. Plate 2(b)

Description: Circular to elliptical trace fossils, preserved on upper bedding surfaces as unfilled epichnial grooves or as casts of these grooves (sand filled convex hyporeliefs). The sandstone casts are slightly lighter in colour compared to the surrounding sediment but of comparable grain size (medium to coarse sand). This trace may occur as isolated or grouped circular to elliptical depressions on bedding surfaces. The maximum diameter measured was 140mm. Specimens with diameters of > 50mm are distributed sparsely throughout the outcrop.

Classification: Arthropod burrow. Similar burrows were described by Rust (1967) as "trilobite" burrows. Anderson (1975) classified the same as being produced by *Malacostraca* rather than *Trilobitina* (Rust, 1977).

**Trace F. Plate 2(c)**

Description: These traces are sets of isolated, slightly curved to straight grooves that are repeated once laterally and may be separated by a faint median groove. Smaller parallel pairs are rarely developed in a direction transverse to the parallel pair. A maximum of two additional pairs is developed in two specimens. Most grooves on this bedding plane occur as individual unpaired depressions, paired depressions and rarer multiple paired depressions. This trace is preserved as concave epireliefs (epichnial grooves) in silt to fine sand. The individual grooves range in length from 10 to 34mm (n=20,  $\bar{x}=20,0$  , s=6,2). This trace is confined to one bedding plane exposure.

Classification: Problematical. These depressions are strongly reminiscent of arthropod swimming-grazing traces (*Monomorphichnus*) or arthropod resting traces. This trace lacks the median slit like depressions of *Arthropodichnus*, the repetition of multiple pairs of parallel or near parallel grooves of *Allcotichnus*, and the repeated pairs of *Tasmandadia*. If the track is incompletely exposed (as illustrated by Hantzschel, 1975 p. W13, Fig. 5) it may be a poorly preserved *Monomorphichnus* Crimes, 1970 or *Allocotichnus* Osgood, 1970. These examples are closer to *Allocotichnus* as illustrated and described in Hantzschel (1975) so this specimen is referred to as being of this ichnogenus. This type of trace has not been previously reported in the Graafwater Formation. Its significance, in conjunction with *Isopodichnus* and *Rusophycus* found elsewhere in the Graafwater Formation, is that these traces are those of trilobites and shows that Class of Arthropoda was extant in this basin during sedimentation.

**Trace G: Not figured**

Description: These traces are simple unbranched to sparsely branched,

unornamented, unlined, cylindrical straight burrows, parallel to bedding with constant diameter ranging from 10 to 15mm in different individuals. The trace length ranges from 50 to 400mm. Traces are preserved as casts of concave epireliefs (epichnial grooves). The casting sediment is the same grain size as the surrounding sediment but is much paler in colour.

Classification: *Planolites* Nicholson, 1873. Not previously reported.

**Trace H: Not figured**

Description: Irregularly meandering to curved unornamented sandstone filled traces are preserved as convex epireliefs (epichnial ridges). The fill is the same grain size (medium to coarse-grained sandstone) and colour (5R 8/2) as the surrounding sediment. Widths of this trace range from 8-22mm ( $n=22$ ,  $x^*=15,6$ ,  $s=3,2$ ). It is found in association with *Planolites* (above). Lengths range up to 10cm.

Classification: Problematical. This trace lacks the longitudinal tubes and internal ornamentation of *Rhizocorallium*, relative straightness of *Planolites*, the narrow median groove of *Didymalichnus*, the median ribbon like crest of *Olivellites* and the median ribbon or striated axis of *Scolicia*. Previous authors (Tankard et al., 1982) have reported "Scolicia type tracks". These traces may be poorly preserved examples.

**Trace I: Plate 2(d)**

Description: Irregularly meandering sandstone filled horizontal trails with a coarse, curved backfill ornamentation, 10-15mm wide. These traces are preserved as full reliefs in medium to coarse-grained sandstone. They occur in association with *Planolites* and ?*Scolicia* on a single bedding plane.

Classification: Problematical. These samples lack the marginal longitudinal tubes of *Rhizocorallium* Type B, the transverse

ornamentation precludes classification as either *Planolites* or *?Scolicia*.

## 2.7. Palaeoenvironmental indicators: Discussion.

Of the palaeoenvironmental indicators present in the Faroo Member at this locality the most diagnostic indicator is the presence of trace fossils. Trace fossils in Ordovician and Cambrian (i.e. early Palaeozoic) sediment occur *exclusively* in marine or nearshore marine sediment (Miller, 1984; Dott *et al.*, 1986).

Polymodal foreset azimuth data are useful indicators in that tidal reversal may be inferred, interpretations consistent with previous work in the lithologically similar Loop and Faroo Members (Rust, 1977). Sandstone petrology, while showing that sediment is texturally and mineralogically mature, cannot discriminate between aeolian and nearshore marine environments.

Sandstone facies are consistent with deposition as washover fans or in the backshore (inferred from the abundant preservation of trace fossils). However the low angle truncation of plane-bedded sandstone is characteristic of deposition on the foreshore and thus this depositional setting cannot be precluded.

Sedimentation conditions appear to have been slow discontinuous deposition alternating with rapid deposition. Bioturbation is a characteristic commonly developed in nearshore sediment from the base of the Cambrian upwards (Howard, 1978 in Basan *et al.*, 1978; Fischer, 1985). Where deposition is continuous, or discontinuous but slow, complete bioturbation is expected. Where deposition is rapid and continuous no bioturbation results. Repeated wave reworking of foreshore sediment is not conducive to the preservation of biogenic traces (Howard, 1978), nor are shifting substrate subaqueous deposits (Seilacher, 1978). Bioturbation is sporadically developed within the outcrop suggesting slow discontinuous deposition alternating with rapid deposition.

Such conditions of sedimentation exist during washover fan deposition in the backshore. The backshore is that portion of beaches normally subaerially exposed and flooded only at the highest water (Reineck and Singh, 1980). Casts of desiccation cracks support such a premise.

## 2.8 CONCLUSIONS

Lithofacies assemblage, palaeocurrent azimuth data and the presence of trace fossils indicate a nearshore marine palaeoenvironmental setting for the Faroo Member at the locality examined. Sandstones may have been deposited in foreshore, backshore and/or washover-fan environments. Such depositional settings are reported from the Peninsula Formation.

The existence of a single facies inferred as nearshore marine should not be taken as indicating that such palaeoenvironmental interpretations are applicable to these two formations (Graafwater and Peninsula) as a whole, precluding other palaeoenvironments. This approach has been followed by previous workers. The distribution of trace fossils (presence or absence) in relation to lithofacies and palaeocurrent data variation are needed before cogent palaeoenvironmental models can be presented.

## REFERENCES

- Anderson, A.M. (1975). The "trilobite" trackways in the Table Mountain Group (Ordovician) of South Africa. Palaeont. Afr., 18, 35-46.
- Basan, P.B. Chamberlain, C.K., Frey, R.W., Howard, J.D. Seilacher, A. and Warne, J.E. (1978). Trace Fossil Concepts. SEPM Short Course Nr. 5, Oklahoma City.
- Cocks, L.R.M. and Fortey, R.A. (1986). New evidence on the South African lower Palaeozoic. Geol. Mag., 123, 437-444.

Crimes, T.P. (1970). The significance of trace fossils in sedimentology, stratigraphy and palaeoecology with examples from lower Palaeozoic strata. In: Crimes, T.P. and Harper, J.C. Eds., Trace Fossils. Seal House Press, Liverpool, 101-126.

Crimes, T.P. and Harper, J.C. (1977). Eds., Trace Fossils 2. Geol. Jour. Spec. Issue Nr. 9, Liverpool, Seal House Press, p.91-138.

Crimes, T.P., Legg, I.C. Marcos, A. and Arboleya, M. (1977). ?Late Precambrian, - low lower Cambrian trace fossils from Spain. In: Crimes, T.P. and Harper, J.C. Eds., Trace Fossils 2. Geol. Jour. Spec. Issue Nr. 9, Liverpool, Seal House Press, p.91-138.

Dott, R.H., Byers, C.W., Fielder, G.W., Stenzel, S.R. and Winfree, K.E. (1986). Aeolian to marine transition in Cambro-Ordovician cratonic sheet sandstones of the northern Mississippi valley, U.S.A. Sedimentology, 33, 345-367.

Ekdale, A.A. and Picard, M.D. (1985). Trace fossils in a Jurassic Eolianite, Entrada sandstone, Utah, U.S.A. In: Curran, H.A. Ed., Biogenic structures: their use in interpreting depositional environments. S.E.P.M., Spec., Pub, 35, 3-13.

Fischer, A.G. (1985). Biological innovations and the Sedimentary Record. In: Holland, H.D. and Trendall, A.F. Eds., Patterns of Change in Earth Evolution. Springer-Verlag, Berlin, 145-157.

Gray, J., Theron, J.N. and Boucot, A.J. (1986). Age of the Cedarberg Formation, South Africa and early land plant evolution. Geol. Mag., 123, 445-454.

Hakes, W.G. (1985). Brackish marine trace fossils. In: Curran, H.A. Ed., Biogenic structures: their use in interpreting depositional environments. S.E.P.M., Spec. Publ., 35, 21-35.

- Hallam, A. (1975). Preservation of trace fossils. In: Frey, R.W. Ed., The study of trace fossils. Springer-Verlag, Berlin, 55-63.
- Hantzschel, W. (1975). Trace fossils and Problematica. In: Teichert, C. Ed., Treatise on Invertebrate Paleontology, Part W. Supplement 1. Geol. Soc. Am. and Univ. of Kansas, 269p.
- Hobday, D.K. and Tankard, A.J. (1978). Transgressive-barrier and shallow shelf interpretation of the lower Paleozoic Peninsula Formation, South Africa. Geol. Soc. Am. Bull., 89, 1733-1744.
- Howard, J.D. (1978). Sedimentology and trace fossils. In: Trace Fossil Concepts. SEPM Short Course Nr. 5, Oklahoma City, 11-42.
- Hunter, C. (1987). Ancient tracks on Table Mountain. Sagittarius, 2/4, 2-3.
- Hurst, A. and Urwin, H., (1982). Geological modelling of clay diagenesis in sandstones. Clay Minerals, 17, 5-22.
- Kochel, R.C. and Dolan, R. (1986). The role of overwash on a Mid-Atlantic coast barrier island. J. Geol., 94, 902-906.
- Kocurek, G. and Dott, R.H. (1981). Distinctions and uses of stratification types in the interpretation of aeolian sand. J. sedim. Petrol., 51, 579-595.
- Kocurek, G. (1981). Significance of interdune deposits and bounding surfaces in aeolian dune sands. Sedimentology, 28, 753-780.
- Kreisa, R.D. and Moila, R.J. (1986). Sigmoidal tidal bundles and other tide generated sedimentary structures of the Curtis Formation, Utah. Geol. Soc. Am. Bull., 97, 381-387.
- Martinsson, A. (1970). Toponymy of trace fossils. In: Crimes, T.P. and Harper, J.C. Eds., Trace Fossils. Geol. Jour. Spec. Issue, 3, 0. 323-

330.

Mason, T.R. (1985). Trace fossils: records of ancient life. S. Afr. J. of Sci., 81, 441-445.

Mazzullo, J., Sims, D. and Cunningham, D. (1986). The effects of aeolian sorting and abrasion upon the shapes of fine quartz sand grains. J. sedim. Petrol., 56, 45-56.

Miller, M.F. (1984). Distribution of biogenic structures in Palaeozoic nonmarine and marine-margin sequences: an actualistic model. J. Palaeont., 58, 550-570.

Nielson, J. and Kocurek, G. (1986). Climbing zibars of the Algodones. Sedim. Geol., 48, 1-15

Plummer, P.S. and Gostin, V.A. (1981). Shrinkage cracks: desiccation or syneresis ? J. sedim. Petrol., 51, 1147-1156.

Potgieter, C.D. and Oelofsen, B.W. (1983). Cruziana Acacensis - The first Silurian index trace fossil from South Africa. Trans. Geol. Soc. S. Afr., 86, 51-54.

Reineck, H.-E. and Singh, I.B. (1980). Depositional sedimentary environments. With reference to terrigenous clastics. 2nd edn. Springer-Verlag, Berlin, 549 pp.

Rust, I.C. (1967). On the sedimentation of the Table Mountain Group. D.Sc. thesis, Univ. Stellenbosch, 110 pp.

Rust, I.C. (1977). Evidence of shallow marine and tidal sedimentation in the Ordovician Graafwater Formation, Cape Province, South Africa. Sedim. Geol., 18, 123-133.

Seilacher, A. (1964). Sedimentological classification and nomenclature of trace fossils. Sedimentology, 3, 253-256.

3. **FACIES DEFINITION, ANALYSIS AND INTERPRETATION OF  
PIEKENIERSKLOOF FORMATION CONGLOMERATES AND SANDSTONES:  
PROCESSES AND IMPLICATIONS FOR PRE-DEVONIAN BRAID PLAIN  
SEDIMENTOLOGY**

## 3.1

**ABSTRACT**

Coarse- to very coarse-grained sandstones, pebbly sandstones and conglomerates of the early Palaeozoic (early Ordovician) Piekenierskloof Formation are well exposed at the coast at Elands Bay and Lambert's Bay and inland at Piekenierskloof Pass, the type area. Five conglomerate and five sandstone facies are defined at these localities.

Of these, two, a coarse, massive, matrix-supported, disorganized, rarely inversely graded conglomerate and a horizontally-bedded coarse-grained sandstone with small cobble-sized clasts are interpreted to have been deposited by processes other than that associated with normal, dilute stream flow. Conglomerates lack the size grading characteristics and imbrication associated with hyperconcentrated flows. Such conglomerate shows the textural characteristics of traction carpet, high density, turbidity currents. This gravel facies is interpreted as a high sediment/fluid ratio high stage deposit. Clast supported, normally graded conglomerates are interpreted to have been deposited from high concentration sediment dispersion as these flows waned. Cross-bedded conglomerates and thin pebble lags represent lower stage reworking of these high stage deposits. Horizontally-bedded coarse-grained sandstones are interpreted as the product of hyperconcentrated flows. These flows are preserved only in the most distal locality examined, Piekenierskloof. Other sandstone facies are those associated with dilute turbulent stream flow, albeit lacking

grain size characteristics on foresets indicative of sandflow cross-strata. This may be a consequence of rapid aggradation. The thickness of some planar cross-stratified sandstones indicates some deep channelisation was present.

The occurrence of these facies, when coupled with other established palaeoenvironmental indicators (unidirectional palaeocurrent data with low variance, fining upward cycles, scour and channelization, marked lateral and vertical facies changes) provide convincing evidence for a fluvial palaeoenvironmental interpretation for this formation.

The palaeodepositional environment is envisaged as having been a rapidly aggrading, bedload dominated, proximal alluvial braid plain that prograded down a SE directed palaeoslope. The preservation of depositional units whose sedimentology is interpreted to indicate mobilisation of large volumes of sediment is taken to mean rapid aggradation. Previous interpretations have inferred moderate slopes and moderate to high runoff. The depositional environment is characterized by 1) the absence of suspended load sedimentation, 2) rare flow of high density sediment dispersions and 3) dominance of bedload sedimentation and reworking of high stage deposits. Channelization is not evident on outcrop scale and the sandstones are apparently sheet bedded.

Recent developments in the methodology of fluvial sedimentology (the development of "architectural elements" and the identification of very large scale bedforms (macroforms) in fluvial flows) cannot be applied with great success at the localities selected due to unsuitable outcrop orientation: facies interpretations of dilute stream flow facies, especially planar and trough cross-bedded sand may be in serious error. Facies interpretations of coarse-grained matrix-supported conglomerates are debatable.

### 3.2 INTRODUCTION

The Piekenierskloof Formation is one of a number of pre-Devonian

formations in the South African rock record whose depositional environment has been interpreted in terms of alluvial, braid-plain sedimentology (Vos and Tankard, 1981). Modern analogues of fluvial systems in vegetation free environments have no actualistic equivalent in pre-Devonian fluvial sedimentation (Fuller, 1985). Previous interpretations of the sedimentology of this formation are therefore suspect, especially where these were made in terms of a fixed number of fluvial end member models, such as that of Miall (1978).

The sedimentology of this formation is re-examined in terms of recent advances in fluvial sedimentology. Not only has the interpretation of fluvial facies in terms of depositional hydrodynamics been advanced (Jackson, 1975; Crowley, 1981, 1983; Lowe, 1982) but the methodology of study (Allen, 1983; Miall, 1985) has changed to adopt more actualistic models. These developments have resulted in the abandonment of the previous spectrum of fixed end member models (Miall, 1985).

Three localities (Elands Bay, Lambert's Bay and Piekenierskloof Pass, the type area) were chosen to examine the Piekenierskloof Formation (Fig. 3.1). At these localities the presence of considerable conglomerate provides some lithological contrast in what is normally an arenaceous succession and abets meaningful environmental interpretation. At Elands Bay and Lambert's Bay on the South Atlantic coast the sequence is well exposed in numerous small inlets, providing good three dimensional exposure. Exposures at the coast dip gently to the E and ENE with dip of  $< 15^{\circ}$ . Outcrop is locally faulted, jointed and gently folded but deformation is less intense and relatively minor relative to exposure inland.

At Piekenierskloof Pass, this formation is well exposed in recently constructed road cuttings. Here the outcrop occurs on an eastward facing monocline (Söhnge, 1983, Fig. 1) and outcrop lacks quality locally due to faulting, intense jointing, thrusting and brecciation.

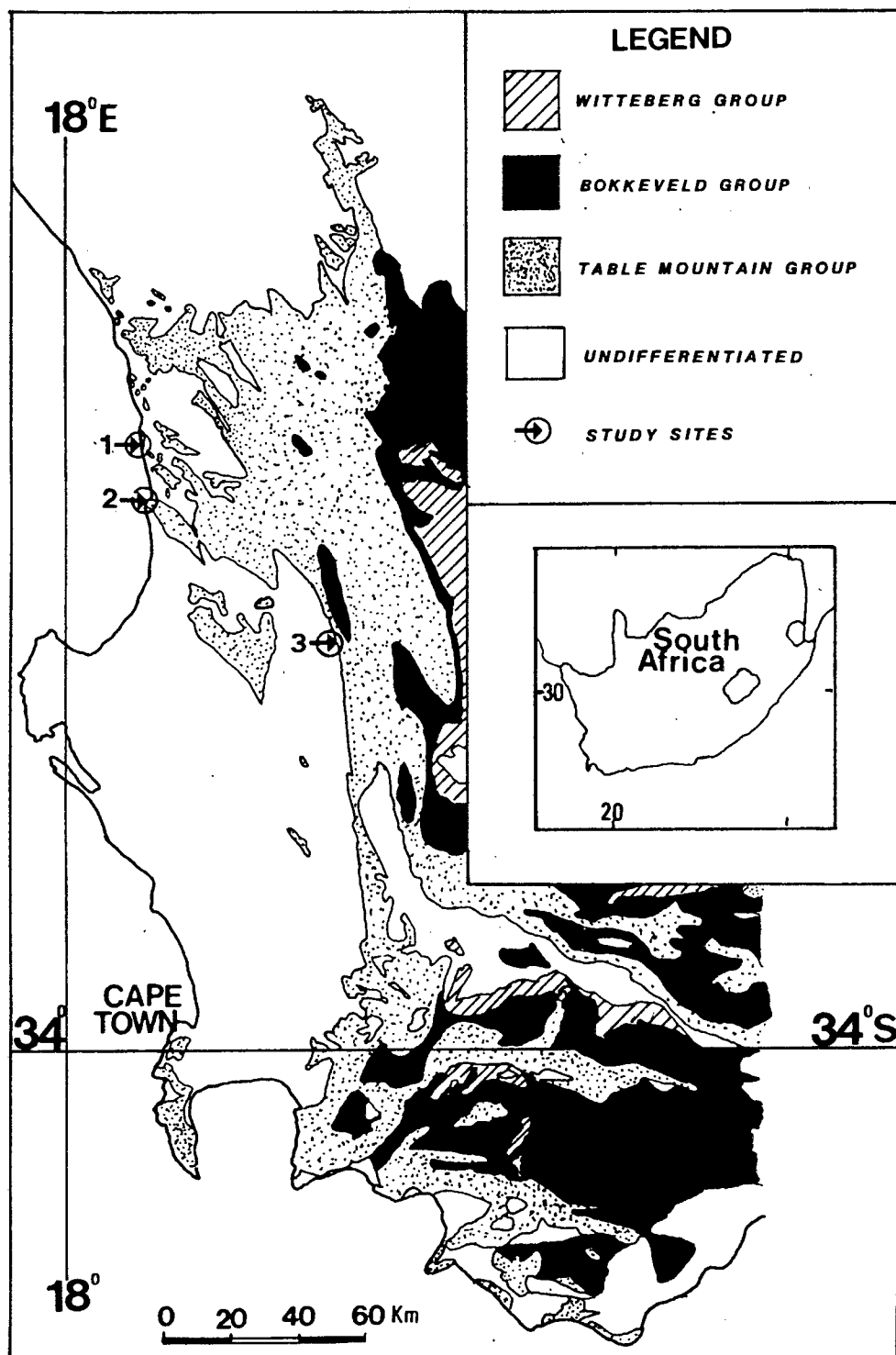


Figure 3.1. Piekenierskloof Formation study sites. Sites 1 & 2 are Lambert's Bay and Elands Bay respectively. Site 3 is Piekenierskloof Pass.

### 3.3 STRATIGRAPHIC SETTING

The Piekenierskloof Formation is the lowermost formation of the Table Mountain Group (Table 1). At Elands Bay the Piekenierskloof Formation overlies the Klipheuwel Formation with a conformable, but locally erosive contact. Here and at other locations to the immediate south and east (at Klein Tafelberg and Redlinghuys, Vos and Tankard (1981), Fig. 1, p. 172) the lower portion of this succession has been interpreted as the more proximal part of a prograding alluvial braidplain - fan delta succession (Vos and Tankard, 1981). At Lambert's Bay neither the base nor the top of this formation is exposed. The stratigraphic position of conglomerates at this location is thus unclear. Conglomerates occur throughout the succession at Piekenierskloof and at the top of the sequence at Aurora (Rust, 1967). Conglomerates occur sporadically throughout this formation and are difficult if not impossible to correlate from outcrop to outcrop. Certainly basin-wide allocyclic events (megasequence scale) have thus far not been recognised: published models (which have recognised a single coarsening then fining upward progression) seem to be applicable only to localized outcrop, such as documented by Vos and Tankard (1981).

Throughout the S.W. Cape this formation is succeeded by the thin bedded, rippled and sporadically burrowed arenaceous Graafwater Formation. The contact between these two formations is conformable and gradational (Rust, 1967).

### 3.4 NEW APPROACH TO FLUVIAL SEDIMENTOLOGY: A SUMMATION

A new method of facies interpretation involving the identification of a hierarchical classification of bedforms (Jackson, 1975; Crowley, 1981, 1983) has been initiated. Microforms, mesoforms and macroforms are the three classes of bedforms in this hierarchy. Microforms are small scale sedimentary structures such as current lineation and small ripple marks (Miall, 1985) generated by turbulence at the

sediment/fluid interface. Mesoforms are produced by varying the intensity of fluid flow and include larger scale flow regime bedforms (dunes, transverse, longitudinal and diagonal 'bars') and are generated by high flow (flood) events. Macroforms are the largest bed configurations, having dimensions commensurate with the size of the turbulent boundary layer (Crowley, 1981, 1983) and reflect the effect of many flood (high stage) events on the scale of tens to thousands of years. These include fluvial features such as compound bars, sand flats and point bars.

Recognition of this hierarchy prompted the development of a new approach to the analysis of fluvial sediment: eight basic architectural elements were defined (Miall, 1985, Table 2). These definitions are based on flow characteristics (microform, mesoform etc), geometry, shape (upper and lower contacts) and scale. Miall identified the following architectural elements: channels, gravel bedforms, sandy bedforms, foreset macroforms, lateral accretion surfaces, sediment gravity flows, laminated sand and sheet overbank fines. Of importance is that each of these architectural elements contains one or a number of lithofacies (as defined in Miall, 1978). Crowley (1981) first demonstrated that foreset macroforms, which are a single bed configuration, consist of upward coarsening Sr-Sp-St lithofacies which are interpreted in terms of a single formational process. Previous interpretations would have interpreted each of these lithofacies separately. Satisfactory differentiation of the architectural elements necessitates good three-dimensional outcrop, with greater than tens of metres in width and height. Such outcrop is not always available, let alone accessible, which reduces the efficacy of this technique.

Further important advances have been made concerning the identification of sediment flows with clast dispersions considerably greater than that of dilute stream flow (Lowe, 1982; Smith, 1986, 1987). The recognition of these flows is based on textural grain size and grain size variation variations (grading) as well as the presence (or absence) of imbrication.

The methodology of study here was to identify facies at the specified localities, based on sedimentary structures, grain size and grain size variations and to assign a facies code to the appropriate observation. The facies codes of Miall (1978), Smith (1987) and Decelles *et al.* (1987) were found to be the most appropriate. These facies/ groups of facies were assigned to an architectural element, if possible. Vertical profiles were prepared on the basis on facies identification. Lithofacies and architectural elements were then interpreted in terms of precedent established for deposits (Long, 1978; Miall, 1978, 1985; Allen, 1983; Eriksson, 1984; Turner, 1984; Smith, 1986, 1987).

### 3.5 FACIES DEFINITIONS

#### 3.5.1. Conglomerates

##### A. Clast type and conglomerate classification

Conglomerates are classified by means of matrix content and clast type (Pettijohn, 1975). Matrix is taken to mean fine grained matrix (grain size less than fine sand (Pettijohn, 1975, p.180). Its use here differs from Pettijohn in that matrix may include grain sizes up to granule conglomerate. The qualifiers "coarse-matrix or coarse-grained matrix" and "fine-matrix" have been applied here in such circumstances. These conglomerates are not paraconglomerates as defined by Pettijohn because fine-matrix is lacking. These conglomerates are orthoconglomerates. The clasts are entirely extraformational at Lambert's Bay and Elands Bay, while a minor intraformational clast type (reworked mudrock, and fine grained sandstone) is present at Piekenierskloof Pass. These conglomerates contain clasts that are mostly quartzose in mineralogy (quartzite, chert and vein quartz are the dominant clast types, Table 11). Some clasts show evidence of foliation and contain quartz veins: the derivation of these clasts may be from a quartzose, low grade metamorphic terrain. Jaspers, hornfelses and acid volcanics constitute a minor proportion of the clasts examined (Table 11).

Oligomictic orthoconglomerates are defined as having > 90% durable quartzose component (Pettijohn, 1975): this classification is most appropriate to Piekenierskloof Formation conglomerates (Table 11). These conglomerates are best classified as oligomictic, sparsely petromict orthoconglomerates. Size analysis of the coarsest clast size of selected conglomerate beds at Lambert's Bay (Table 12) indicates that the mean of the largest 30 clasts, measured 1-5m either side of the line of section, is in the -7 phi size fraction. Clasts coarser than 256mm (-8 phi) are rare. Beds of conglomerate of this clast size were not encountered during examination of these three localities in this study. However conglomerate beds with clasts in that size range have been reported (Vos and Tankard, 1981).

B: Inversely graded to ungraded matrix-supported, disorganized conglomerates

Facies code: Gm(d)

These conglomerates rarely show coarse-tail inverse grading in the pebble to cobble size range. Pebbles and cobbles float in a matrix of (and defined here as) polymodal sediment with grain size ranging from medium sand to granule conglomerate (Plate 3e). These conglomerates have abrupt, non-erosive planar bases. Upper surfaces are commonly irregular with relief on the order of a few cm. Bed thickness is usually in the order of less than one metre. Some beds show a rare transition from matrix to clast support, without matrix in the upper few 10's of cm. Beds with well developed inverse coarse-tail grading are rarely interbedded with thin beds of indistinctly laminated to thickly bedded medium- to coarse-grained sand. Most beds are unstratified, show little to no grain size variation in the coarse tail or matrix and contain no identifiable sedimentary structure (Plate 3e). An A axis parallel, A axis imbrication ( A[p]A[i] ) is rarely observed on favourably orientated outcrop.

C: Clast supported, normally graded to ungraded conglomerate

Facies code: Gm

This facies comprises massive, unstratified, clast supported pebble to cobble conglomerates. These conglomerates are commonly ungraded. Few beds show normal grading (Plate 3b). The interstices between the clasts are rarely void. If filled, the sediment is of the calibre of medium to coarse sand. Bed thickness rarely exceeds 1m. These conglomerates have either planar or concave up erosive bases. Upper surfaces can be irregular or show gradation upwards into low angle cross-bedded coarse sand to granule conglomerate. No obvious imbrication was observed in these conglomerates although Vos and Tankard (1981) report an A[p]A[i] imbrication (p.180, Fig. 7) from conglomerates at Elands Bay.

D: Gravel lag

Facies code: G1

Thin, laterally extensive, pebble to cobble conglomerates are 2-3 pebble diameters thick (Plate 3 g&h). These sheet-like conglomerates are usually clast-supported, with sand filling in the interstices between clasts. No obvious imbrication is visible. These conglomerates are erosively based and are overlain by sandy Sp, St facies. Rare transitions are observed into Gi facies (below)

E: Low-angle cross-stratified conglomerate (and pebbly sandstone)

Facies code: Gi

Low-angle (5-20°) cross-stratified clast and matrix-supported conglomerate (Plate 3 c&d) is commonly interbedded with pebbly very coarse sand to granule conglomerate. These conglomerates are erosively based with a planar to concave upward lower bounding surface. Azimuth

directions of the foresets are at an angle ( $10 - 30^{\circ}$ ) to the azimuths of local trough axes. Imbrication, where present, is of the A[t]B[i] variety. Where foresets are interbedded with coarse sand a coarse-tail (conglomerate grain size) normal grading is present with an inverse grading in the sand sized fraction. These conglomerates may grade down set from Gp facies (definition below). Bed thickness varies from 0.5 to 1m. Sedimentation units are solitary and can be seen to act as nuclei for successive finer grained (sand sized) sedimentation units.

F: Planar cross-stratified conglomerate (and pebbly sandstone)

Facies code: Gp

High angle ( $> 20^{\circ}$ ) planar cross-stratified pebble to cobble conglomerates (Plate 3 a&f) may be entirely clast supported or interbedded with coarse sand (Plate 3f). Further, these conglomerates may grade down set into Sp facies (described below) or into Gi facies. Sedimentation units are solitary and are erosively based with planar or lenticular geometry.

### 3.5.2 Sandstones

A: Planar cross-bedded sandstones

Facies code: Sp

Planar cross-bedded, pebbly, medium- to very coarse-grained sandstone (Plate 4 a,b, c&f) occurs in sets of up to 2m thick. Sets thicker than 1m tend to be solitary. Foresets in this facies may intersect the lower bounding surface tangentially or at a higher acute angle. Foreset inclination ranges from  $10 - 20^{\circ}$ . Grain size variations are absent down or across foresets. Solitary sets usually extend for the length of the outcrop and are 10's of metres wide. Some sets are planar tabular with parallelism in upper and lower bounding surface. Most sets are wedge shaped. Small scale ( $< 30\text{cm}$ ) sets may show downclimbing relationships relative to the underlying set. Coarsening

upward relationships within sets or upwards through several sets or other sandstone facies are very rare: only one set at the outcrop at Lambert's Bay showed this relationship.

B: Trough cross-bedded sandstone (and pebbly granule conglomerate)

Facies code: St-Gt

Trough cross-bedded sandstones (Plate 4 d&e) occur in small to medium sets up to 50cm thick. Set widths vary from < 1m to several m. (Plate 4 d&e). Grain sizes range from medium sand to very coarse sand and granule conglomerate. These sandstones commonly contain sporadic pebbles and small cobbles. Coset thicknesses may exceed several metres. The set lower bounding surface is scoop shaped and erosive. Sets are eroded by the succeeding set. Coset boundaries are planar with relief in the order of a few centimeters and are marked by a thin layer of extraformational conglomerate a few pebble diameters thick. Grain size in successive sets may rarely fine upwards. Set thickness and grain size do not diminish allowing the development of ripple cross-bedded sandstones. This may be a consequence of the coarse calibre of sand.

C: Low-angle cross-stratified medium- to coarse-grained sandstone, may be pebbly

Facies code: S1

Low-angle ( $< 10^{\circ}$ ) cross-bedded medium- to coarse-grained sandstones (Plate 3h) occur in sets up to 50cm thick. Lowermost sets may rest on a thin pebble lag. Sets at Piekenierskloof Pass can be seen to fill-in shallow channels and scours up to 0.75 m deep and up to 30-40 m wide. Paucity of extensive outcrop as well as stream-wise orientation of outcrop prevents these relationships being observed at Elands and Lambert's Bay, although this facies is present at these two localities. Coarser grained sets may contain sporadic clasts up to small cobble (70mm) size.

## D: Horizontally plane bedded sandstone

Facies code: Sh(b)

Sheet-like horizontally-bedded coarse- to very coarse-grained sandstone commonly contain sporadic pebbles up to cobble grade (Figure 3.3). These sandstones are thinly bedded, with indistinct contacts between beds that have limited lateral extent. These sandstones are coloured purple and contain dispersed iron oxide heavy minerals. This facies was located only at Piekenierskloof Pass.

## E: Horizontally laminated sandstone

Facies code: Sh(a)

Fine to medium grained, well sorted, laminated sandstone occurs (Plate 4g) very rarely at all three localities. At the coast it occurs as rare solitary sheet-like beds 20-50cm thick. At Piekenierskloof Pass it occurs as thin sheets, that may fine upwards, that fill wide (> 10m) scours (channels?). One such bed at Piekenierskloof contains heavy minerals (zircon, tourmaline, rutile and iron oxides) and has been assayed at 0.1 g/t Au. At Piekenierskloof Pass these sandstones are coloured a deep purple as opposed to other sandstones and conglomerates, which are coloured orange-brown).

## F: Mudrock

Facies code: M

Sediment finer than medium sand is very rare in the Piekenierskloof Formation. At both Lambert's Bay and Elands bay this facies is absent. At Piekenierskloof this facies is present as intraformational conglomerate within coarse clastics as well as thin drapes at the tops of minor channel fills. Where present, this facies is massive with no apparent internal structure. A summary of facies definitions is presented as Table 14.

### 3.6 FACIES INTERPRETATIONS

#### 3.6.1. Conglomerates

##### A: Gm(d) and Gm facies

These conglomerates are assigned the Gm(d) (conglomerate, massive, disorganized) facies code as defined by Decelles *et al.* (1987). This facies code differs from the Gms code (conglomerate, matrix-supported, may be massive) in that the Gms code "matrix" is a clay to fine sand (rarely coarser) in which the conglomerate clasts are dispersed while in the Gm(d) facies code the "matrix" is poorly sorted medium sand to granule conglomerate. Where referred to hereafter these two matrix types will be called "coarse-matrix or coarse-grained matrix" (for matrix in the Gm(d) facies code) and fine-matrix (for matrix in the Gms facies code).

Conglomerates with massive, fine-matrix supported texture are usually interpreted as the product of cohesive debris flows (Miall, 1978, 1985; Decelles *et al.*, 1987; Allen, 1981; Smith, 1986). In these deposits the clasts are supported in the matrix by the cohesive strength and density of the matrix in a debris flow whose mechanical behavior approximates a Bingham plastic (Lowe, 1982). Turbulence and grain dispersive pressure are supporting mechanisms in the non-cohesive debris flow type. Cohesive debris flows are characteristically deposited on alluvial fans, where sediment of varying calibre (mud to boulder conglomerate) is transported in such flows on moderate to steep slopes.

These coarse-grained matrix-supported conglomerates were first reported from the Piekenierskloof Formation in Rust (1967) who called them "conglomerates with disrupted framework" and concluded that "this texture results from very rapid deposition with no further reworking". No mention is made of this facies in Vos and Tankard (1981) or Tankard *et al.* (1982). Similar deposits are reported in the rock record from the Archean, (Buck and Minter, 1985), where interpreted as rapidly

deposited pebbly bedload, the Palaeozoic (Allen, 1981), where interpreted as a non-cohesive debris flow and the Neogene (Smith, 1987), where interpreted as form of non-cohesive debris flow, the "hyperconcentrated flow".

In the argument developed hereafter it is the intention of the author to show that 1) these conglomerates possess grain size and textural characteristics of non-cohesive debris flow and 2) that these conglomerates are related to other conglomerate facies by changes of sediment/fluid ratio.

Conglomerates showing transition from coarse-matrix support to clast are rare in the succession and are very similar to Type 'B' conglomerates as defined by Allen (1981). These inversely graded and ungraded coarse-matrix supported conglomerates were inferred by that author to have been deposited from a high concentration dispersion rather than by viscous flow.

The conglomerates lack imbrication characteristics of hyperconcentrated flow, as defined by Smith (1986). The combination of A-axis transverse to flow direction, imbricated in the pebble and small cobble size fraction, and A-axis parallel to flow and imbricated in the size fraction greater than small cobble, is absent in these conglomerates. Other characteristics of hyperconcentrated flow (Table 15) such as clast support are absent. However, these Piekenierskloof Formation conglomerates are similar to hyperconcentrated flow deposits in that the matrix is coarse grained, polymodal and poorly sorted. Imbrication is very weakly developed, and where visible, shows the A axis parallel to flow and imbricated. Imbrication itself is not diagnostic: A axis parallel to flow orientations are reported from both cohesive debris flows and hyperconcentrated flows (Smith, 1986).

Hyperconcentrated flow was first defined by Smith (1986) as sediment mass flows whose transport and deposition mechanisms were intermediate between cohesive debris flows and dilute, turbulent stream flow. These sediment mass flows are characteristic of regions where

vast volumes of sediment and fluid (water) are rapidly mobilized. Hyperconcentrated flows are not sediment gravity flows. These deposits were first recognised in volcanoclastic sediment deposited by the 1980 Mount. St. Helens eruption (Smith, 1987).

Some of these coarse-grained matrix-supported conglomerates show development of thin, interbedded, coarse grained, indistinctly, laminated sand (Fig. 3.2) which grades upward into Gm(d) conglomerate. This upward coarsening strongly resembles the traction carpet deposits reported by Lowe, (1982, Fig. 6a), deposited from sandy and gravelly high density turbidity currents. These deposits are characterised by sediment deposition in three stages: an initial traction sedimentation



---

Figure 3.2. Coarse-grained matrix-supported conglomerate at Lambert's Bay. Gm(d) facies. Note interbedded laminated and thinly bedded sand . These conglomerates are inferred to have been deposited by processes similar to those for traction carpet deposits as described by Lowe (1982). Lens cap (centre) diameter 45mm for scale.

---

stage is followed by a traction carpet stage which is succeeded by a suspension sedimentation stage as the flow collapses and becomes more dilute.

In the first stage, sand is deposited from a slightly unsteady turbulent flow and shows flat lamination: as flow unsteadiness increases, suspended load is progressively concentrated on the bed and transport in the bed load layer is dominated by grain collisions leading to the formation of a basal particle layer maintained by dispersive pressure. Deposition is terminated when flow collapses due to continual sediment fallout (Lowe, 1982). This mechanism, and the formation of new carpets at the rising bed surface (Lowe, 1982) is thus inferred for rare cycles of coarse sand interbedded with coarse matrix-supported conglomerates. Such surging is characteristic of many sediment flows.

Rapid sedimentation from both suspension and traction are characteristic of hyperconcentrated flow (Smith, 1986) and non-cohesive debris flow (Lowe, 1982). Sediment transport mechanisms are inferred to have been fluid turbulence, buoyancy and grain dispersive pressure. Thus these processes are inferred to have been operative in Piekenierskloof Gm(d) facies conglomerates.

Thus to summarize these coarse-grained matrix-supported pebble and small cobble conglomerates are inferred to have been deposited from non-cohesive debris flows, akin to hyperconcentrated flows. These deposits, where ungraded or show poorly developed inverse grading, and lack interbedded sand may be more similar to density modified grain flows, which are a non-cohesive sediment flow where clasts are supported by dispersive pressure. A spectrum of transportation mechanisms is thus inferred: dispersive pressure, buoyancy and turbulence are the supporting mechanisms and it is difficult to determine the relative importance of each of these processes.

Conglomerates with 2-5% by volume clay content in the matrix may have behaved as cohesive debris flows (Rust and Jones, 1987). This

possibility may be discounted for coarse-grained matrix-supported conglomerates at Lambert's Bay and Elands Bay given the paucity of mudrock within the succession as a whole in the conglomeratic parts of the succession in particular. Throughout the Table Mountain Group, where mudrock is present within arenites (or coarser grain sizes) as intraformational mud chips and as infiltrated clay, it has been diagenetically reddened and is very obvious in thin section as well as at outcrop. Such features are absent at the localities selected.

These coarse-matrix sediment flows can evolve down flow into pebble and cobble clast supported, relatively matrix poor conglomerates (Lowe, 1982, Fig. 12). Clast supported, normally graded pebble and cobble conglomerate (Facies Gm) may represent a distal evolution of coarse-grained matrix-supported pebble to cobble conglomerates. Cohesive debris flows can evolve into inversely graded traction carpets down flow. Further, traction carpets evolve into high density turbidity currents and normally graded gravelly and sandy turbidity currents down flow (Lowe, 1982). Various conglomerate facies can represent different sediment/fluid mixtures (Decelles *et al.*, 1987). These two conglomerate facies are inferred to be part of a depositional spectrum of sediment gravity, and turbulent flows that are intimately related to sediment /fluid ratio.

On pre-Devonian braid plains, without vegetation or stiff mud to aid channelization by stabilizing channel banks, channels are inferred to have been very wide. Channel width to depth ratios of 100-1000:1 have been inferred (Fuller, 1985). High stage events are here thus thought to have mobilized much sediment and produced deposits reminiscent of hyperconcentrated flow, non-cohesive debris flow and density modified grain flows. Cross-stratified conglomerates are inferred to have been deposited within channels at high stage, albeit at lower sediment/fluid ratios than Gm(d) facies conglomerates. These deposits are assigned to the architectural element SG (sediment gravity flows) as defined by Miall (1985). This architectural element is characteristic of alluvial fans and the most proximal part of alluvial braid-plains where both slope and discharge can be relatively high.

B: G1, Gi and Gp facies (cross-stratified conglomerates)

These conglomerate lithofacies define a range of mesoforms characteristic of architectural element GB.

G1 facies is a conglomerate containing pebbles to small cobbles in layers up to 2-3 clasts thick and is reminiscent of "thin diffuse gravel sheets" (Miall, 1985). These thin conglomerate sheets are inferred to move only during high discharge and accrete upwards and down stream to form "longitudinal bars". G1 facies can also be interpreted as thin conglomerate lag, associated with fluvial scour, defining channel bases formed during high discharge events in shallow braided channels.

Bars accreting into deeper areas (scour pools, channels) develop lee side separation eddies and foreset stratification may result. Such conglomerates in this study are solitary, clast supported pebble to cobble conglomerates.

Planar cross-bedded conglomerates are interpreted as having been deposited in the lee of bar cores as dilute, stream flows waned. Some clast supported conglomerates are interbedded with medium to thickly cross-stratified pebbly very coarse-grained sandstone and granule conglomerate. Their foresets have a sharp base and coarsen upwards from coarse-grained, pebbly, sand to pebble and cobble conglomerate. Such stratification may develop during turbulent, dilute high stage flow where gravel sheets are swept over, and deposited in the lee of bar cores (Miall, 1985). Low-angle cross-stratified conglomerate (Gi facies) occurs as solitary, large scale gravelly bedforms as much as 1m thick. Foresets are interbedded with thin to medium cross-bedded, pebbly, coarse- to very coarse-grained sand. Clast supported foresets commonly contain < 0.5mm sand filling in the interstices between the clasts. Such sand is undersized relative to the coarser fraction (Walker, 1975, Fig. 7-3). These sand size void fills are interpreted as lower stage sieve deposits.

Sand size detritus coarsens upwards into > 1000 $\mu$  sand, granule conglomerate and pebble conglomerate. Such conglomerates may armour the bedform foresets from erosion during lower stage flow. Gi facies are interpreted as accretion deposits of conglomerate bedforms. Some may be lateral accretion surfaces. Foreset orientation in these cases is at a high angle to sandy foresets in underlying or overlying trough cross-stratified sands. Conglomerates may have aggraded in shallower part of braid plain channels: conglomerates are interbedded with some very thick planar cross-bedding (Plate 3d) which is normally deposited in deeper channels (Turner, 1977, 1984; Rust and Jones, 1987)

### 3.6.2 Sandstones

#### A: St facies (Trough cross-bedded sandstone)

Trough cross-bedded sandstones (Gt-St facies) are interpreted as minor channel fills and lower flow-regime dunes (Miall, 1985). This facies, with underlying conglomerate lag and basal erosion suggests a fluvial channel origin, characterized by basal scour, bedload deposition and dune migration. Trough cross-bedded sandstone is commonly reported (Turner, 1977, 1984; Eriksson, 1984; Buck and Minter, 1985; Miall, 1985) in the rock record in braided fluvial deposits.

Trough cross-bedding overlying planar cross-bedding are facies associated with macroform migration (Crowley, 1981, 1983). Trough cross-bedding does not occur in this association at the localities examined.

Shallow foreset inclinations, tangential bottomsets and the superimposition of trough scours are all characteristic of deposition from small subaqueous dunes at low aggradation rates (Buck and Minter, 1985). Trough cross-bedded sands have been observed to form with the migration of dunes across the deeper portion of braided stream channels if the bedload is dominantly sand (Miall, 1985).

Trough cross-bedded sandstones are one of a number of lithofacies

defining architectural element SB (sandy bedforms) as defined by Miall (1985). At these localities this facies is further inferred to be part of architectural element CH (channels).

B: Sp facies (Planar cross-bedded sandstones)

Planar cross-bedded sandstones may have planar tabular or wedge-shaped geometry. Foreset intersections with the lower bounding set surface may be tangential or sharp. Where tangential, high velocity flow separation is indicated (Minter, 1986). Planar, sharp foresets lack grain size characteristics (down foreset coarsening, across foreset coarsening) associated with sand flow avalanching (as defined by Hunter, 1985; Buck, 1985): foreset accretion may be continuous and include some suspension fallout.

This type of cross-stratification (straight tabular foresets, discordant basal contact) is associated with slipface advance, at near the angle of repose along the lee face of bars at high current velocities within the deeper part of channel systems (Turner, 1977; Rust and Jones, 1987).

Planar cross-stratification was considered to result from the migration of "transverse bars" (Smith, 1972), lingoid dune fields (Miall, 1978) and "simple bars" (Allen, 1983) in bedload dominant braided alluvial streams. This type of cross-stratification is further associated with macroform slipface advance (Crowley, 1981, 1983). Not all planar cross-stratification may be associated with macroform slipface advance (Miall, 1985 p. 279). On macroforms this facies occurs as part of a characteristic upward coarsening from ripple cross-stratified sand at the base of the macroform to planar cross-stratified sand and finally trough cross-stratified sand. These transitions are absent at the localities examined. Thus planar cross-stratified sandstone is assigned to the architectural element SB (sandy bedforms) rather than element FM (foreset macroforms).

These bedforms are the result of sediment movement in normal, dilute turbulent stream flow (Leeder, 1982; Smith, 1986, 1987).

C: S1 facies (Low angle cross-stratified sandstone)

Low angle cross-stratified sandstones are interpreted as scour fills, crevasse splays and antidunes (Miall, 1978, 1985). This facies may also represent low amplitude, small scale bedforms or channel bar accretion surfaces.

---



---

Figure 3.3. Coarse-grained, horizontally-bedded sandstone, Piekenierskloof Pass. Note indistinct bedding contacts. This facies is interpreted as being the result of deposition from hyperconcentrated flow as described by Smith (1986, 1987).

---

D: Sh(a) and Sh(b) facies (Horizontally-bedded and laminated sandstone)

Horizontally-laminated, medium- to fine-grained sandstones [Sh(a) facies] are formed in the turbulent boundary layer of the upper flow regime (Allen, 1984; Smith, 1987). Distinction between lamination and bedding permits the recognition of Sh(b) facies (Decelles *et al.*, 1987): very coarse-grained, horizontally-bedded sandstone with pebble to cobble sized clasts result from deposition from sandy hyperconcentrated flows (Smith, 1987).

E: Facies M (Mudrock)

This facies is indicative of suspension settling and reduced flow velocity. Mudrock facies occurs at the top of minor channel fills at Piekenierskloof Pass and may indicate lower velocities and progressive abandonment as channels aggraded and filled.

### 3.7 VERTICAL PROFILES

The Piekenierskloof Formation was examined during vertical traverses at the localities given. During the first traverse facies were defined: during the second traverse facies relationships were observed, palaeocurrent indicators measured and vertical profiles erected. The distribution of facies defined and interpreted (above) in this study area are given here and presented diagrammatically (Figs. 3.4 and 3.6).

Palaeocurrent indicators measured were trough axes, foreset bedding and the orientation of minor channels. Trough axes and foreset bedding are Rank 5 palaeocurrent indicators (Miall, 1974) and minor channels are Rank 4. Rank 1, 2 & 3 indicators are river systems, individual rivers and major channels respectively (Miall, 1974). These indicators are rarely if ever used as suitably large outcrop is lacking.

Trough cross-bedding and foreset bedding data were corrected for tectonic dip. Corrected data were processed using a circular normal distribution (Leeder, 1982, p. 129). No weighting factors were applied.

Mean azimuth is calculated by taking cumulative sines and cosines of corrected azimuth data (Table 13). A vectorial mean, vectorial magnitude, consistency ratio, angular deviation (radians) and the square of angular deviation [variance in degrees<sup>2</sup>) were calculated for each locality and at minor outcrop nearby. Of importance in palaeoenvironmental interpretation are the consistency ratio and the variance (Miall, 1974; Long, 1978). The values of variance obtained by combining trough axis and foreset bedding at outcrop scale (Table 13) is well within the published range of variance of palaeoenvironmental indicators of this rank (Miall, 1974 Table 1.). Variance values obtained here are within the range of values (295- 650, Rank 4) obtained from cross-bedding in recent sand bars in braided rivers (Miall, 1974, Table 1) and is less than the range variance obtained from marine palaeocurrent indicators (range 6000-8000, Long, 1978).

Palaeocurrent statistics were subjected to a test for uniformity (a  $\chi^2$  test with 2 degrees of freedom, after Turner, 1977). Palaeocurrent distribution from the examined Piekenierskloof Formation outcrop are unimodal.

Palaeocurrent roses were drawn with data fitted into 30° intervals. Vector mean and number of data readings is given for each rose. Consistency ratios of data obtained from the Piekenierskloof Formation at the given localities and the Klipheuwel Formation below it (at Elands Bay) are usually > 0.70.

Compared to a consistency ratio (0.30) obtained from the Graafwater Formation at Carstensberg Pass (Section 2, this thesis), the consistency ratio is higher and variance lower in Piekenierskloof Formation data sets. Thus consistency ratio may prove to be a powerful environmental discriminator if applied on a basin-wide scale.

### 3.7.1. Elands Bay

A vertical profile (Fig. 3.4) was measured across the contact between Klipheuwel and Piekenierskloof Formations, south of the railway line on the slopes of Bobbejaansberg (Fig. 3.5). Klipheuwel Formation arenites contain fine to coarse-grained trough cross-bedding that fines upwards. Cross-laminated ripples are rarely found at the top of cosets. Gt-St cosets overlie oligomictic pebble - cobble conglomerate lags (G1 facies). Gm facies conglomerates are rare but occur near the contact with the Piekenierskloof Formation. The contact has local relief of up to 3m at this and other (Vos and Tankard, 1981 Fig. 11) localities. Relief on the contact is filled in by Gm and G1 facies conglomerates interbedded with minor Gt-St facies granule conglomerates and sandstones. Conglomerates are oligomictic.

At Elands Bay, conglomerates occur above the contact and define the top of a coarsening upwards megasequence (megasequence used in the sense of Heward, 1978). The succession then fines upwards from the basal conglomerates. Cyclicity of such large scale (> 100's of m, Heward, 1978) is usually the result of tectonic activity and uplift in the source area and such a mechanism has been inferred here (Vos and Tankard, 1981). The coarsening upwards in the Klipheuwel Formation culminates in a scoured (eroded) surface (defining the base of the Piekenierskloof Formation), which is overlain by oligomictic pebble to cobble conglomerate. Such upward coarsening and scour result from fluvial degradation as fluvial activity increases or tectonic activity induces relief at the basin margins (Buck and Minter, 1985). Aggradation of conglomerate may be a response to the initial topography and the subsequent fining upwards the result of denudation of the uplifted source area and retreat of the locus of conglomerate deposition.

The erosional episode that produced the scour surface was followed by a period of rapid initiation of sedimentation and progradation of conglomerate to this site in the depositional basin. Allocyclic mechanisms are not necessary to produce such a sequence of

MEASURED SECTION:  
ELANDS BAY: 32°19'S, 18°20'E

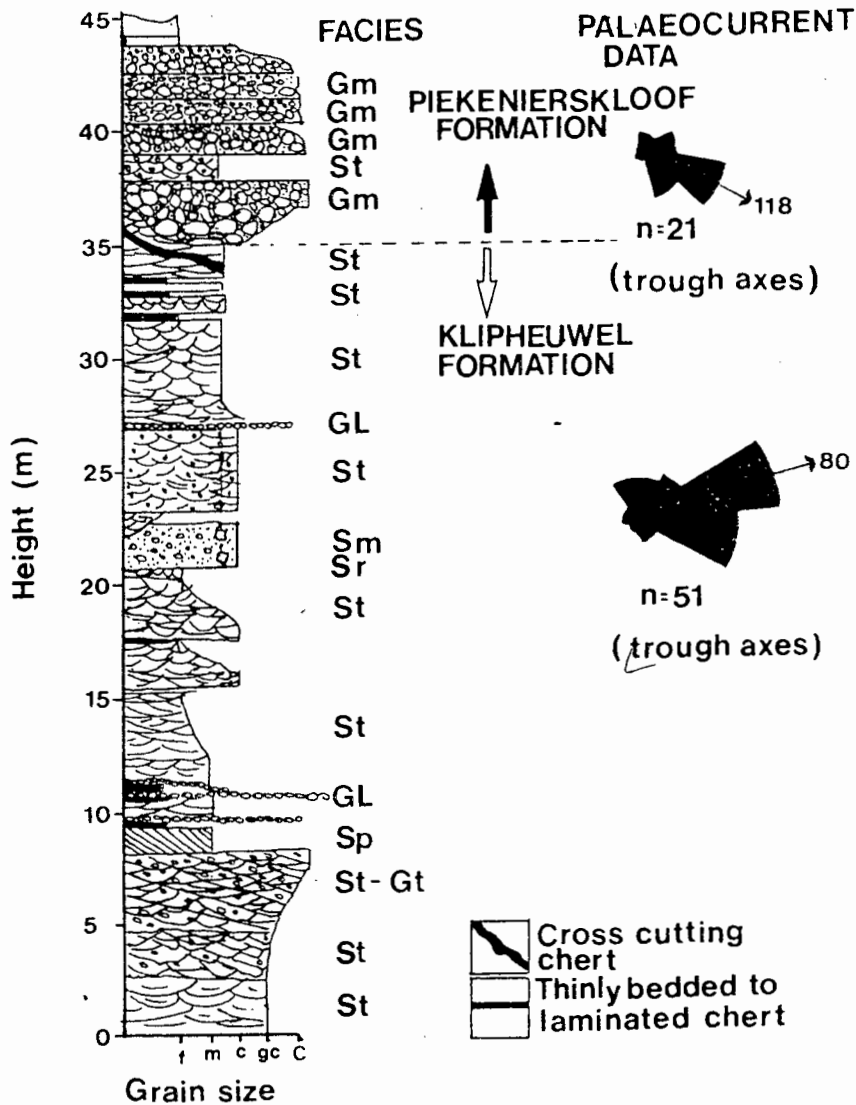


Figure 3.4. A vertical profile measured in the Piekenierskloof Formation at Elands Bay, showing the vertical distribution of facies. This section was measured immediately southwest of the fish factory. Latitude and longitude of section given above. Palaeocurrent data are drawn at 30° intervals, with vector means and number of readings indicated. Palaeocurrent statistics are presented in Table 13.

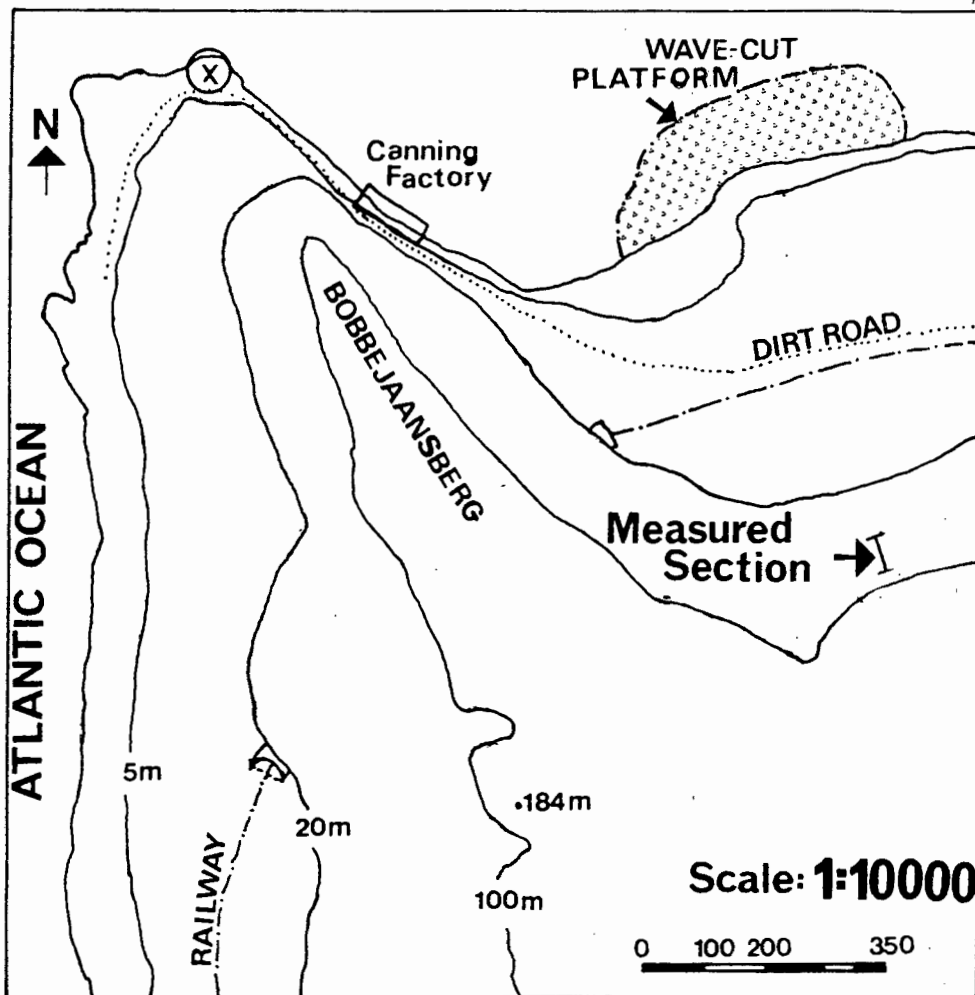


Fig. 3.5. Location of measured section at Elands Bay. Palaeocurrent data for the Klipheuwel Formation measured on the wave cut platform. Palaeocurrent data for the Piekenierskloof Formation measured at X. At both these localities good bedding plane exposures allows easy measurement of the orientation of trough axes.

sedimentation events. On alluvial fans, fan head entrenchment of short to moderate duration may result in the abandonment of portions of the fan surface (and resultant erosion) and the establishment of an active depositional lobe elsewhere (Heward, 1978, Table 4). Later avulsion may re-establish sedimentation at this locus.

Allocyclic processes such as changes of sea level (base level) would have a basin-wide effect on sedimentation style and have a demonstrable effect over large parts (> 200km parallel to depositional strike and 120 km perpendicular to strike) of a particular basin (Grotzinger, 1986). Periodic rejuvenation of relief along fault lines will produce cyclicity in alluvial fan - proximal braid-plain successions (Heward, 1978).

Given that conglomerates occur at different stratigraphic levels in the Piekenierskloof Formation, and are not correlatable, autocyclic processes such as avulsion or feeder channel capture appear to provide a parsimonious interpretation of available data. Avulsion on alluvial braid plains can be very rapid: the Kosi River on the Himalayan Foreland has shifted 113 km to the west in 228 years in episodic jumps of up to 19 km/yr (Wells and Dorr, 1987). Shifts of locus of sedimentation are episodic, cross watersheds and occur as channels aggrade and are unable to contain sediment flux. Avulsion appears in this case to have no correlation with tectonic events. Klipheuwel Formation palaeocurrent indicators have a vector mean of  $080^{\circ}$  True which differs slightly from Piekenierskloof Formation directional indicators (vector mean  $118^{\circ}$  True). Consistency ratios and variance for these two formations (Table 13) are low and comparable. This may be a consequence of deposition on different deposition lobes.

### 3.7.2. Lambert's Bay

A vertical profile (Fig. 3.6) was measured immediately south of the town (Fig. 3.7). Facies developed here are Gm(d), Gm, Gl, Gt-St, Gp-Sp, Sh(a) and Sl. The vector mean of palaeocurrent indicators is  $132^{\circ}$  (True). Outcrops of sandstone south of this exposure on the coast yielded similar results ( $130^{\circ}$  True, Loc. 5, Table 13.). Thus sediment is inferred to have been transported down a SE-directed palaeoslope. Palaeocurrent indicators at this locality show increased variance and a lower consistency ratio relative to data generated from other Piekenierskloof Formation outcrop: this may be a consequence of the

MEASURED SECTION:  
 LAMBERTS BAY: 32°05'S, 18°18'E

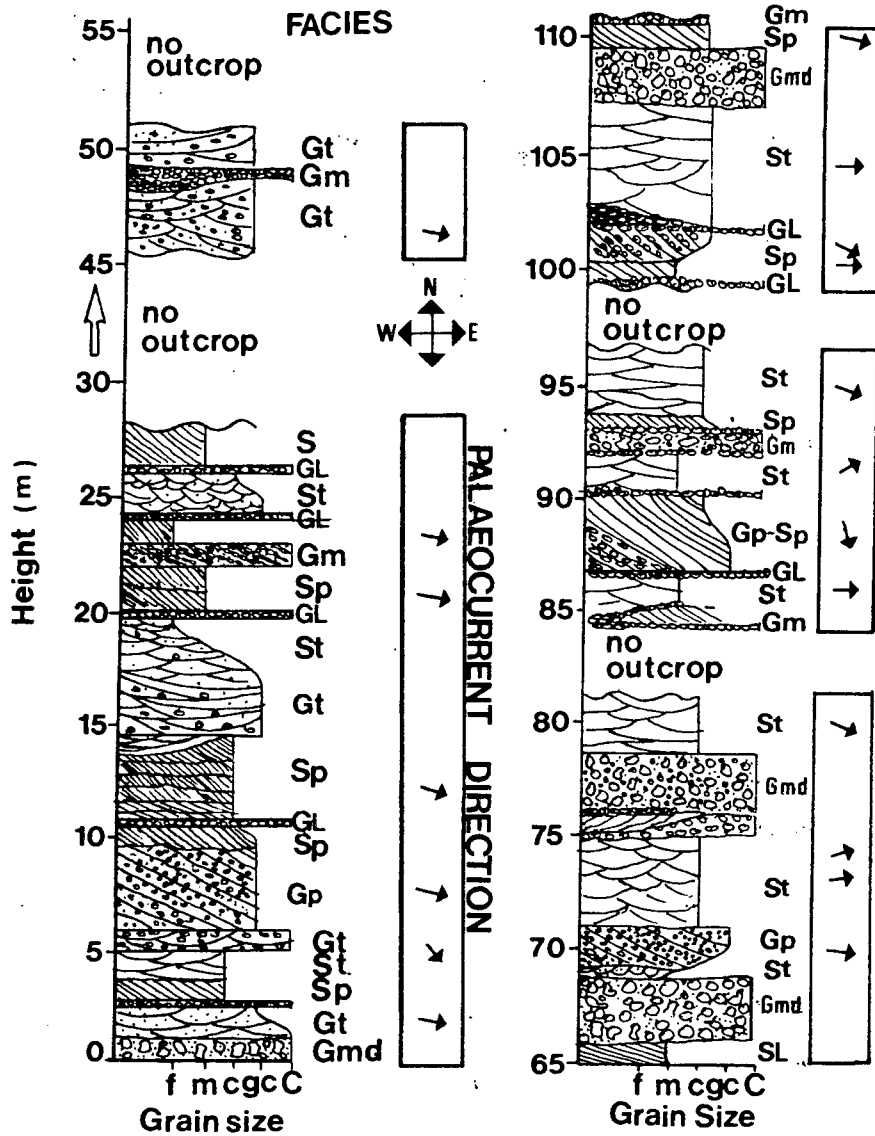


Figure 3.6. Vertical profile measured in the Piekenierskloof Formation at Lambert's Bay, immediately south of the town. Section shows vertical variation of facies. Facies codes are given in the text. Palaeocurrent variations with increasing height in the section are indicated.

MEASURED SECTION:  
LAMBERT'S BAY: CONTINUED

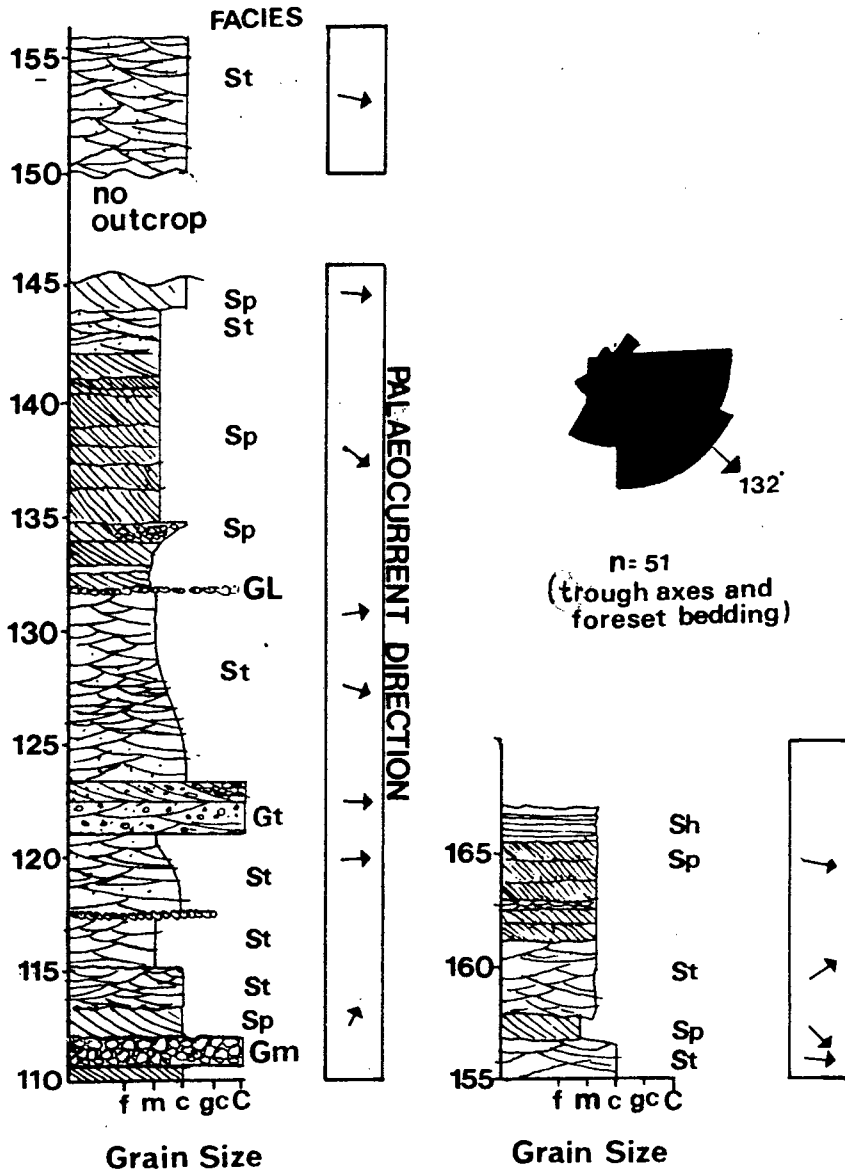


Figure 3.6. (cont.) Vertical profile measured at Lambert's Bay. Facies codes, definitions and interpretations are given in the text.

Palaeocurrent rose is for combined data measured within the section.

Vector mean and number of readings given. Palaeocurrent statistics are given in Table 13.

greater thickness of section measured, the greater number of readings taken, the inclusion of planar cross-bedding foreset directions as well as the inclusion of data from several, stacked channel systems.

No scour surface underlies the conglomeratic succession here and palaeocurrent directions are similar (Table 13, Locations 3&5). Directions obtained are similar to those illustrated in Rust

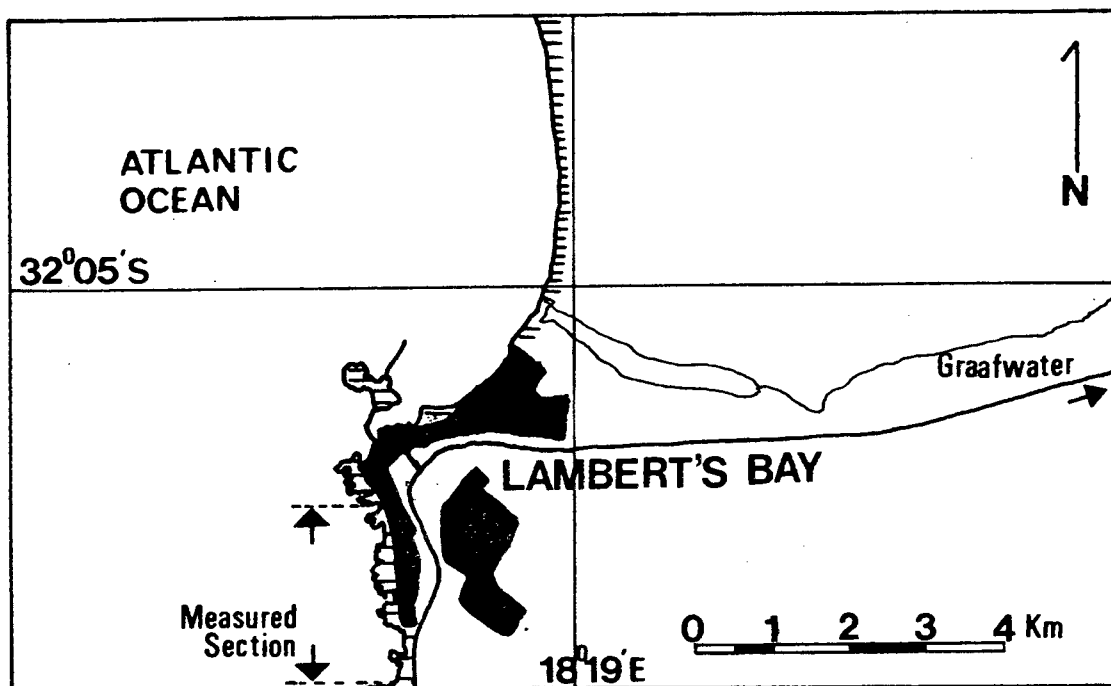


Figure 3.7. Lambert's Bay: vertical profile location

(1967). However, palaeocurrent indicators to the west of the coastal outcrop (Location 4, Table 13 immediately to the west of the Sishen-Saldahna railway line, west of Lambert's Bay, Fig. 3.8) show a marked difference. The direction of the vector mean is  $227^{\circ}$  True (coastal

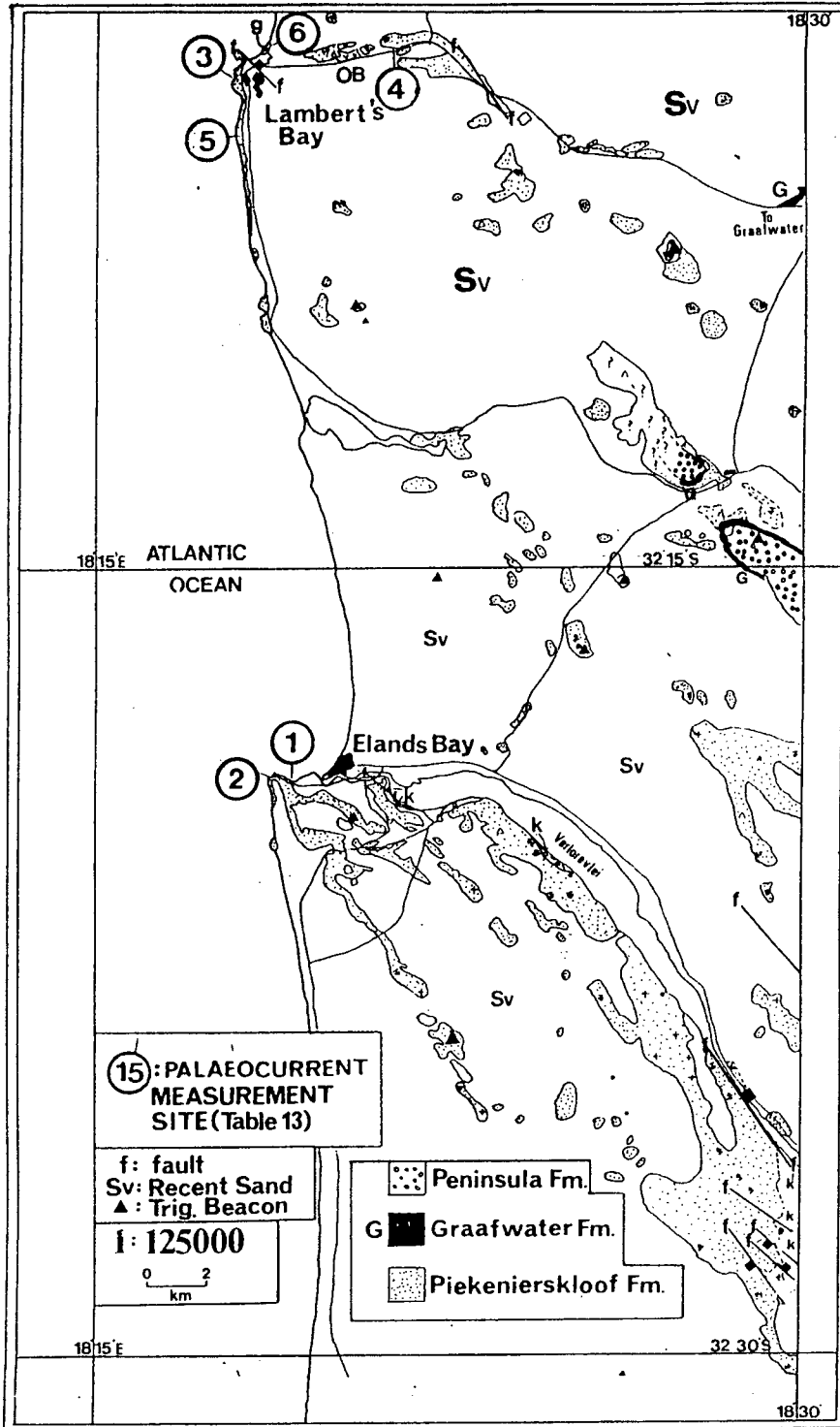


Figure 3.8. Location of palaeocurrent measurement sites (Table 13) and general geology along the Atlantic seaboard. Abbreviations: Sv = Recent sand, f = fault, K = Klipheuwel Formation outcrop.

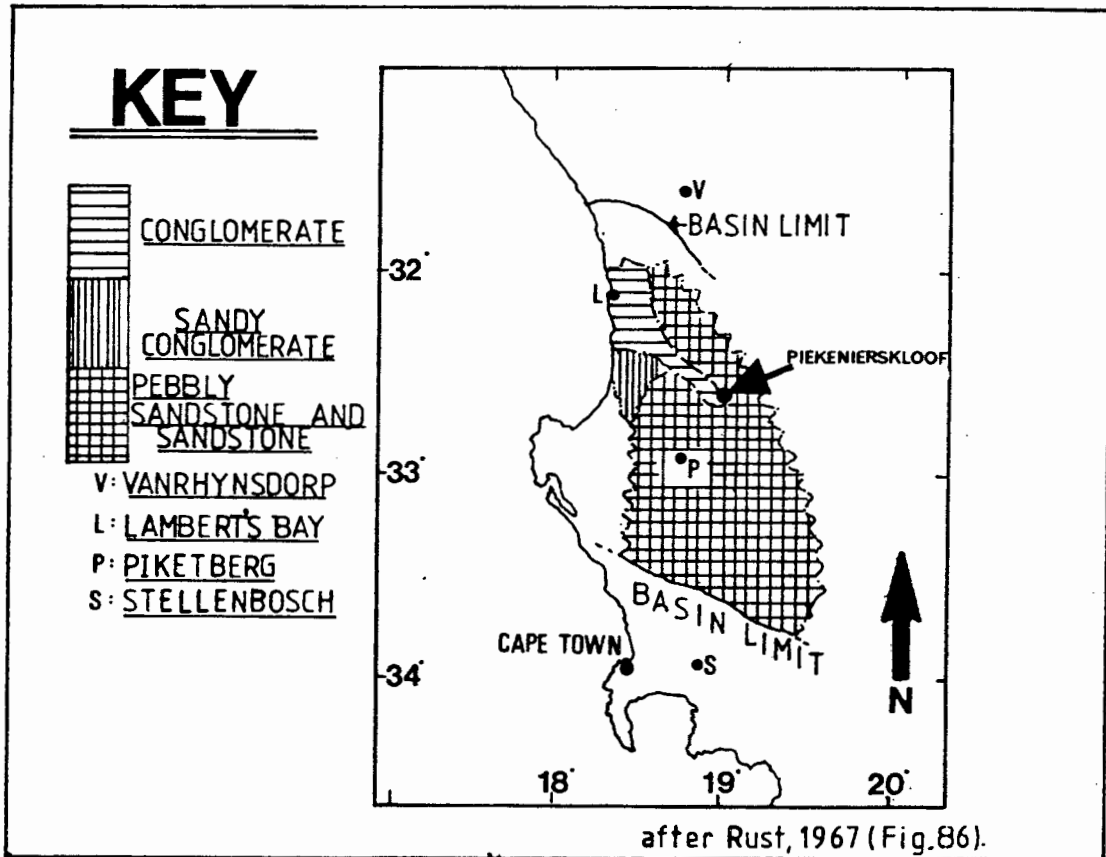


Figure 3.9. Distribution of sediment type in the Piekenierskloof Formation (after Rust, 1967, Fig. 86). Abbreviations: V = Vanrhynsdorp, L = Lambert's Bay, P = Piketberg, S = Stellenbosch.

outcrop have vector means  $\sim 130^{\circ}$  True). This outcrop is separated from the outcrop at the coast by an inferred fault (Fig. 3.8). The outcrop is correlated with the Piekenierskloof Formation but its exact stratigraphic position relative to the coastal outcrop is unknown.

If the occurrence of conglomerates was confined to the coastal outcrop alone, then tectonic processes could be invoked to explain their presence in an otherwise arenaceous succession. Given that conglomerates at these localities are probably developed in proximal depositional environments and that their distribution is limited, a close analogy can be found amongst documented basin margin conglomerates, within which cyclicity is explained by allocyclic processes (Heward, 1978; Blair, 1987). However, conglomerate is not confined to the most proximal region (Fig. 3.9). If drainage basin erosion and fan sedimentation exceed the rate of subsidence during periods of tectonic quiescence, incision of the most proximal fan occurs and the locus of deposition is moved down fan (Heward, 1978; Blair, 1987).

### 3.7.3. Piekenierskloof Pass.

Piekenierskloof Pass (the stratigraphic type area) is the most distal conglomeratic outcrop in the Piekenierskloof Formation. Conglomerate (Gm(d), Gm, Gt, Gp and G1 facies) and coarse-grained pebbly sandstones (St and Sp facies) occur throughout the succession. Over 1200m of outcrop is exposed, albeit discontinuously. Dips are moderate ( $25^{\circ}$ - $35^{\circ}$ ) at the base of the Pass and steepen abruptly near the top ( $75^{\circ}$ ). Strike remains constant throughout ( $057^{\circ}$  True, dip to SE). This outcrop occurs on a eastward facing monocline (Söhnege, 1983, Fig. 1) and much tectonic disturbance (pervasive jointing, large scale normal and small scale reverse faults) is evident. The lower contact with the Klipheuwel Formation shows a small angular discordance of less than  $5^{\circ}$  (J.N. Theron, pers. comm., 1985). The upper contact with the Graafwater Formation is not exposed.

Gm, Gm(d), Gt-St, Gp-Sp, Sh(a) & (b) and mudrock facies are exposed in the section. Large, very thickly bedded ( $> 0.5\text{m}$ , up to  $3\text{m}$ ) sheets with a complex geometry of Gm, Gm(d), Gp-Sp and Gt-St facies (facies association A) are overlain by sheet bedded and or channelised Sh (a) & (b), pebbly St and Sp facies (facies association B). Where channelised an erosional scour with G1 or Gm facies separates these two facies

associations. Mudrock facies occur as rare uppermost channel-fill or as extraformational conglomerate clasts within Gm or Gm(d) facies.

Palaeocurrents are directed to the SE (vector mean  $158^{\circ}$  True). The palaeocurrent distribution is unimodal (Table 13) with consistency ratios and variance well within the range of values obtained at other outcrops of the Piekenierskloof Formation.

### 3.8 DISCUSSION

Five conglomerate and five sandstone facies are defined in the Piekenierskloof Formation at the three localities examined, Elands Bay, Lambert's Bay and Piekenierskloof Pass. Of these, two, a coarse-matrix supported, oligomictic pebble to cobble conglomerate and a pebbly, horizontally-bedded, coarse-grained sandstone are inferred to be deposited from sediment flows with sediment/fluid ratios higher than that of dilute, turbulent stream flow. The former shows textural characteristics indicative of traction carpet deposits. The latter is inferred to have been deposited from hyperconcentrated flow. Pre-Devonian alluvial sediment conceptually must have responded to high flow events differently from modern alluvium. It is evident that this braided alluvium contains a spectrum of deposits representing different sediment/fluid ratios ranging from dilute normal stream flow (lower sediment/fluid ratios) to more concentrated flows.

The preservation of these two facies, coupled with the observation that the foresets of sediment normally associated with dilute stream flow lack the grain size characteristics of avalanching, suggests rapid aggradation.

Planar cross-stratified sandstone foresets commonly have a tangential contact with the lower bounding surface. This is inferred to be the result of strongly turbulent, three dimensional flow over bedform crests.

Large scale planar cross-stratified sandstone are considered to

represent large bedforms in shallow channels. Because of the preserved height of these bedforms (2-3m in some cases) and the inferred channel width to depth ratios of 100-1000:1, it is deduced that channels were at least 200-2000m wide. The size of these channels, relative to the dimensions of available outcrop, coupled with a lack of a finer grained sediment component, makes identification difficult. Sandstones thus appear sheet bedded. Channel bases can be defined by the presence of scour (erosion surfaces) on which GL facies occur. Smaller scale channels (< 100m wide, < 1m preserved depth) are evident at Piekenierskloof Pass. Distal decrease in channel size is not commonly reported in recent literature on braided alluvium (Heward, 1978, Table 4) but may occur distally in the zone of infiltrated water expulsion (Heward, 1978), which may be applicable here.

Interpretation of Sp and St facies may be in serious error. These facies occur together as part of upward coarsening cycles of Sr-Sp- and St facies on preserved, modern macroforms. Such cycles are absent at the localities examined. No literature exists on ancient macroforms other than Minter (1986). The terminology relating to, and definition of, bedforms is in a state of flux at present. Thus these two facies cannot be interpreted convincingly. Facies interpretations here are those of Miall (1978) and Miall (1985).

Facies defined in this study can easily be fitted into one or more of Miall's new architectural elements. This technique loses considerable effect where outcrop is poor or lacks three dimensional aspect (it would be very difficult to apply this technique of facies analysis to core samples, for instance).

At the localities examined conglomerate is interbedded with sandstone. An analogy can be sought from Pleistocene outwash gravel and sandstone deposits (Enynon and Walker, 1974) where sand is deposited in the deeper part of channels and conglomerate in the shallower portions. At the locations examined the preserved thickness of conglomerate rarely exceeds the preserved thickness of associated sandstone, which occurs in marginal or overlying relationships.

The single upward coarsening and then upward fining megacycle recognised by Vos and Tankard (1981) at Elands Bay is not recognised throughout the basin or at any other outcrop examined. Conglomerates are not confined to the most proximal parts of the deposystem (inferred to be at the present coast), thus allocyclic processes (tectonism, relief rejuvenation, base level fall) alone cannot explain the appearance of conglomerate. Avulsion of the lobe of active sedimentation is as plausible. Where allocyclic processes are inferred to have been operative their effects should be evident at several localities (Grotzinger, 1986).

Palaeocurrent data are unimodal, have high consistency ratios and low variance relative to data generated from strata of probable marine origin (Faroo Member, Graafwater Formation, Carstensberg Pass). Such data may prove to be a powerful palaeoenvironmental discriminator if applied to other outcrop in the Piekenierskloof Formation and other formations in the Table Mountain Group.

### 3.9 CONCLUSION

Sedimentation in the Piekenierskloof Formation is adequately explained by deposition from wide, rapidly aggrading bedload dominated channel systems characterized by the migration of bedforms. Local accumulation of conglomerate may be associated with avulsion during periods of tectonic quiescence, incision and progradation. The more proximal and coarser part of the alluvial braid plain then prograded locally over more distal deposits. Some conglomerates were deposited with higher sediment/fluid ratios than dilute stream flow. This may be a consequence of rapid mobilisation of vast volumes of sediment during high stage flows on unvegetated Pre-Devonian braid plains.

### REFERENCES

- Allen, J.R.L. (1983). Studies in fluvial sedimentation: Bars, bar complexes and sandstone sheets (low sinuosity braided streams) in the Brownstones (L.Devonian), Welsh Borders. *Sedim. Geol.*, 33, 237-293.

- Allen, J.R.L. (1984). Parallel lamination developed from upper stage plane beds: a model based on the larger coherent structures of the turbulent layer. Sed. Geol., 39, 227 - 242.
- Allen, P.A. (1981). Sediments and processes on a small, stream flow dominated, Devonian alluvial fan, Shetland Islands. Sedim. Geol., 29, 31-66.
- Blair, T.C. (1987). Tectonic and hydrologic controls on cyclic alluvial fan, fluvial and lacustrine rift-basin sedimentation, Jurassic-lowermost Cretaceous Trodos Santos Formation, Chipas, Mexico. J. sedim. Petrol., 57, 845-862.
- Buck, S.G. (1985). Sand-flow cross-strata in the tidal sands of the lower Greensand, (lower Cretaceous), southern England. J. sedim. Petrol., 55, 895-906.
- Buck, S.G. and Minter, W.E.L. (1985). Placer formation by fluvial degradation of an alluvial fan sequence: the Proterozoic Carbon Leader placer, Witwatersrand Supergroup, South Africa. J. geol. Soc. London, 142, 757-764.
- Crowley, K.D. (1981). Origin, structure and internal stratification of three hierarchical classes of bedforms in unidirectional flows: examples from the Platte River Basin in Colorado and Nebraska. Ph.D. Thesis, Princeton Univ., 227 pp.
- Crowley, K.D. (1983). Large scale bed configurations (macroforms), Platte River Basin, Colorado and Nebraska. Geol. Soc. Am. Bull., 94, 117-133.
- Decelles, P.G., Tolson, R.B., Graham, S.A., Smith, G.A., Ingersoll, R.V., White, J., Schmidt, C.J., Rice, R., Moxon, I., Lemke, L., Handschy, J.W., Follo, M.F., Edwards, D.P., Cavazza, W., Caldwell, M. and Bargar, E. (1987). Laramide thrust-generated alluvial-fan sedimentation, Sphinx Conglomerate, Southwestern Montana. Bull. Am.

Assoc. Petrol. Geol., 71, 135-155.

Eriksson, P.G. (1984). A palaeoenvironmental analysis of the Molteno Formation in the Natal Drakensberg. Trans. Geol. Soc. S. Afr., 87, 237-244.

Eynon, and Walker, R.G. (1974). Facies relationships in Pleistocene outwash gravels, southern Ontario: a model for bar growth in braided rivers. Sedimentology, 21, 43-70.

Fuller, A.O. (1985). A contribution to the conceptual modelling of pre-Devonian fluvial systems. Trans. Geol. S. Afr., 88, 189 - 194.

Groztinger, J.P. (1986). Cyclicity and palaeoenvironmental dynamics, Rocknest Platform, N.W. Canada. Geol. Soc. Am. Bull., 97, 1208 - 1231.

Heward, A.P. (1978). Alluvial fan sequence and megasequence models: with examples from the Westphalian D. and Stephanian B. coalfields, northern Spain. In: Miall, A.D. Ed., Fluvial Sedimentology, Can. Soc. Petrol. Geol., Calgary Alberta, 669-702.

Hunter, R.E. (1985). Subaqueous sand-flow cross-strata. J. sedim. Petrol., 55, 557-562.

Jackson, R.G. (1975). Hierarchical attributes and a unifying model of bedforms composed of cohesionless material and produced by shearing flow. Geol. Soc. Am. Bull., 86, 1523 - 1533.

Leeder, M.R. (1982). Sedimentology. Processes and Product. George Allen and Unwin, London, 344 pp.

Long, D.G.F. (1978). Proterozoic stream deposits: some problems of recognition and interpretation of ancient sandy fluvial systems. In: Miall, A.D. Ed., Fluvial Sedimentology, Can. Soc. Petrol. Geol., Calgary, Alberta, 313-342.

Lowe, D.R. (1982). Sediment gravity flows: II. Depositional models with special reference to the deposits of high density turbidity currents. J. sedim. Petrol., 52, 279-297.

Miall, A.D. (1974). Palaeocurrent analysis of alluvial sediment: a discussion of directional variance and vector magnitude. J. sedim. Petrol., 44, 1174-1185.

Miall, A.D. (1978). Lithofacies types and vertical profile models in braided river deposits: a summary In: Miall, A.D. Ed., Fluvial Sedimentology. Can. Soc. Petrol. Geol., Calgary, Alberta, 597-604.

Miall, A. D. (1985). Architectural-element analysis: A new method of facies analysis applied to fluvial deposits. Earth Sci. Rev., 22, 261-308.

Minter, W.E.L. (1986). Very large ancient fluvial bedforms in the Steyn placer, Welkom Goldfield. Abstr. Geol.Soc. of S.A. Gecongress 86, 465-468.

Pettijohn, E.J. (1975). Sedimentary Rocks. Harper and Row, New York, 628 pp.

Rust, I.C. (1967). On the sedimentation of the Table Mountain Group. D.Sc. thesis, (unpubl.), Univ. Stellenbosch, 110 pp.

Rust, B.R. and Jones, B.G. (1987). The Hawkesbury sandstone south of Sydney, Australia: Triassic analogue for the deposition of a large braided river. J. sedim. Petrol., 57, 222-233.

Smith, G.A. (1986). Coarse-grained nonmarine volcanoclastic sediment: terminology and depositional process. Geol. Soc. Am. Bull., 97, 1-10.

Smith, G.A. (1987). The influence of explosive vulcanism on fluvial sediments: the Deschutes Formation (Neogene), in Central Oregon. J. sedim. Petrol., 57, 613-629.

Smith, N.D. (1972). Some sedimentological aspects of planar cross-stratification in a sandy braided river. J. sedim. Petrol., 42, 624-634.

Söhnge, A.P.G. (1983). The Cape Fold Belt - Perspective. In: Söhnge, A.P.G. and Halbich, I.W. Eds., Geodynamics of the Cape Fold Belt. The Geological Society of South Africa Spec. Pub., 12, 1-6.

Tankard, A.J. and Hobday, D.K. (1977). Tide dominated back-barrier sedimentation, Early Ordovician Cape Basin, Cape Peninsula, South Africa. Sed. Geol., 18, 135-159.

Tankard, A.J., Jackson, M.P.A., Eriksson, K.A., Hobday, D.K., Hunter, D.R. and Minter, W.E.L. (1982). The Crustal Evolution of Southern Africa: 3.8 Billion Years of Earth History. Springer-Verlag, Berlin, 523 pp.

Turner, B.R. (1977). Fluvial cross-bedding in the upper Triassic Molteno Formation of the Karoo (Gondwana) Supergroup in South Africa and Lesotho. Trans. Geol. soc. S. Afr., 80, 241-252.

Turner, B.R. (1984). Palaeogeographic implications of braid bar deposition in the Triassic Molteno Formation of the eastern Karoo Basin. Paleont. Afr., 25, 29-38

Vos R.G. and Tankard, A.J. (1981) Braided fluvial sedimentation in the lower Palaeozoic Cape Basin, South Africa. Sed. Geol., 29, 171-193.

Walker, R.G. (1975). Conglomerate: sedimentary structures and facies models. In: Harms, J.C., Southard, J.B., Spearing, D.R. and Walker, R.G. Eds., Depositional environments as interpreted from primary sedimentary structures and stratified sequences. Short Notes, Soc. Econ. Palaeon. Mineral., 2, 133-161.

Wells, N.A. and Dorr, J.A. Jr. (1987). Shifting of the Kosi River, northern India. Geology, 15, 204-207.

#### 4. PUBLISHED WORK

Three publications co-authored or written by the author are submitted as published contributions to the geology of the Table Mountain Group. "Palaeoenvironmental significance of Nardouw Formation clast shape" is a re-evaluation of the author's Honours project, and suggests a fluvial palaeoenvironment for parts of the Nardouw Formation at its most proximal extremity. The abstracts on "The diagenesis of some Table Mountain Group Arenites" are the result of co-operative research between the author and Mr. Peter Chadwick under the supervision of Professor Arthur Fuller. The abstract written by the author solely was delivered at the Biennial Conference of the Mineralogical Society of South Africa, in September, 1987. The co-authored abstract has been accepted for presentation by the author on his research group's behalf at the Biennial Congress of the Geological Society of South Africa (Geocongress 88) to be held at the University of Natal (Durban) in July, 1988.

DIAGENESIS AND CLAY MINERALOGY OF SOME TABLE  
MOUNTAIN GROUP ARENITES  
IN THE S.W. CAPE:  
A PRELIMINARY NOTE

BY

A.G. Thamm

ABSTRACT

Quartzose and feldspathic arenites of the Table Mountain Group and Klipheuwel Formation respectively contain small, but significant amounts of neoformed, authigenic clay minerals. Species identified by X-ray diffraction and electron microprobe (WDS) include kandite group minerals, illite, illite/smectite (ISII), and pyrophyllite. These clay minerals occur as framework grain replacements and (more commonly) as pore fills that occlude porosity post-dating pervasive quartz cementation.

Kandite group minerals occlude porosity after the dissolution of quartz framework grains and syntaxial quartz overgrowths, as well as replacing framework grains. Texturally, in thin section, this appears as neoformed kandites that infill (secondary) porosity associated with embayed and pitted quartz framework grains and cement. Such features are strongly suggestive of kandite replacement of carbonate cement. Some oversized and elongate pores are occluded by kandite minerals and are more suggestive of kandite replacement of feldspar.

Kandite replacement of feldspar and/or replacement carbonate cement requires influx of acid groundwater. In oilfield brines the thermal maturation of kerogen releases such acidic groundwater and can result in the formation of secondary porosity, as well as contributing to the increased flux of alumina as organic complexes. This is an unlikely process in the dominantly arenaceous Table Mountain Group (Which is lacking in shale, organic rich or otherwise). The observation that the amount of kandite occluding porosity increases towards the basin margin, indicates influx of acidic (meteoric) groundwater into Table Mountain Group arenites.

Given the low solubility of alumina reported in most formation water (and the absence of organic complexing) the source of alumina was probably local, ie Al-bearing silicates such as feldspar or mica. Kandite group minerals are subsequently replaced by illite, illite/smectite and pyrophyllite with increasing diagenetic grade.

The quartz rich nature of these arenites is ascribed to derivation from older, Pan-African or Namaqua age orogenic

terrains (which would have resulted in the liberation of quartz rich sediment). The subsequent dissolution of chemically unstable framework grains and clay neoformation is a product of groundwater flux during diagenesis. These arenites from the Klipheuwel, Piekenierskloof and Graafwater Formations show improving rounding and loss of polycrystalline quartz framework grains up stratigraphic section as the succession becomes marine. Earlier models of sandstone petrogenesis involving sustained abrasion and attrition of the framework component may apply to marine facies only.

ooOoo

DIAGENESIS AND PETROLOGY  
OF SOME TABLE MOUNTAIN GROUP  
ARENITES IN THE S.W. CAPE SANDVELDT

BY

A.G. Thamm (presenter)  
GEOLOGICAL SURVEY, BELLVILLE

and

A.O. Fuller & P.J. Chadwick  
DEPARTMENT OF GEOLOGY, UNIVERSITY OF CAPE TOWN

ABSTRACT

Quartzose and feldspathic arenites of the Table Mountain Group (Graafwater and Piekenierskloof Formations) and Klipheuwel Formation respectively contain small, but significant amounts of neoformed, authigenic clay minerals. Species identified by X-ray diffraction, electron microprobe (WDS) and scanning electron microscope include kandite group minerals, illite, illite/smectite, and pyrophyllite (Chadwick, 1987; Thamm, 1988). These clay minerals occur as framework grain replacements and (more commonly) as pore fills that occlude porosity post-dating pervasive quartz cementation.

Kandite group minerals occlude porosity after dissolution of quartz framework grains and syntaxial quartz overgrowths as well as replacing framework grains. Texturally, in thin section, this appears as neoformed

kandites that infill (secondary) porosity associated with embayed and pitted quartz framework grains and cement. Such features are reported during kandite replacement of carbonate cement (Burley and Kantorowicz, 1986). Some oversized and elongate pores are occluded by kandite minerals and are more suggestive of kandite replacement of feldspar.

Kandite replacement of feldspar and/or replacement of carbonate cement requires influx of acid groundwater. In oilfield brines the thermal maturation of kerogen releases such acidic groundwater and can result in the formation of secondary porosity, as well as contributing to the increased flux of alumina as organic complexes (Surdam et al., 1984). This is an unlikely process in the dominantly arenaceous lower Table Mountain Group (which is lacking in shale, organic rich or otherwise). The amount of kandite occluding porosity increased towards the basin margin. Such features are indicative of influx of acidic (meteoric) groundwater beneath unconformities.

Given the low solubility (500 pbb) of alumina reported in most formation water (and the absence of organic complexing) the source of alumina was probably local, i.e. Al-bearing silicates such as feldspar or mica. Kandite group minerals are subsequently replaced by illite and illite/smectite or pyrophyllite with increasing diagenetic grade.

The quartz rich nature of these arenites is ascribed to derivation from older, orogenic terrains. Such provenance areas result in the liberation of quartz rich sediment (Dickenson et al., 1983; Potter, 1984, 1986). The subsequent dissolution of chemically unstable framework grains and clay neoformation is a product of groundwater flux during diagenesis.

The necessity for sustained abrasion and attrition of sediment in nearshore sedimentary environments, favoured in earlier models of Table Mountain group quartzarenite petrogenesis (Visser, 1974), is obviated by the diagenetic processes described. An increase in textural and framework maturity is observed in arenites whose ichnology and lithofacies distribution are compatible with nearshore sedimentary palaeoenvironments. Such arenites are rare.

#### REFERENCES

Burley, S.D. and Kantorowicz, J.D. (1986). Thin section and S.E.M. textural criteria for the recognition of cement dissolution porosity in sandstones. Sedimentology, 33 587-604.

Chadwick, P.J. (1987). A 32<sup>o</sup> traverse through the Table Mountain Group in the western Cape Province. A stratigraphic, mineralogical and petrographic study. B.Sc.(Hons). thesis, Univ. of Cape Town, 50pp.

Dickenson, W.R., Beard, S.L., Brakenridge, G.R., Erjavec, J.L., Ferguson, R.C., Inman, K.F., Knepp, R.A., Lindberg, F.A. and Ryberg, P.T. (1983). Provenance of North American Phanerozoic sandstones in relation to Tectonic Setting. Geol. Soc. Am. Bull., 94, 222-235.

Potter, P.E. (1984). South America and a few grains of sand. Nature, 311, 645-648.

Potter, P.E. (1986). South America and a few grains of sand Part 1: Beach sands. J.Geol., 94, 301-319.

Surdam, P.C., Boese, S.W. and Crossey, L.J. (1984). The Chemistry of Secondary Porosity. In: McDonald, D.A. and Surdam, R.C. *Clastic Diagenesis*. Amer. Assoc. Petrol. Geol., Tulsa, Oklahoma, 127-149.

Thamm, A.G. (in prep.). Contributions to the Geology of the Table Mountain Group. M.Sc. thesis, Univ. of Cape Town.

Visser, J.N.J. (1974). The Table Mountain Group: A study in the deposition of quartz arenites on a stable shelf. Trans. Geol. Soc. S. Afr., 77, 229-237.

\*\*\*\*\*

# Palaeoenvironmental significance of clast shape in the Nardouw Formation, Cape Supergroup

A.G. Thamm

Department of Geology, University of Cape Town, Private Bag, Rondebosch 7700, Republic of South Africa

Accepted 31 December 1986

Given adequate residence time within a particular environment clasts should develop shapes characteristic of abrasion within that environment. Clasts from the Silurian to early Devonian Nardouw Formation (Table Mountain Group) suggest shaping within a fluvial palaeoenvironment. Conglomerates and pebbly sandstones sampled in four localities and classified into 13 groups have mean sphericities and coefficients of flatness greater than 0,65 and 45, respectively. The clasts selected are composed of vein quartz and are unlikely to have had any significant inherited form. Published palaeoenvironmental syntheses of the Nardouw Formation rely on analogy to the Peninsula Formation (Table Mountain Group) for which a shallow siliciclastic shelf and barrier island model has been proposed. The lack of shape characteristics indicative of marine palaeoenvironments may be a consequence of short residence time or lack of 'energy' in the beach and/or nearshore. An alternative hypothesis that these conglomerates are of fluvial origin is presented in this paper.

Indien genoeg vestigingstyd in 'n sekere omgewing toegelaat word, behoort klaste vorms te ontwikkel wat kenmerkend is van afskuiwing in daardie omgewing. Klaste van die Siluriese tot vroeë Devoniese Formasie Nardouw (Groep Tafelberg) dui op vorming in 'n fluviale paleo-omgewing. Konglomerate en rolsteenhoudende sandstene wat in vier lokaliteite gemonster en in 13 groepe geklassifiseer is, het gemiddelde sferisiteite en koëfisiënte van platheid groter as 0,65 en 45, respektiewelik. Die klaste wat geselekteer is, is saamgestel uit aarkwarts en dit is onwaarskynlik dat dit enige betekenisvolle geërfde vorm het. Gepubliseerde paleo-omgewingsinteses van die Formasie Nardouw is gebaseer op die analogiese verband tussen die Formasie Skiereiland (Groep Tafelberg) waarvoor daar 'n vlaksiliclastiese-bank-versperring-eilandmodel voorgestel is. Die gebrek aan vormkenmerke wat dui op seepaleo-omgewings kan 'n gevolg wees van kort verblyftydperk van gebrek aan 'energie' in die strandgebied en/of nabygeleë kus. 'n Alternatiewe hipotese dat hierdie konglomerate van fluviale oorsprong is, word hier aangebied.

## Introduction

Thick arenaceous formations of pre-Devonian age, that are unfossiliferous and lack mudrock facies, present complex problems to the palaeoenvironmentalist. Coarse-grained marine deposits that lack bimodal-bipolar cross-stratification or flaser bedding, and which are dominated by high-angle planar and trough cross-stratification, are difficult to distinguish from braided fluvial sediments deposited by sheet flooding and channel migration (Long, 1978).

The Nardouw Formation is an arenaceous, coarse-grained and sheet bedded sequence dominated by high angle-planar and trough cross-bedding (Rust, 1967). North of 31°40' S it is the sole representative of the Table Mountain Group, the underlying formations (Cedarberg, Pakhuis and Peninsula) having overlapped onto Cambrian-Precambrian metasediments (Rust & Theron, 1964). Published interpretations favour a shallow marine palaeoenvironment (Rust, 1973; Tankard *et al.*, 1982). This paper postulates an alternative fluvial origin, based on clast shape studies.

The study area (Figure 1) in the Bokkeveldberge in the vicinity of Niewoudtville, Cape Province is the northernmost outcrop of the Nardouw Formation. The Nardouw Formation is flat-lying and tectonically undisturbed.

The study of clast shape has been shown to be a useful environmental discriminator. Sphericity (Sneed & Folk, 1958) and coefficient of flatness (Luttig, 1962) have been used to discriminate between modern beach and river

gravels (Dobkins & Folk, 1970; Stratten, 1974). Application to ancient deposits to determine sedimentation history have met with similar success (Russell, 1980).

## Shape analysis

### Method

Thirteen samples comprising 378 clasts in the pebble and cobble size range were obtained from the basal conglomerate and from lag horizons separating multistorey sand bodies. The basal conglomerate underlies the entire study area. The lag horizons are continuous on outcrop scale.

Sphericity and coefficient of flatness were calculated from triaxial measurements. Three orthogonal axes (A, B, C) were defined, but do not necessarily intersect at a common point. Clasts were orientated so that the AB plane was viewed, and the long (A) and intermediate (B) axes measured. The AB plane was rotated through 90° and the short axis (C) measured. The A, B, and C axial lengths were used to calculate

$$(i) \text{ Sphericity: } \left( \frac{C^2}{AB} \right)^{1/3}$$

$$(ii) \text{ Coefficient of flatness: } \frac{100 C}{A}$$

## Results

A mean sphericity and coefficient of flatness were calculated for each sample (Table 1). These values, other than



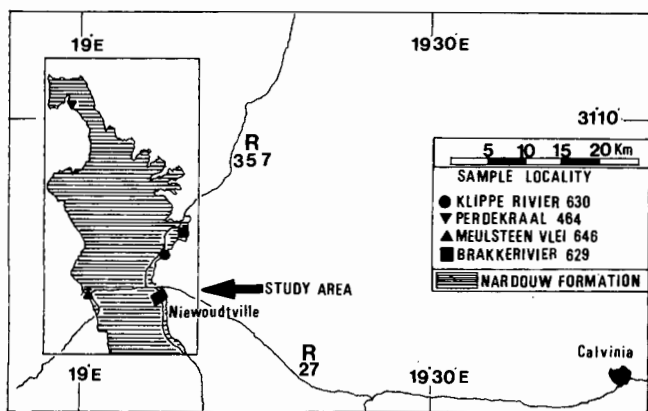


**Figure 1** Location of the sample sites in the study area, showing main roads. Sample sites are named after local farms.

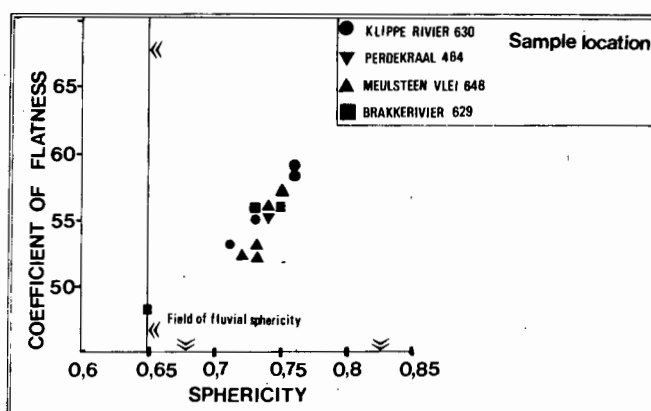


**Figure 2** Graphical representation of coefficient of flatness and sphericity data in the study area. Boundaries of the field of fluvial shape indices (after Stratten, 1974) are indicated by the double arrow.

**Table 1** Nardouw Formation clast shape indices

Locality	Sample No.	Type	n	Sphericity		Coefficient of flatness	
				( $\bar{x}$ )	(s)	( $\bar{x}$ )	(s)
Brakkerivier	1	lag	19	0,73	0,08	56,66	9,82
Brakkerivier	2	lag	70	0,73	0,11	56,63	14,64
Brakkerivier	3	basal	54	0,65	0,11	47,46	14,12
Perdekraal	4	lag	23	0,74	0,09	55,45	12,84
Meulsteenvlei	5	basal	61	0,74	0,10	56,51	12,78
Meulsteenvlei	6	lag	25	0,72	0,08	53,38	10,59
Meulsteenvlei	7	lag	10	0,73	0,08	53,95	11,82
Meulsteenvlei	8	lag	17	0,73	0,09	52,01	12,40
Meulsteenvlei	9	lag	16	0,75	0,10	57,66	14,56
Klipperivier	10	lag	25	0,73	0,09	55,34	10,34
Klipperivier	11	lag	11	0,76	0,14	59,53	18,49
Klipperivier	12	lag	22	0,76	0,10	58,14	14,39
Klipperivier	13	basal	25	0,71	0,09	53,18	10,80
Mean sphericity			378	0,74	0,10		

$\bar{x}$  is the sample mean.

s is the sample standard deviation.

n is the number of clasts in each sample.

sample 3 which has an ambiguous mean sphericity value, fall in the field of fluvial shape indices as defined by Stratten (1974), which is defined by a coefficient of flatness greater than 45 and sphericity greater than 0,65 (Figure 2).

The sphericity and coefficient of flatness are believed to be normally distributed (Dobkins & Folk, 1970; Barrett, 1980). A 'goodness of fit test' (Underhill, 1981) confirms this hypothesis for the sphericity data at the 95 per cent confidence level (Table 2).

Replicate analyses indicate that the axial measurements are precise to within 5,8 per cent. A distribution free test, the Kruskal Wallis one-way analysis of variance, tested the equality of sphericity sample means. A null hypothesis that the sphericity sample means have the same location parameter is rejected at the 95 per cent confidence level. If the sample means are

tested against an alternative hypothesis that sphericity and coefficient of flatness are greater than 0,65 and 45, respectively using Student's 't' test, the samples (other than sample 3) accept the alternate hypothesis at the 95 per cent confidence level.

**Discussion**

Clasts shaped in fluvial environments have been reported in what are interpreted to be marine sediment (McBride, 1966; Ricci Lucchi, 1969; Russell, 1980). These studies are concerned with resedimented deposits, specifically turbidites. Processes involve 'some down-slope mass-transport mechanism from an original fluvial deposit' (Blatt *et al.*, 1980). The Nardouw Formation arenites bear no resemblance to turbidite deposits and hence this model can be ruled out.

Further misfit classifications have been reported from estuaries with low wave energy, as well as pocket beaches associated with cliffs (Dobkins & Folk, 1970). The latter is clearly not applicable (Rust, 1967; 1973; 1981; Tankard *et al.*, 1982). The former case makes the migration of large, very coarse-grained bedforms (the planar and trough cross-bedded sandstones reported by Rust, 1967) implausible.

Palimpsest fluvial gravels have been reported from the North Sea (McCave, 1985) emplaced during Pleistocene low sea-level stands and subsequently drowned by the Holocene-transgression. Transgressive-regressive episodes have been interpreted in the transition from marine to nonmarine depositional environments (Clifton, 1981) and have been interpreted in the Bokkeveld Group stratigraphically above the Nardouw Formation (Theron, 1972; Tankard & Barwis, 1982). It is here suggested that the conglomerates with fluvial shape indices were emplaced in the Nardouw Formation as an allocyclic response to an as yet unreported combination of changes of relative sea level, basement subsidence and sediment influx.

It should be noted that the Nardouw Formation is of Silurian — early Devonian age (Cooper, 1982; Potgieter & Oelofsen, 1983); the late Silurian is characterized by a

**Table 2** 'Goodness of fit' test data

The 'goodness of fit' test uses all the sphericity data combined. The null hypothesis is that the sphericity data are normally distributed.

Interval	Observed Frequency	Theoretical Probability	Expected Frequency
0,383-0,505	9	0,0135	5,10
0,505-0,627	52	0,1375	51,97
0,627-0,749	144	0,4028	152,25
0,749-0,871	142	0,3503	132,41
0,871-0,991	31	0,0959	36,25

The test statistic is

$$D^2 = \sum_{i=1}^k (O_i^2/E_i) - N,$$

where N is the number of values (378), and has k-d-1 degrees of freedom (k is the number of subsets (5) and d=2 as a mean and variance have been estimated).  $O_i$  is the observed frequency of data in interval i,  $E_i$  the expected frequency, based on theoretical probability. The test statistic ( $D^2$ ) = 4.895.

Chi square (with 2 degrees of freedom) = 5,991 at the 95% confidence level.

Thus  $D^2$  lies in the region of null hypothesis acceptance.

eustatic *sea-level fall*, the earliest Devonian by a eustatic *sea-level rise* (Vail *et al.*, 1977; Hallam, 1984). These fluvial gravels may therefore record the progradation of the coastal plain that bordered the Nardouw siliciclastic shelf and its subsequent drowning under such circumstances.

The textural and mineralogical maturity of the Nardouw Formation arenites is attributed to sustained abrasion and attrition in the beach environment (Visser, 1974). These conglomerates, with fluvial shape indices, are thus anomalous given published process-response models for this Formation. If the sandstones represent reworked fluvial deposits this implies that the conglomerates were deposited below a 'null' point (where wave velocity asymmetry results in onshore, hence beachward, sediment movement), thus retaining their fluvial shape characteristics.

### Conclusions

Shape indices show that the last process that shaped clasts in the Nardouw Formation was a fluvial one. Conglomerates in the most northern (landward) part of this formation are thus inferred to have been fluvially deposited. The extent to which fluvial processes can be applied to the Nardouw Formation in other geographical localities is currently under investigation.

### Acknowledgements

The author wishes to acknowledge the criticism, advice and support of Professor Arthur Fuller and Dr. John Rogers who are thanked for their critical scrutiny of earlier versions of this manuscript. The reviewers provided

**Table 3** Kruskal Wallis test statistic data

The 378 sphericity values were classified into 13 groups (samples) on the basis of geographic locality and type. The  $j^{\text{th}}$  sample contains n observations. All the sphericity values are ranked 1 to N (N=378). Tied values are assigned an average rank.  $R_j$  is the sum of the ranks for sample j.

The Kruskal Wallis test statistic is

$$H = \frac{12}{N(N+1)} \sum_{j=1}^g \left( \frac{R_j^2}{n_j} \right) - 3(N+1)$$

Sample	Frequency	Rank sum
1	19	3708,0
2	70	15109,5
3	54	6120,5
4	23	4723,5
5	61	12263,5
6	25	4545,5
7	10	1940,5
8	17	3055,0
9	16	3291,0
10	25	5117,0
11	11	2363,0
12	22	4968,0
13	25	4426,0

The test statistic (H) is = 36,02.

The empirical level of significance = 0,0003, using the chi square distribution with 12 degrees of freedom. The chi square value for 12 degrees of freedom and 0,05 significance level is 21,026 (Underhill, 1981).

The null hypothesis that the samples are drawn from the same population is rejected.

by the Geological Society of South Africa are also thanked for their comments. The author acknowledges financial support from the CSIR and from Anglo-American Exploration Services (Orkney) without which this work would not have been possible.

### References

- Barrett, P.J. (1980). The shape of rock particles, a critical review. *Sedimentology*, **25**, 291-303.
- Blatt, H., Middleton, G. & Murray, R. (1980). *Origin of Sedimentary Rocks*. 2nd Edn. Prentice-Hall, Inc., New Jersey, 782pp.
- Clifton, H.E. (1981). Progradational sequences in Miocene shoreline deposits, southeastern Caliente Range, California. *J. sedim. Petrol.*, **51**, 165-184.
- Cooper, M.R. (1982). A revision of Devonian (Emsian-Eifelian) Trilobita from the Bokkeveld Group of South Africa. *Ann. S. Afr. Mus.*, **89**, 1-174.
- Dobkins, J.E. & Folk, R.L. (1970). Shape development on Tahiti-Nui. *J. sedim. Petrol.*, **40**, 1167-1203.
- Hallam, A. (1984). Pre-Quaternary sea level changes. *A. Rev. Earth Planet. Sci.*, **12**, 205-243.
- Long, D.G.F. (1978). Proterozoic stream deposits: some problems of recognition and interpretation of ancient

**Table 4** 't' Test data

Sample	N	't'test	't'calc (Spher.)	't'calc (C.o.F.)	Result (Spher.)	Result (C.o.F.)
1	19	1,729	4,47	5,31	Reject H <sub>0</sub>	Reject H <sub>0</sub>
2	70	1,667	7,61	6,65	Reject H <sub>0</sub>	Reject H <sub>0</sub>
3	54	1,674	0,67	1,21	Accept H <sub>0</sub>	Accept H <sub>0</sub>
4	23	1,714	4,80	3,90	Reject H <sub>0</sub>	Reject H <sub>0</sub>
5	61	1,671	7,03	7,02	Reject H <sub>0</sub>	Reject H <sub>0</sub>
6	25	1,708	4,38	3,48	Reject H <sub>0</sub>	Reject H <sub>0</sub>
7	10	1,812	3,16	2,40	Reject H <sub>0</sub>	Reject H <sub>0</sub>
8	17	1,740	3,30	2,33	Reject H <sub>0</sub>	Reject H <sub>0</sub>
9	16	1,746	3,64	3,48	Reject H <sub>0</sub>	Reject H <sub>0</sub>
10	25	1,708	4,44	3,53	Reject H <sub>0</sub>	Reject H <sub>0</sub>
11	11	1,796	2,63	2,60	Reject H <sub>0</sub>	Reject H <sub>0</sub>
12	22	1,717	4,69	4,28	Reject H <sub>0</sub>	Reject H <sub>0</sub>
13	25	1,708	3,33	3,79	Reject H <sub>0</sub>	Reject H <sub>0</sub>

The null hypothesis (H<sub>0</sub>) is that the population mean is 0,65 (Sphericity) and 45 (Coefficient of flatness). The alternate hypothesis is that the population mean is greater than 0,65 and 45 for sphericity and coefficient of flatness, respectively. 't' Test is one-sided and at the 95% confidence level. The 't' test data are derived from Underhill (1981). The 't' calc values are derived from the mean ( $\bar{x}$ ) and standard deviation (s) data given in Table 1 using

$$t = \frac{(\bar{x} - u)}{s/B}$$

where  $\bar{x}$  is the sample mean, s<sup>2</sup> the sample variance, u the population mean and B the square root of the number of values in each sample (N).

The level of significance is 0,05.

sandy fluvial systems.,313-341. In: Miall, A.D. Ed., *Fluvial Sedimentology*. Can. Soc. Petrol. Geol., Calgary, Alberta, 859pp.

Lüttig, G. (1962). The shape of pebbles in the continental, fluvial and marine facies. *Internat. Union of Geology and Geophysics — Internat. Assoc. of Sci. Hydrology*, **59**, 253-258.

McBride, E.F. (1966). *Sedimentary petrology and history of the Haymond Formation (Pennsylvanian), Marathon Basin, Texas*. Texas Bur. Econ. Geol. Rept. Inv., **57**, 101pp.

McCave, I.N. (1985). *Recent shelf clastic sediments*, 49-65. In: Brenchley, P.J. & Williams, B.P.J. Eds., *Sedimentology, Recent Developments and Applied Aspects*. The Geol. Soc., Blackwell Scientific Pubs., 342pp.

Potgieter, C.D. & Oelofsen, B.W. (1983). *Cruziana acacensis*

— the first Silurian index trace fossil from southern Africa. *Trans. geol. Soc. S.Afr.*, **86**, 51-54.

Ricci Lucchi, F. (1969). Composizione e morfometria di un conglomerato risedimento nel flysch Miocenico romagnolo. *Gionale di Geol., Ann. Mus. Geol. Bologna, Ser. 2a*, **36**, 1-47.

Russell, T. (1980). *Use of clast shape in determining the sedimentation history of the Devonian Keepit conglomerate, Australia*. *Sedim. Geol.*, **25**, 277-290.

Rust, I.C. (1967). *On the sedimentation of the Table Mountain Group in the Western Cape Province*. D.Sc. thesis (unpubl.). Univ. Stellenbosch.

--- (1973). The evolution of the Paleozoic Cape Basin, southern margin of Africa, 247-276. In: Nairn, A.E.M. & Stehli, F.G., Eds., *The Ocean Basins and Margins. 'The South Atlantic'*, Plenum, New York, 583pp.

--- (1981). Lower Paleozoic rocks of Southern Africa, 165-187. In: Holland, C.H., Ed., *Lower Paleozoic of the Middle East, Eastern and Southern Africa and Antarctica — (Lower Paleozoic Rocks of the World 3)*. John Willey and Sons, New York, 331pp.

--- & Theron, J.N. (1964). *Some aspects of the Table Mountain Series near Vanrhynsdorp*. *Trans. geol. Soc. S.Afr.*, **67**, 133-137.

Sneed & Folk, R.L. (1958). *Pebbles from the lower Colorado River, Texas, a study in particle morphogenesis*. *J. Geol.*, **66**, 114-150.

Stratten, T. (1974). Notes on the application of shape parameters to differentiate between beach and river deposits in Southern Africa. *Trans. geol. Soc. S.Afr.*, **77**, 59-64.

Tankard, A.J. & Barwis, J.H. (1982). Wave dominated deltaic sedimentation in the Devonian Bokkeveld basin of South Africa. *J. sedim. Petrol.*, **53**, 959-974.

---, Jackson, M.P.A., Eriksson, K.A., Hobday, D.K., Hunter, D.R. & Minter, W.E.L. (1982). *Crustal Evolution of Southern Africa — 3.8 billion Years of Earth History*. Springer-Verlag, Berlin, 523pp.

Theron, J.N.J. (1972). *The stratigraphy and sedimentation of the Bokkeveld Group*. D.Sc. thesis (unpubl.), Univ. Stellenbosch.

Underhill, L.G. (1981). *Introstat*. 3rd Edn. Juta & Co., Cape Town, 383pp.

Vail, P.R., Mitchum, R.M.Jr. & Thompson, S. (1977). *Seismic Stratigraphy and Global Changes in Sea Level, Pt. 4: Global Cycles of Relative Changes in Sea Level*, 83-97. In: Payton, C.E., Ed., *Seismic Stratigraphy — Application to Hydrocarbon Exploration*. Mem. Amer. Assoc. Petrol. Geol., **26**, 516pp.

Visser, J.N.J. (1974). *The Table Mountain Group: a study in the deposition of quartz arenites on a stable shelf*.



## Plate 1

### Captions

- a) Quartz overgrowths (qo) intersecting at a triple junction occluding pore space, arenite G 114. (Sample codes given in Appendix 1).
- b) Quartz overgrowths (arrowed) and detrital grain; arenite G 114.
- c) Small blocky kaolinite; arenite G 114.
- d) Large vermiform kaolinite and late stage quartz euhedra (arrowed); arenite G 114.
- e) Vermiform kaolinite intergrown with quartz (q); arenite G 303.
- f) Quartz dissolution etch pits; arenite P107.
- g) Triangular etch pits and euhedral laths of illite; arenite K 204.
- h) Illite laths and ragged edge, resorbed, kaolinite; arenite G 303.
- i) Pyrophyllite flakes; arenite P 121.
- j) Euhedral illite laths, neoformed in open pore space; arenite K 205.

# Plate 1

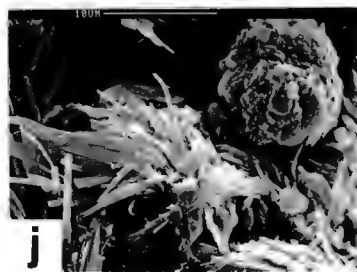
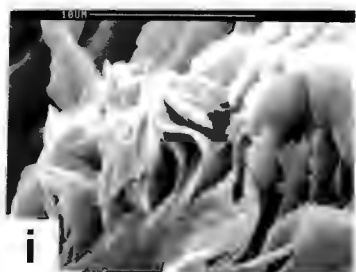
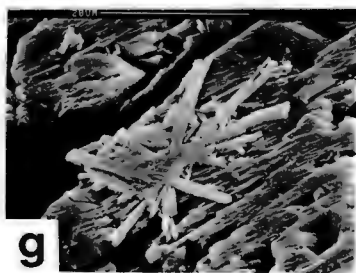
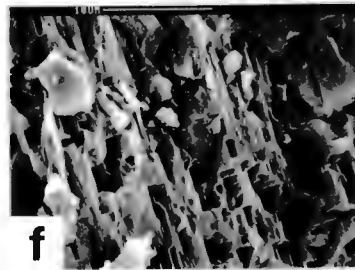
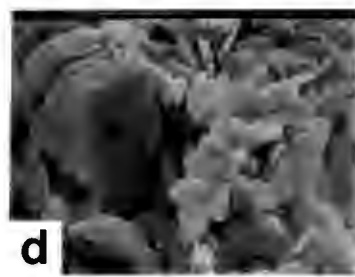
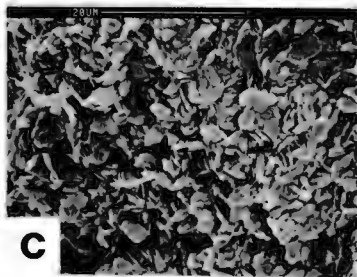
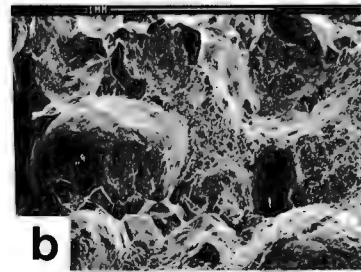
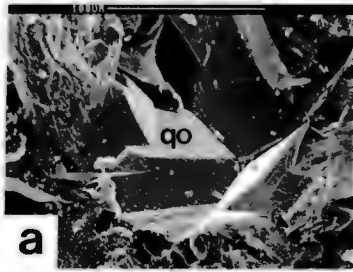


## Plate 2

### Captions

- a) Graafwater Formation stratigraphy at Heerenlogement, north of Graafwater village. The succession is capped by the Peninsula Formation which is underlain by the Faroo (arrowed) Tierhoek, Loop and Middlepos Members of the Graafwater Formation respectively. The thin bedded Loop and Faroo Members contain a diverse trace fossil assemblage.
- b) Circular burrow, with coarser sand infill, Faroo Member, Graafwater Formation, R364, Carstensberg Pass. Similar features were interpreted as trilobite burrows by Rust (1967) and as the ichnogenera Metaichna by Anderson (1975). Compare with Rust (1967), Plate 14 a-f.
- c) Bedding plane view of small grooves (epichnial grooves), Faroo Member, R 364 which are reminiscent of the ichnogenera Allocotichnus or Monomorphichnus. These may be trilobite resting or swimming-grazing traces.
- d) Sinuous trail, with coarse backfill, and indistinct marginal grooves, Faroo member, R364. Preserved on a upper bedding surface as a convex epirelief and full relief. This trace may be poorly preserved Rhizocorallium, type B.
- e) Ichnospecies Trichichnus linearis, Faroo Member, R364, Carstensberg Pass. Preserved as clay filled exichnia.
- f) Skolithos, preserved as exichnia, Faroo Member, R364 Carstensberg Pass. View onto bedding plane.
- g) Solitary Arenicolites, height ~45 mm, Faroo member, R364 Carstensberg Pass.
- h) Casts of mudcracks, Faroo Member, R364, Carstensberg Pass. Note orthogonal and triple junction intersection and irregular size. These features suggest origin by desiccation rather than syneresis.

# Plate 2

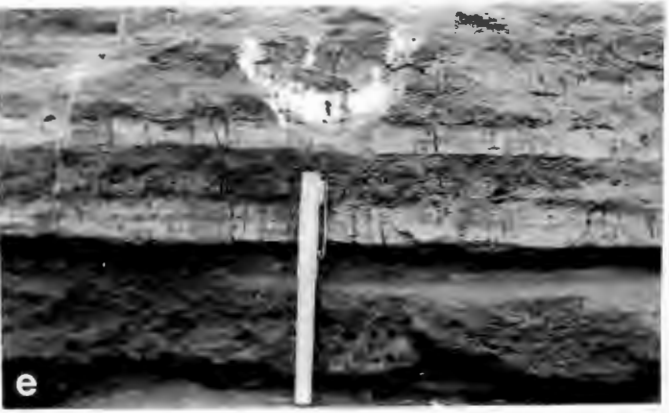
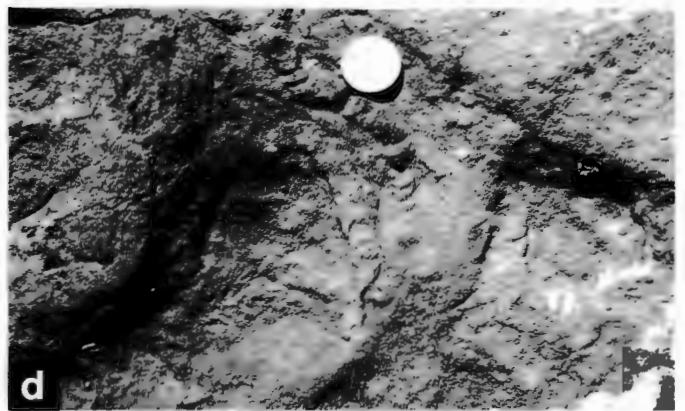
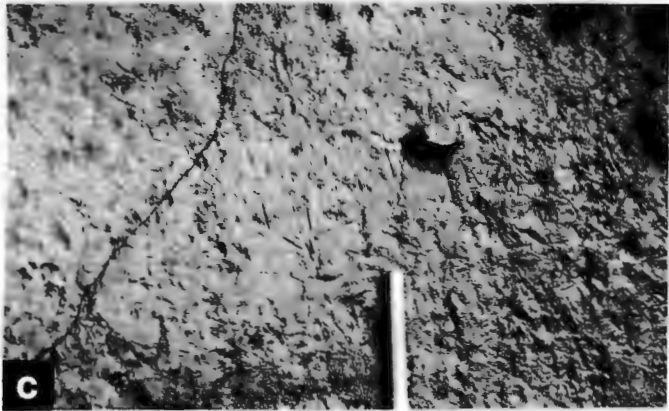
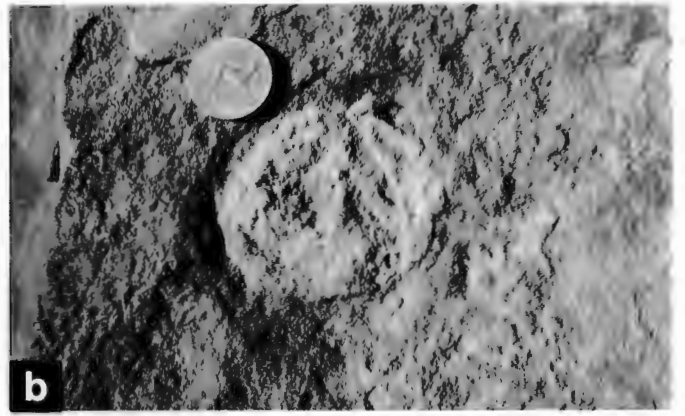


### Plate 3

#### Captions

- a) Planar cross-stratified conglomerate. Note grain size variations and coarser grain size at the base of foresets (Gp facies), Elands Bay. Scale 1m.
- b) Normally graded, clast supported conglomerate. Gm(a) facies, Elands Bay. Scale 0,75m.
- c) Low-angle, cross-stratified conglomerate, Lambert's Bay. Rock hammer for scale.
- d) Sandstone stratification and bar evolution, Lambert's Bay. Note low-angle cross-stratified, clast supported conglomerate at base, capped by sets of planar cross stratified, pebbly, very coarse grained sandstone, with discordant, non-erosional contacts. Scale 30 cm.
- e) Matrix-supported conglomerate, Lambert's Bay. The matrix is very coarse grained to coarse grained sand and granule conglomerate. Divisions on scale bar are 10 cm.
- f) Planar cross-stratified conglomerate grading down set into planar cross-stratified sandstone. Gp-Sp facies, Lambert's Bay. Scale 25 cm.
- g) Clast supported lag, a few pebble diameters thick. G1 facies Lambert's Bay. Rock hammer for scale.
- h) Low-angle, cross-stratified sand interbedded with clast supported conglomerate (G1 facies), Lambert's Bay. Scale 30 cm.

# Plate 3

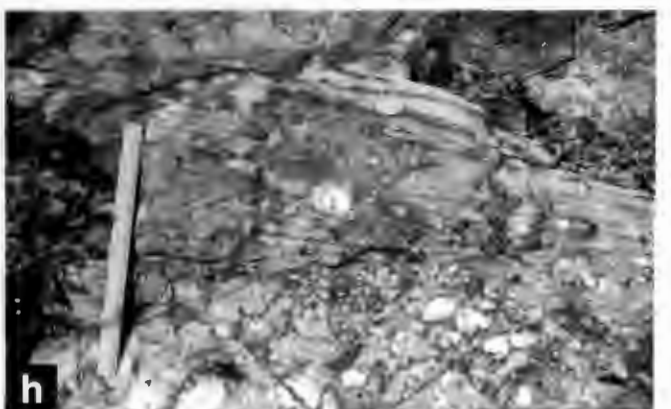
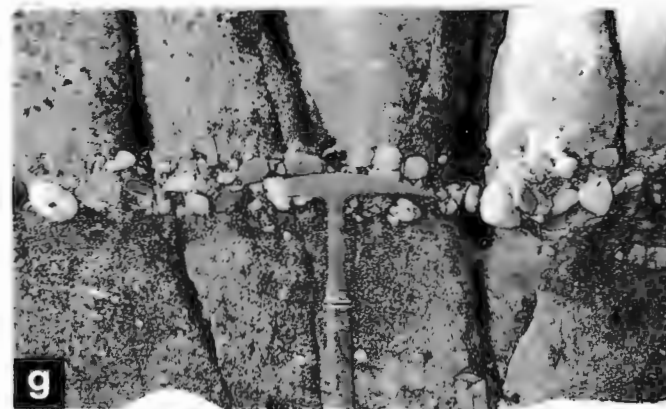
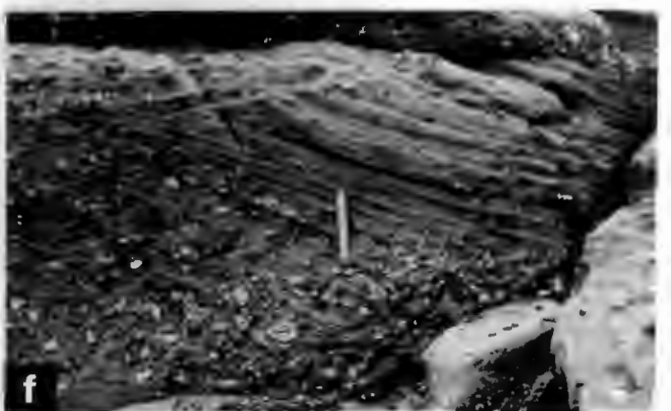
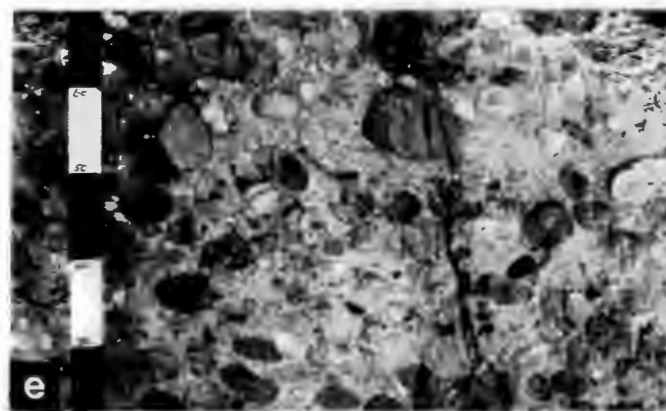
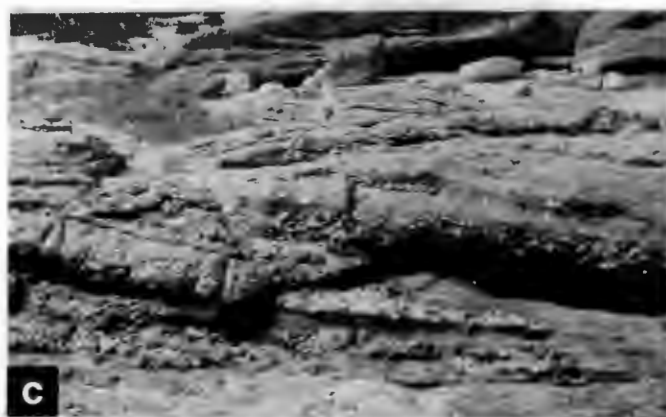
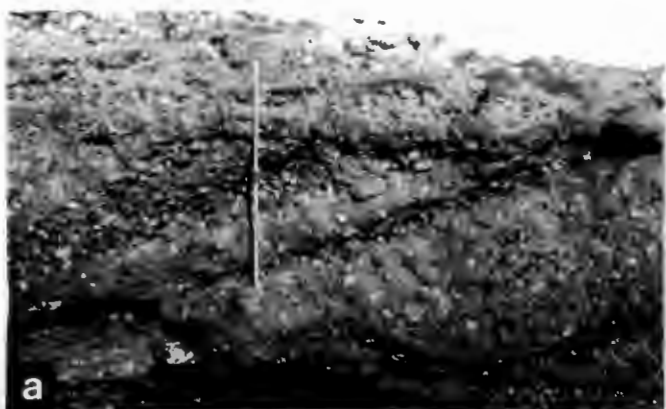


## Plate 4

### Captions

- a) Large scale cross-bedding (Sp) without pronounced basal scour, Lambert's Bay. Note asymptotic foreset intersection with lower bounding surface, indicative of high suspended load or high separation eddy turbulence. Scale bar gradations in 10's of cm.
- b) Planar cross-stratified, pebbly, coarse-grained sandstone (Sp facies), Lambert's Bay. Scale bar divisions in 10's of cm.
- c) Planar tabular cross-stratified sandstone, Lambert's Bay. Scale as in (b) above.
- d) Medium scale trough cross-bedding (St facies). Elands Bay. Hand lens for scale. Bedding plane view.
- e) Large scale trough cross-bedded sandstone, Steenbokfontein, just south of Lambert's Bay. Scale bar 1,5 m.
- f) Planar cross-bedded pebbly sandstone (Sp facies), Lambert's Bay. Compare with Vos and Tankard, 1981.
- g) Horizontally bedded medium-grained sandstone. Sh (a) facies, Lambert's Bay. Rock hammer for scale.
- h) St facies, Lambert's Bay. Transverse view. Scale bar length to swivel, 25 cm.

# Plate 4

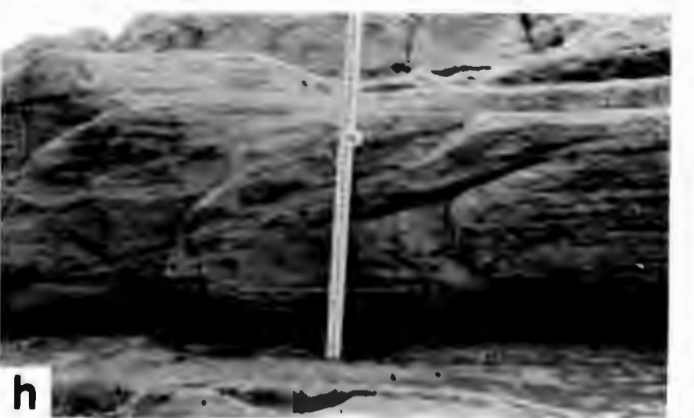
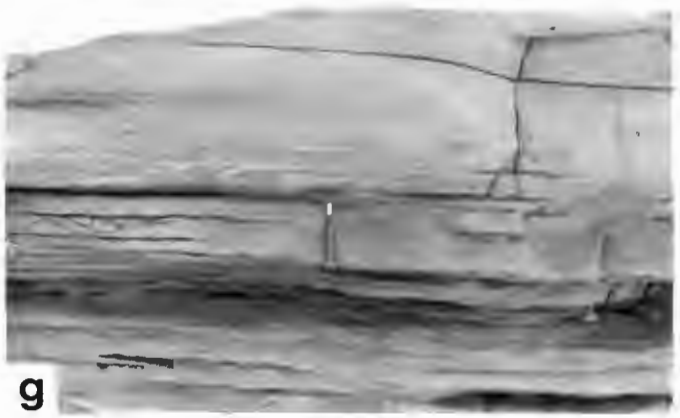
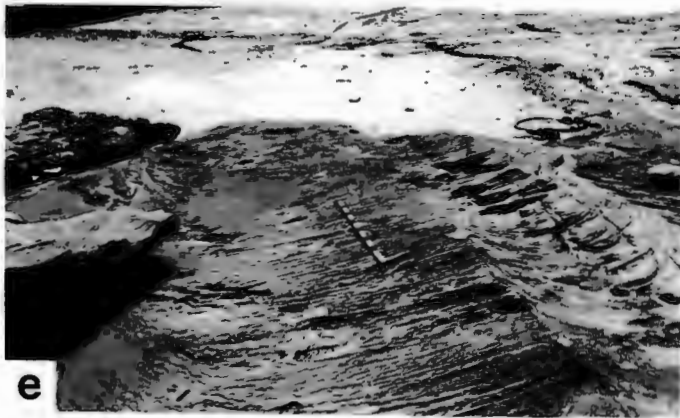
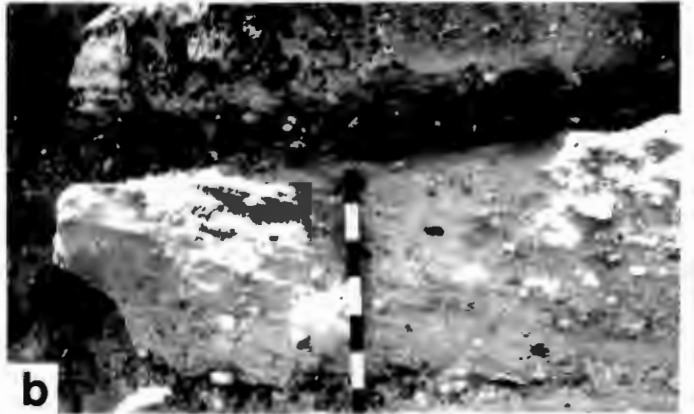
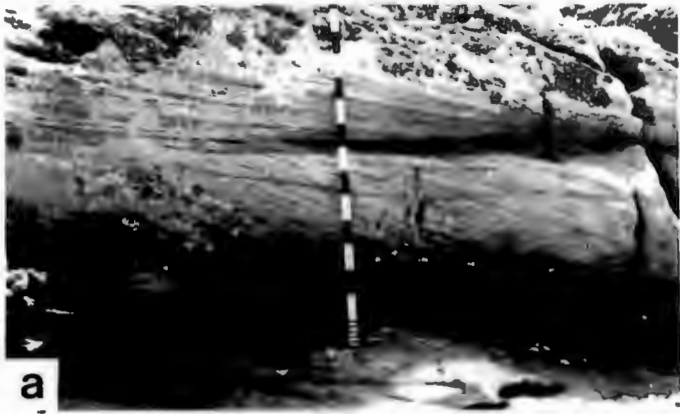


**Table 1**  
**Stratigraphy of the Table Mountain Group**  
 (after SACS\*, 1980)

Group	Formation	Lithology
Table Mountain	Nardouw <sup>\$\$</sup>	Arenite
	Cedarberg	Shale and siltstone
	Pakhuis	Diamictite

(minor local unconformity)

Peninsula	Arenite
Graafwater <sup>##</sup>	Arenite, shale and (minor) conglomerate
Piekenierskloof <sup>##</sup>	Arenite and conglomerate

(major regional unconformity except where Klipheuwel Formation  
developed)

Klipheuwel <sup>##</sup>	Arenite, shale and conglomerate.
--------------------------	-------------------------------------

<sup>##</sup>: Aspects of these Formations dealt with in this thesis.

<sup>\$\$</sup>: Raised to Subgroup status by J.N. Theron and co-workers at the Geological Survey, P.O. Box 572 Bellville, 7535, South Africa, but lacks formal SACS approval to date (July, 1988).

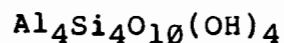
\*: Abbreviation for the South African Committee for Stratigraphy, (SACS), 1980. Stratigraphy of South Africa, South West Africa/Namibia, and the Republics of Bophuthatswana, Transkei, and Venda. (Comp., L.E. Kent). Geol. Surv. Handbook Nr. 8.

**TABLE 2**

**Microprobe analyses of euhedral kaolinites in Graafwater  
Formation Arenites**

F	-	0.24	-	-	-	-
Na <sub>2</sub> O	-	-	-	0.03	-	0.04
K <sub>2</sub> O	-	-	-	-	0.04	0.05
SiO <sub>2</sub>	42.75	45.35	46.78	46.85	47.11	46.59
TiO <sub>2</sub>	-	-	-	-	-	-
Al <sub>2</sub> O <sub>3</sub>	37.43	39.14	39.37	39.22	39.76	39.54
Cr <sub>2</sub> O <sub>3</sub>	-	-	-	-	-	-
FeO	0.11	-	-	0.13	-	0.18
MnO	-	-	-	-	-	0.05
MgO	0.03	-	0.03	0.04	-	0.07
CaO	0.07	0.04	0.05	-	0.04	-
NiO	-	-	-	-	-	-
<b>Total</b>	<b>80.39</b>	<b>84.76</b>	<b>86.23</b>	<b>86.27</b>	<b>86.95</b>	<b>86.52</b>
<b>Molecular</b>	<b>1.94</b>	<b>1.97</b>	<b>2.02</b>	<b>2.03</b>	<b>2.01</b>	<b>2.00</b>
SiO <sub>2</sub> / Al <sub>2</sub> O <sub>3</sub>						

**Ideal Kaolinite is**



**Atomic proportions based on 14(O)**

Si	3.941	3.971	4.011	4.020	4.008	3.989
Al	4.063	4.037	3.978	3.962	3.985	3.989
Fe	0.011	-	-	0.010	-	0.015
Mg	-	-	0.005	0.005	-	0.010
Ca	0.006	0.005	0.005	-	0.005	-
Na	-	-	-	0.002	-	0.010
K	-	-	-	-	0.004	0.010
Mn						0.005
<b>Sum</b>	<b>8.017</b>	<b>8.013</b>	<b>7.999</b>	<b>7.999</b>	<b>8.002</b>	<b>8.028</b>

‡ 2 ‡ 5 ‡ 6 ‡ 7 ‡ 8 ‡ 9

**TABLE 3**

**Microprobe analyses of pyrophyllite in  
Piekenierskloof Formation Arenites**

	# 1	# 8	# 10	# 11	# 12	# 13
Na <sub>2</sub> O	0.06	-	0.07	0.11	0.14	0.10
K <sub>2</sub> O	-	0.03	0.09	0.05	0.12	-
SiO <sub>2</sub>	67.44	65.73	61.18	58.14	52.63	64.84
TiO <sub>2</sub>	-	-	-	-	0.04	-
Al <sub>2</sub> O <sub>3</sub>	29.04	28.75	27.04	25.86	22.94	28.09
FeO	0.24	0.28	0.35	0.36	0.64	0.34
MgO	-	0.02	0.05	0.09	0.20	0.07
CaO	-	0.03	0.05	0.07	0.04	0.07
<b>Total:</b>	<b>96.86</b>	<b>94.84</b>	<b>88.83</b>	<b>84.68</b>	<b>76.75</b>	<b>93.51</b>
<b>Molecular</b>						
SiO <sub>2</sub> / Al <sub>2</sub> O <sub>3</sub>	3.9	3.9	3.8	3.8	3.9	3.9

**Atomic proportions based on 22 oxygens  
Ideal pyrophyllite is Al<sub>4</sub>Si<sub>8</sub>O<sub>20</sub>(OH)<sub>4</sub>**

Na	0.013	0.004	0.016	0.030	0.042	0.023
K	-	0.004	0.015	0.008	0.023	-
Si	7.947	7.916	7.884	7.860	7.877	7.920
Ti	-	-	-	-	0.004	-
Al	4.032	4.080	4.106	4.120	4.047	4.040
Fe	0.031	0.029	0.037	0.040	0.080	0.035
Mg	-	0.02	0.009	0.019	0.044	0.013
Ca	-	0.004	0.006	0.010	0.006	0.009
<b>Sum:</b>	<b>12.023</b>	<b>12.037</b>	<b>12.073</b>	<b>12.087</b>	<b>12.123</b>	<b>12.056</b>

**TABLE 4**

Microprobe analyses of authigenic illites  
Graafwater and Klipheuwel Formation Arenites

	#10	#12	#13	#14	#15	#16
Na <sub>2</sub> O	0.05	0.10	0.06	0.08	0.06	0.15
K <sub>2</sub> O	8.99	9.34	9.27	8.76	8.64	8.99
F	-	0.11	-	-	-	-
SiO <sub>2</sub>	48.01	47.70	46.06	46.78	47.44	46.28
TiO <sub>2</sub>	0.09	0.16	0.07	-	-	0.04
Al <sub>2</sub> O <sub>3</sub>	31.93	31.32	30.81	33.99	33.80	34.92
Cr <sub>2</sub> O <sub>3</sub>	-	-	-	-	-	-
FeO	1.99	2.37	1.83	1.41	1.55	1.83
MnO	-	-	-	-	-	-
MgO	1.26	1.77	1.50	0.80	0.82	0.61
CaO	0.21	0.12	0.17	0.16	0.21	0.12
Total:	92.53	92.99	89.77	91.98	92.52	92.94

Atomic Proportions Based on 22 Oxygens

Na	0.013	0.027	0.018	0.021	0.015	0.039
K	1.556	1.619	1.661	1.519	1.488	1.550
F	-	0.049	-	-	-	-
Si	6.512	6.484	6.469	6.356	6.403	6.253
Ti	0.009	0.016	0.008	-	-	0.004
Al	5.104	5.018	5.101	5.442	5.377	5.560
Cr	-	-	-	-	-	-
Fe	0.226	0.270	0.215	0.161	0.175	0.207
Mn	-	-	-	-	-	-
Mg	0.255	0.358	0.313	0.161	0.165	0.124
Ca	0.031	0.018	0.025	0.023	0.030	0.017
Sum:	13.706	13.859	13.810	13.683	13.653	13.754

- = not detected

# 10, 12, 13, 14, 15 & 16 : Rock K204

Table 4 cont.

	#17	#18	#22	# 4	# 6	#16
Na <sub>2</sub> O	0.02	0.05	0.08	0.07	0.04	0.09
K <sub>2</sub> O	7.53	8.31	7.49	9.14	8.66	8.73
F	-	-	-	-	-	-
SiO <sub>2</sub>	43.86	47.55	46.89	47.87	45.91	48.11
TiO <sub>2</sub>	-	-	-	0.06	-	0.54
Al <sub>2</sub> O <sub>3</sub>	30.42	33.94	30.17	35.84	34.03	30.91
Cr <sub>2</sub> O <sub>3</sub>	-	-	-	-	-	-
FeO	1.80	1.64	3.08	1.84	2.29	5.84
MnO	-	-	-	-	-	-
MgO	1.26	0.83	0.84	0.27	0.29	1.11
CaO	0.14	0.29	0.18	-	0.21	-
Total	:85.03	92.61	88.71	95.09	91.43	95.33

## Atomic proportions based on 22 (O)

Na	0.007	0.012	0.016	0.018	0.011	0.023
K	1.410	1.427	1.349	1.536	1.518	1.494
F	-	-	-	-	-	-
Si	6.436	6.401	6.613	6.304	6.304	6.455
Ti	-	-	-	0.006	-	0.054
Al	5.261	5.385	5.015	5.562	5.507	4.888
Cr	-	-	-	-	-	-
Fe	0.221	0.184	0.364	0.202	0.263	0.656
Mn	-	-	-	-	-	-
Mg	0.275	0.167	0.177	0.054	0.059	0.222
Ca	0.022	0.042	0.026	-	0.031	-
Sum:	13.632	13.618	13.560	13.682	13.693	13.792

- = not detected

# 17, 18 &amp; 22 : Rock K204

# 4, 6, &amp; 16 : Rock K206

Table 4 cont.

	#17	#15	#14	#13	#12	#11
Na <sub>2</sub> O	0.04	0.52	0.05	0.08	0.32	0.04
K <sub>2</sub> O	8.84	10.60	8.66	8.80	9.73	9.44
F	-	0.35	-	-	-	-
SiO <sub>2</sub>	47.85	44.44	47.96	49.51	45.00	41.73
TiO <sub>2</sub>	-	0.73	-	0.06	0.34	-
Al <sub>2</sub> O <sub>3</sub>	35.11	35.34	30.86	35.51	34.26	30.97
Cr <sub>2</sub> O <sub>3</sub>	-	-	-	-	-	-
FeO	2.75	1.50	3.17	2.08	2.32	2.40
MnO	-	-	-	-	-	-
MgO	0.36	0.58	1.44	0.36	0.53	0.51
CaO	0.09	-	0.13	0.12	-	-
Total:	95.11	94.06	92.27	96.52	92.50	85.09

## Atomic proportions based on 22 ( O )

Na	0.010	0.137	0.012	0.020	0.084	0.011
K	1.489	1.837	1.508	1.453	1.703	1.801
F	-	0.151	-	-	-	-
Si	6.321	6.041	6.551	6.406	6.174	6.239
Ti	0.006	0.074	-	0.006	0.035	-
Al	5.466	5.662	4.968	5.415	5.539	5.457
Cr	-	-	-	-	-	-
Fe	0.303	0.171	0.362	0.225	0.267	0.299
Mn	-	-	-	-	-	-
Mg	0.072	0.118	0.294	0.069	0.108	0.114
Ca	0.013	-	0.019	0.017	-	-
Sum :	13.680	14.191	13.714	13.611	13.910	13.578

# 17, 15, 14, 13, 12 &amp; 11 : Rock K207

Table 4 cont.

	#10	#23	#25
Na <sub>2</sub> O	0.04	0.20	0.16
K <sub>2</sub> O	8.50	6.50	6.83
F	-	-	-
SiO <sub>2</sub>	49.28	52.42	51.35
TiO <sub>2</sub>	0.07	-	-
Al <sub>2</sub> O <sub>3</sub>	36.01	35.13	32.80
Cr <sub>2</sub> O <sub>3</sub>	-	-	-
FeO	2.01	0.73	0.88
MnO	-	-	-
MgO	0.21	1.03	1.16
CaO	0.20	-	-
Total:	96.35	96.01	93.18

## Atomic proportions based on 22 ( O )

Na	0.018	0.050	0.041
K	1.402	1.051	1.143
F	-	-	-
Si	6.375	6.647	6.734
Ti	0.007	-	-
Al	5.490	5.250	5.424
Cr	-	-	-
Fe	0.218	0.078	0.097
Mn	-	-	-
Mg	0.040	0.195	0.227
Ca	0.028	-	-
	13.578	13.271	13.312
Sum :			

# 10: Rock no: K206

# 23 &amp; 25 : Rock no : K207

TABLE 5

Illite Data

#	K/A	S/A	T*	O*	IL	K <sub>2</sub> O	A%	B%	C%
-----									
Rock	K 204								
10	0.30	2.55	-1.48	-0.23	+1.63	8.99	46	52	2
12	0.32	2.59	-1.50	-0.19	+1.69	9.34	47	50	3
13	0.33	2.53	-1.52	-0.20	+1.73	9.27	48	49	3
14	0.28	2.34	-1.64	+0.05	+1.59	8.76	43	55	2
15	0.28	2.38	-1.60	+0.01	+1.56	8.64	43	55	2
16	0.28	2.25	-1.74	+0.12	+1.62	8.99	43	56	1
17	0.27	2.45	-1.56	-0.08	+1.46	8.73	41	56	3
18	0.27	2.38	-1.60	+0.06	+1.52	8.31	42	56	2
22	0.27	2.64	-1.39	-0.04	+1.42	7.49	41	57	2
-----									
Rock	K 206								
4	0.28	2.27	-1.69	+0.13	+1.66	9.14	42	57	1
6	0.28	2.29	-1.70	+0.07	+1.59	8.66	43	56	1
16	0.31	2.64	-1.50	-0.05	+1.52	8.73	42	56	2
17	0.27	2.31	-1.68	+0.16	+1.53	8.84	42	58	0
10	0.26	2.32	-1.62	+0.13	+1.48	8.50	41	58	1
11	0.33	2.29	-1.76	-0.08	+1.81	9.44	44	53	3
14	0.30	2.64	-1.45	-0.13	+1.56	8.66	44	53	3
13	0.27	2.34	-1.59	+0.07	+1.51	8.80	42	54	4
15	0.33	2.13	-1.69	+0.50	+1.98	10.6	49	49	2
12	0.31	2.23	-1.79	0.0	+1.79	9.73	46	53	1
-----									
Rock	K 207								
25	0.20	2.53	-1.27	+1.1	+1.10	6.50	34	64	2
23	0.23	2.65	-1.35	+0.25	+1.18	6.83	36	61	3
-----									

Table 5 cont.

Column Headings :

# : Analysis number. K/A : molecular ratio of  $K_2O$  to  $Al_2O_3$   
S/A : molecular ratio of  $SiO_2$  to  $Al_2O_3$   
T\* : tetrahedral site charge, calculated from the atomic proportions based on 22 (O) .  
+ or - : excess or charge deficiency present in calculation  
O\* : octahedral site charge  
Il : interlayer charge  
K<sub>2</sub>O : %  $K_2O$  in raw microprobe analysis

A%, B% and C% are co-ordinates in a triangular plot, where A is the  $MR^3$  component, B the  $2R^3$  component and C the  $3R^2$  component and these components are calculated from the atomic proportion data as follows :

- (1) - Convert the raw microprobe analysis to relative atomic proportions of the elements present;
- (2) - Set the  $Na + K + 2Ca$  as =  $M^+R^3$  component;
- (3) - The  $R^3$  component is calculated by adding  $Al + Fe^{3+}$  . Since  $R^{3+}$  is present in the  $MR^3$  component one must subtract the value of the  $M^+R^{3+}$  component from the  $Al + Fe^{3+}$  . The remainder is halved to give  $2R^3$ .
- (4)  $Mg$  and  $Fe^{2+}$  is summed and divided by three to give  $3R^2$  ;
- (5) the values of the three components are **summed** and each component is divided by the total to give atomic percentages.

These are given above as A, B, and C.

This method of calculating these components is that of :

Velde, B. (1985) Clay Minerals. A physico-chemical explanation of their occurrence. Developments in sedimentology 40. Elsevier , Amsterdam, 427pp.

The method given above is outlined on p. 39, and several of these plots are illustrated in this text on p. 41 (Figure 6), p. 73 (Figure 14a), p. 74 (Figure 14.b) and p. 75 (Figure 15).

Table 5 cont.

The analyses given above conform to the standard set by Velde, (1985 p. 4) where the following site occupancies disqualified an analysis from use : > 6.1 octahedral ions, >8.1 tetrahedral ions and > 2.2 interlayer ions per  $O_{20}(OH)_4$ .

There are problems with the allocation of Fe in microprobe analysis, as both  $Fe^{2+}$  and  $Fe^{3+}$  are present. As all Fe is calculated as  $Fe^{2+}$  in these analyses and the proportion of Fe is usually small, the  $MR^3-2R^3-3R^2$  diagram is not badly distorted.

---

TABLE 6

## Representative Feldspar Analyses

Na <sub>2</sub> O	0.91	1.15	1.08	2.06	1.18	1.19
K <sub>2</sub> O	14.91	14.85	15.04	13.27	15.13	15.19
SiO <sub>2</sub>	66.07	66.34	66.32	65.96	65.98	65.76
Al <sub>2</sub> O <sub>3</sub>	17.81	18.42	18.05	18.29	18.10	17.83
FeO	0.17	-	-	-	-	-
MgO	-	-	-	-	-	-
CaO	-	0.04	-	-	-	-
Total:	99.93	100.80	100.49	99.58	100.39	99.97
Ab:	8.46	10.48	9.7	19.06	10.60	10.61
Or:	91.25	89.32	90.13	80.94	89.40	89.39
An:	0.30	0.20	-	-	-	-
Rock No:	K207	K207	K205	K205	K205	K205
Analysis No:	3	7	25	26	28	42
K <sub>2</sub> O	15.03	14.57	14.78	15.19	16.05	15.37
SiO <sub>2</sub>	65.04	65.48	65.29	65.86	66.57	66.88
Al <sub>2</sub> O <sub>3</sub>	18.46	17.88	18.39	18.01	17.94	18.05
FeO	-	0.19	-	-	-	-
MgO	-	-	-	-	-	-
CaO	0.07	0.06	0.08	-	-	-
Total	99.39	99.30	99.41	99.83	101.10	101.24
Ab	7.33	10.43	8.18	7.17	4.88	8.52
Or	92.31	89.27	91.42	92.72	95.06	91.40
An	0.36	0.30	0.40	0.11	0.07	0.08
Rock no:	K207	K207	K207	K207	K207	K207
Analysis#:	1	2	4	5	6	8

Table 6 cont.

Na <sub>2</sub> O	0.87	0.75	0.60	0.93	0.94	0.82
K <sub>2</sub> O	15.73	16.02	15.97	14.77	15.49	15.44
SiO <sub>2</sub>	65.51	64.86	65.97	66.53	65.08	65.43
Al <sub>2</sub> O <sub>3</sub>	18.11	17.85	18.08	18.61	17.94	18.02
FeO	-	-	0.11	-	-	-
MgO	-	-	-	-	-	-
CaO	-	-	-	-	-	-
Total	100.22	99.48	100.73	100.84	99.45	99.71
Ab	7.75	6.63	5.37	8.74	8.48	7.47
An	92.25	93.37	94.63	91.26	91.52	92.53
Rock no:K205	K205	K205	K205	K205	K205	K205
Analysis#: 1	4	5	6	17	18	
Na <sub>2</sub> O	0.80	0.64	0.84	0.75	0.64	0.96
K <sub>2</sub> O	15.73	15.75	15.32	15.47	15.51	15.36
SiO <sub>2</sub>	65.21	65.58	65.10	65.28	65.74	65.24
Al <sub>2</sub> O <sub>3</sub>	17.97	18.14	17.96	17.62	18.09	18.00
FeO	-	-	-	0.14	0.12	-
MgO	-	-	-	-	-	-
CaO	-	-	-	-	-	-
Total:	99.71	100.12	99.22	99.26	100.10	99.56
Ab:	7.21	5.89	7.69	6.88	5.93	8.65
Or:	92.79	94.11	92.31	93.10	94.07	91.29
An:	-	-	-	0.02	-	0.07
Rock No: K205	K205	K205	K204	K204	K204	K204
Analysis#: 38	39	40	1	2	3	

Table 6 cont.

Na <sub>2</sub> O	0.79	0.37	0.75	1.08	0.86	0.92
K <sub>2</sub> O	15.61	16.41	15.56	15.17	11.11	15.43
SiO <sub>2</sub>	66.08	64.80	65.56	64.91	68.46	64.96
Al <sub>2</sub> O <sub>3</sub>	17.96	17.41	17.71	17.85	18.93	18.03
FeO	0.14	0.11	0.14	-	0.14	-
MgO	-	-	-	-	-	-
CaO	-	-	-	-	-	-
Total:	100.58	99.10	99.72	99.01	99.50	99.34
Ab:	7.11	3.27	6.80	9.73	10.48	8.32
Or:	92.75	96.73	93.15	90.15	89.52	91.62
An:	0.14	-	0.05	0.12	0.01	0.06
Rock no:	K204	K204	K204	K204	K204	K204
Analysis#:	6	7	8	10	12	14



Table 7 cont.

Point count data				
	mean	s	range	N
Qm	26,9	5,9	20,5-37,9 %	10
Qp1	6,2	3,0	1,8-12,1 %	10
Qp2	11,5	9,0	2,4-29,7 %	10
F	16,4	8,9	3,6-33,2 %	10
L	14,1	4,6	6,6-23,0 %	10
Q*	0,63	0,16	0,38-0,83	
Q	59,0	12,0	37,2-73,2 %	10
F1	19,5	10,4	5,4-42,9 %	10
L1	14,0	4,6	6,6-23,0 %	10
Qm1	36,1	8,2	26,6-47,7 %	10
Lt	41,3	9,0	25,3-59,5 %	10
M	15,8	3,8	10,0-21,6 %	10
C	6,7	6,2	0,5-20,1 %	10
Sum A (sum of number of points in original analyses of sandstones in this group)				5394
Sum B (sum of number of points in recalculated analyses of sandstones in this group)				4028

Component mean: mean percentage of indicated component in N samples. Component standard deviation (s): standard deviation of indicated component in N samples (here each sample is one thin section).

**TABLE 8**

**Mean Modal Analyses of Piekenierskloof Formation  
Arenites in Volume Percent  
(arenites containing pyrophyllite)**

-----  
Point count data  
-----

	mean	s	range	N
Qm	48,6	7,5	37,0-59,0 %	12
Qp1	11,4	4,9	3,0-20,0 %	10
Qp2	12,8	7,6	4,0-25,0 %	10
F	-	-	- - -	12
L	4,0	3,6	0 -10,3 %	12
Q*	0,67	0,12	0,46-0,82	
Q	94,4	5,0	85,3-100 %	12
Fl	-	-	- - -	12
L1	5,0	4,7	0 -14,7 %	12
Qm1	63,8	11,6	41,4-80,5 %	12
Lt	35,9	11,5	19,5-58,6 %	12
M	14,6	8,5	2,5-24,8 %	12
C	7,6	3,6	2,5-14,2 %	12

-----  
Sum A (number of points in the original analyses) 5813  
Sum B (number of points in the recalculated analyses) 4608  
-----

**TABLE 9**

Mean Modal Analyses of Piekenierskloof Formation  
 Arenites in Volume Percent  
 (Arenites without pyrophyllite)

---

Point count data

---

Component	mean	s	range	N
Qm	54,2	6,6	40,1-63,6 %	11
Qp1	9,6	3,6	5,3-16,4 %	11
Qp2	14,0	8,7	8,0-38,8 %	11
F	-	-	- - -	11
L	2,3	1,7	0 - 5,4 %	11
Q*	0,704	0,100	0,48-0,80	11
Q	96,8	2,3	92,7-100 %	11
F1	-	-	- - - %	11
L1	2,9	2,3	0 - 7,3 %	11
Qm1	68,1	9,3	46,4-76,4 %	11
Lt	31,7	9,6	21,7-53,6 %	11
M	9,7	3,5	5,0-14,8 %	9
C	11,7	5,4	5,2-19,1 %	11

---

Sum A (number of points in the original analyses)      6202  
 Sum B (number of points in the recalculated analyses) 4979

---

TABLE 10

Mean Modal Analyses of Graafwater Formation  
Arenites in Volume Percent

---

Point count data

---

	mean	s	range	N
Qm	52,6	11,9	22,5-66,8 %	22
Qp1	7,2	3,7	3,5-18,8 %	22
Qp2	11,7	10,8	1,0-36,7 %	22
F	1,6	2,0	0 - 6,0 %	22
L	5,1	4,6	0 -22,7 %	22
Q*	0,75	0,15	0,33-0,92	22
Q	91,1	5,6	74,51-98,2 %	24
F1	2,0	2,6	0 - 7,7 %	24
L1	6,8	4,7	0,8-24,0 %	24
Qm1	68,8	15,8	24,3-90,2 %	24
Lt	29,2	15,7	14,2-75,2 %	24
M	8,7	6,9	1,1-20,3 %	24
C	12,0	7,6	1,7-26,5 %	22

---

Sum A (Number of points in original analyses) 14267

Sum B (Number of points in recalculated\* analyses) 11215

---

\*Recalculated analyses are matrix and cement free analyses based on Dickenson's scheme.

TABLE 11

CLAST COMPOSITIONS AND PROPORTIONS  
AT SELECTED SITES AT LAMBERT'S BAY

nA	%A	nB	%B	nC	%C	nD	%D	nE	%E	nF	%F	NN
60	45.5	21	15.9	36	27.3	2	1.5	5	3.8	8	6.1	132
45	38.8	4	3.4	50	43.1	-	-	9	7.8	8	6.9	116
60	53.1	3	2.7	39	34.5	3	2.7	-	-	8	7.1	113
82	68.9	3	2.5	26	21.8	-	-	1	-	7	5.9	119
55	50.9	2	1.9	35	32.4	-	-	8	7.4	8	7.4	108
65	57.0	6	5.3	37	32.5	-	-	1	0.9	5	4.4	114
61	53.8	1	0.9	39	34.2	-	-	7	6.1	6	5.3	114
64	59.3	-	-	25	23.1	2	1.9	11	10.2	6	5.6	108
56	52.3	16	15.0	22	20.6	1	0.9	7	6.5	5	4.7	107
78	66.1	2	1.7	23	19.5	-	-	7	5.9	8	6.8	118
												Sum
<b>A</b>		<b>B</b>		<b>C</b>		<b>D</b>		<b>E</b>		<b>F</b>		
626		58		332		8		56		69	<b>TOTAL:</b>	1149
<b>Percentages</b>												
<b>A</b>		<b>B</b>		<b>C</b>		<b>D</b>		<b>E</b>		<b>F</b>		
54.4		5.0		28.9		0.7		4.9		6.0	<b>TOTAL:</b>	100

**Methodology**

The clast type was noted on horizontal exposure for between 100-200 clasts in a 1m<sup>2</sup> grid at 10 localities selected at random in Gm(d), Gm, Gp, Gl and Gi facies.

**Clast types**

A: quartzite and chert B: sandstone C: veinquartz D: conglomerate

E: quartzose metamorphic, foliated and quartz veined, jointed

F: other petromict clasts including red jasper, acid volcanic, and melanocratic hornfels.

**TABLE 12**  
**PIEKENIERSKLOOF FORMATION PEBBLE SIZE DATA**  
 (LAMBERT'S BAY VERTICAL PROFILE)  
 (Long axis only)

Pebble length measurements were made at given heights on the Lambert's Bay vertical profile. Measurements are estimates of the largest clast size and are calculated by measuring the long axes of the 30 (in one case 27) largest clasts encountered 1-5m either side of the line of section (Heward, 1978).

Height (m)	Number of measurements	Length in mm		Length in phi	
		X	S	X	S
122	30	142.3	21.2	-7.14	0.21
117	30	112.8	23.4	-6.92	0.26
111	30	129.4	25.0	-7.00	0.26
109	30	142.0	24.9	-7.13	0.24
102	30	133.5	26.4	-7.03	0.26
99	30	139.5	22.1	-7.11	0.22
92	30	98.8	19.3	-6.60	0.26
86	30	130.6	31.7	-6.99	0.31
75	30	123.0	22.7	-6.92	0.25
68	30	109.7	19.2	-6.76	0.26
49	30	107.0	21.8	-6.72	0.26
22.5	27	122.3	28.5	-6.90	0.31
11	30	128.4	25.1	-6.98	0.26
5.5	30	179.7	22.5	-7.47	0.19
0	30	114.0	23.4	-6.80	0.28

X and S (mm): mean and standard deviation of N clasts, clast A axis in millimeters.

X and S (Phi): mean and standard deviation of N clasts, Clast A axis calculated phi value where

$$\text{phi} = -(\log_{10} (\text{mm}) / \log_{10} 2).$$

Maximum clast size is thus usually in the cobble range.

**TABLE 13**  
**PALAEOCURRENT STATISTICS**

**STATISTICS AND ABBREVIATIONS:**

n = number of palaeocurrent measurements at a particular locality  
 v = sum of cosines of azimuthal data  
 w = sum of sines of azimuthal data  
 Vm = vectorial mean ( $= \tan^{-1} w/v$ )  
 r = vectorial magnitude ( $(v^2 + w^2)^{1/2}$ )  
 l = consistency ratio ( $r/n$ )  
 s = angular deviation ( $[2(1-l)^{1/2}]$ )  
 s<sup>2</sup> = square of angular deviation (in degrees squared)

Loc.	n	v	w	Vm	r	l	s	s <sup>2</sup>
1	51	4.50	24.27	79	24.68	0.822	0.60	1163
2	21	8.99	16.80	118	19.05	0.907	0.43	610
3	51	-25.65	28.84	132	37.67	0.724	0.70	1600
4	14	-8.40	-9.15	227	12.42	0.887	0.48	740
5	11	-6.22	7.14	130	9.68	0.879	0.49	791
6	30	-10.50	19.98	117	22.57	0.752	0.70	1625
7	20	-1.66	-5.84	254	6.07	0.304	1.18	4570
8	14	-11.50	4.64	158	12.40	0.889	0.48	749

Location 1: Trough axes measured on the wave cut platform, Elands Bay, Klipheuwel Formation.

Location 2: Trough axes measured in the Piekenierskloof Formation, west of the fish factory, Elands Bay.

Location 3: Trough axes and foreset azimuths measured in the Piekenierskloof Formation between Lambert's Bay Canning Factory and the tidal pool.

Location 4: Trough axes and foreset azimuths measured in the Piekenierskloof Formation, west of the Sishen-Saldanha railway line.

Location 5: Trough axes measured in the Piekenierskloof Formation south of Lambert's Bay.

Location 6: Foreset azimuths measured in the Graafwater Formation on the beach below the caravan site, Lambert's Bay.

Location 7: Foreset azimuths measured in the Faroo Member, Graafwater Formation, at Carstensberg Pass, R364.

Location 8: Foreset azimuths measured in the Piekenierskloof Formation at Piekenierskloof Pass.

0  
TABLE 14

PIEKENIERSKLOOF FORMATION FACIES DEFINITIONS AND INTERPRETATIONS

FACIES CODE	DESCRIPTION	INTERPRETATION
Gm(d)	Massive, inversely graded to ungraded matrix* supported pebble to cobble conglomerate; poorly sorted, poor to no stratification; poor a(p)a(i) imbrication.	Traction carpet, high stage flow; deposition from decelerating high concentration dispersion; sediment gravity flow.
Gm	Massive, ungraded to normally graded clast supported pebble to cobble conglomerate.	Deposition from decelerating high concentration dispersion, gravel bedform. bedform.
Gi	Low-angle cross-bedded pebble to cobble conglomerate; may be interbedded with coarse sand to granule conglomerate on foreset with coarse tail normal grading and matrix* inversely graded.	Gravel bedform margin; lateral accretion surfaces; reworked low stage dilute flow gravel bedform and lateral accretion surface.
G1	Thin, 2-3 pebble diameters, pebble to cobble lag; may be clast supported, matrix infiltrated.	Channel floor or bar top armour; dilute stream flow.
Gp	Planar cross-bedded pebble to cobble conglomerate; may be clast or matrix supported, other foresets may be pebbly coarse sand to granule conglomerate.	Gravel bar accretion surface.
Gt-St	Trough cross-bedded pebbly coarse-grained sand to granule conglomerate; solitary or grouped bedforms. May be gradational down set or upwards into St facies which is finer grained.	Two to three dimensional dunes, channel fills; lower flow regime sandy and gravel bedforms, (macroform component).
Sp	Sand, medium- to very coarse-grained, may be pebbly; solitary or grouped bedforms may have tangential or sharp foreset intersection with lower bounding surface.	Lingoid and transverse sandy bedforms; if grain size coarsens upwards may be macroform.

Sl	Sand, medium- to coarse-grained may be pebbly; low-angle (lee < 10°) cross-bedded.	Suspension fallouts in lee of low amplitude bedform, scour fills, bedform accretion surface.
Sh	(a) Sand, medium- to coarse-grained, laminated and horizontally bedded.  (b) Rare medium- to coarse-grained sand, indistinctly bedded, gradational intrastratal contacts, oversized pebble to cobble clasts present.	Lower to upper regime regime planar flow flat bed phase; bar top sands. Hyperconcentrated flood flow.
M	Mudrock, finer grained than fine sand, massive, coloured red and purple, oxidised.	Suspension fallout abandoned channel fill.

---

\*: matrix: medium to very coarse sand and granule conglomerate.

---

TABLE 15

CLASSIFICATION AND CHARACTERISTICS  
OF FLOW PROCESSES AND DEPOSITS  
after, Smith, 1986

Flow type:	Debris flow	Hyperconcentrated flow	Normal stream flow
Character:	Laminar at time of deposition, may be turbulent on steep slopes	Partly turbulent at all times	Fully turbulent
Sediment support mechanism	Matrix strength, grain dispersive pressure and buoyancy	Turbulence, grain dispersive pressure and buoyancy	Turbulence
Mode of deposition	En masse	Rapid grain by grain aggradation from both suspension and traction	Grain by grain dominated by traction
Stratification	None within depositional units	None or horizontal stratification, no cross stratification	Conglomerate: massive or horizontal stratification. Sandstone: cross stratification and horizontal stratification
Grading	None, reverse to normal	Commonly normal	Variable as a result of sequential processes
Conglomerate	Matrix support rarely clast support	Clast support with polymodal, poorly sorted matrix	Clast support with distinctly finer matrix of infiltrated sand
Clast A axis orientation	Variable flow parallel minor imbrication	Larger pebbles perpendicular smaller clasts parallel, poor imbrication	Perpendicular, well imbricated

## APPENDIX 1

### SAMPLE LOCATION AND DESCRIPTION

Each sample number contains a Formation code: K for the Klipheuwel Formation, P for the Piekenierskloof Formation and G for the Graafwater Formation.

-----  
 UCT Collection \* Field Sample \* Grain \* Latitude \* Longitude  
 Number \* Number \* Size \* \*  
 -----

13373	K 204a	vcs	32°32' S	18°27' E
13374	K 205	ms	32°32.5' S	18°27' E
13375	K 202	fs	32°19' S	18°20' E
13376	K 206	ms	32°32' S	18°27' E
13377	K 204b	vcs	32°32' S	18°27' E
13378	K 105	ms	32°19' S	18°20' E
13379	K 107	ms	32°19' S	18°20' E
13380	K 207a	ms	32°19' S	18°20' E
13381	K 208	fs	32°19' S	18°20' E
13382	K 207b	ms	32°19' S	18°20' E

13383	P 6115a	cs	32°30' S	18°50' E
13384	P 1853	vcs	32°37' S	18°58' E
13385	P 6120	cs	32°13' S	18°27' E
13386	P 6108	cs	32°30' S	18°49' E
13387	P 6112	ms	32°20' S	18°45' E
13388	P 9102	cs	32°37' S	18°58' E
13389	P 6852	cs	32°37' S	18°58' E
13390	P 6110	cs	32°27' S	18°48' E
13391	P 6501	cs	32°55' S	19°02' E
13392	P 1851	cs	32°37' S	18°58' E
13393	P 6115b	cs	32°37' S	18°58' E
13394	P 9678	cs	32°05' S	18°20' E
13395	P 6107	vcs	32°19' S	18°20' E
13396	P 6104	ms	32°31' S	18°51' E
13397	P 5851	ms	32°43' S	18°38' E
11382	P 1382	ms	32°43' S	18°38' E

appendix 1 cont.

11384	P 1384	cs	32°43'	S	18°38'	E
13398	P 6103	cs	32°56'	S	18°45'	E
11385	P 1385	ms	32°43'	S	18°38'	E
11383	P 1383	ms	32°43'	S	18°38'	E
13399	P 1852	cs	32°05'	S	18°18'	E
13400	P 1851	vcs	32°37'	S	18°58'	E

---

13401	G 9852	cs	34°05'	S	18°26'	E
13402	G 6121	fs	32°05'	S	18°03.5'	E
13403	G 6406	ms	31°59'	S	18°34.5'	E
13404	G 6403	cs	31°54'	S	18°38'	E
13405	G 6302	fs	31°59'	S	18°34.5'	E
13406	G 2385	ms	34°05.2'	S	18°25.8'	E
13407	G 6303	vcs	31°59'	S	18°34.5'	E
13408	G 6309	ms	31°59'	S	18°34.5'	E
13409	G 6114	ms	32°08'	S	18°38'	E
11390	G 1390	ms	32°43'	S	18°38'	E
11389	G 1389	ms	32°43'	S	18°38'	E
11391	G 1391	ms	32°43'	S	18°38'	E
11386	G 1386	ms	32°43'	S	18°38'	E
11387	G 1387	ms	32°43'	S	18°38'	E
11388	G 1388	ms	32°43'	S	18°38'	E
13410	G 6402	cs	31°54'	S	18°38'	E
13411	G 6307	fs	31°59'	S	18°34.5'	E
13412	G 6308	ms	31°59'	S	18°34.5'	E
13413	G 6305	ms	31°59'	S	18°34.5'	E
13414	G 6304	vfs	31°59'	S	18°34.5'	E
13415	G 6407	ms	31°59'	S	18°34.5'	E
13416	G 6409	ms	31°54'	S	18°38'	E
13417	G 6400	ms	31°54'	S	18°38'	E
13418	G 6401	gC	31°54'	S	18°38'	E

gC: granule conglomerate, 2-4mm grain size.

vcs: very coarse grained sandstone, 1-2mm grain size.

cs: coarse grained sandstone, 0.5-1mm grain size.

ms: medium grained sandstone, 0.25-0.5mm grainsize.

fs: fine grained sandstone, 0.125-0.25mm grain size.

vfs: very fine grained sandstone, 0.0625-0.125mm grain size.

Grain size scale after Udden - Wentworth, (1922).



Appendix 2 cont.

In the plate tectonic classification of sandstone mineralogy (Dickenson, W.R., and Suczek, C.A. (1979). Plate tectonics and sandstone compositions. Am. Assoc. Petrol. Geol. Bull., 63, 2164-2182, Fig. 1.) the notation used is abbreviated as follows:

In the Q-F-L triangle :

CI : craton interior	RO : recycled orogen
TC : transitional continental	BU : basement uplift
DA : dissected arc	TA : transitional arc
UA : undissected arc	

In the Qm-F-Lt triangle, in addition to the above :

M : mixed	QR : quartzose recycled
TR : transitional recycled	LR : lithic recycled

---

Next to each component in the analysis a two standard deviation reliability estimate is given, calculated by the method outlined by Van der Plas and Tobi, (1965), (Van der Plas, L. and Tobi, A.C.(1965), A chart for judging the reliability of point counting results. Amer. J. Sci., 263, 87-90.)

where  $E = 2(100P/N - P^2/N)^{1/2}$

and

N = the number of points ( $N_a$  or  $N_b$ )

P = the percentage of the component

E = two standard deviations

---

Sandstone classification is after McBride, 1963 (McBride, E.F., (1963). A classification of common sandstones. J. sedim. Petrol., 33, 664-669.)

In this classification quartz, chert and quartzite are all grouped at the quartz pole and granite and gneiss at the lithic pole. None of the examined sandstones contain discrete granite or gneiss framework grains so the the inclusion of these components at the lithic pole is not a complicating factor.

Appendix 2 cont.

Component	K204 E	K205 E	K202 E	K206 E	K204 E
Qm	22,5 3,4	24,5 3,7	26,4 3,5	31,5 3,7	21,4 3,7
Qp1	12,1 2,7	3,4 1,6	3,1 1,4	5,8 1,9	6,6 2,2
Qp2	24,9 3,5	9,7 2,6	2,4 1,2	9,5 2,3	29,7 4,1
F	12,9 2,7	33,2 4,0	11,8 2,6	3,6 1,5	10,6 2,8
L	12,2 2,6	6,6 2,1	19,8 3,2	15,7 2,9	10,6 2,8
C	0,5 0,6	1,9 1,2	10,1 2,8	13,2 2,7	3,0 1,5
M	10,6 2,5	18,3 3,3	17,1 3,0	19,4 3,1	17,9 3,4
H	4,3 1,7	0,5	6,1 1,0	1,6 1,0	- -
Q*	0,38	0,65	0,83	0,67	0,37
R	SA	SA-SR	SA-R	A	SA
S	PS	MS	WS	MS	MS
Q	69,5 4,1	48,7 4,9	50,2 5,7	70,8 4,4	73,2 4,5
F	15,3 3,2	42,9 4,9	18,6 3,9	5,4 2,2	13,4 3,4
L	15,2 3,2	8,4 2,7	32,2 4,6	23,8 4,1	13,4 3,4
T1	RO	TC	RO	RO	RO
QM	26,6 3,9	31,8 4,6	41,6 4,9	47,7 4,8	27,1 4,5
LT	48,4 4,4	25,3 4,3	39,8 2,4	46,9 4,9	59,5 5,0
T2	M-TR	DA	M	TR	TR-LR
N <sub>a</sub>	602	536	636	645	501
N <sub>b</sub>	510	415	404	425	395

Appendix 2 cont.

Component K105 E      K107 E      K207a E      K208 E      K207a E

---

Qm	34,1 4,2	37,9 4,1	22,2 3,8	20,5 3,8	28,2 4,1
Qp1	9,1 5,2	6,2 2,1	6,0 2,1	1,8 1,2	7,9 2,5
Qp2	6,3 4,4	12,1 2,8	10,8 2,8	3,1 1,6	6,2 2,2
F	15,2 3,2	16,7 3,2	29,0 4,1	20,3 3,7	10,8 2,9
L	14,4 3,2	12,9 2,9	11,8 2,9	23,0 4,0	13,8 3,2

C	2,4 1,4	4,7 1,9	3,4 1,6	7,8 2,5	20,1 3,7
M	13,6 3,0	10,0 2,6	14,8 3,2	14,4 3,3	21,6 3,8
H	3,3 1,6	0,8 0,8	1,2 1,0	2,4 1,4	1,1 0,9

Q*	0,69	0,66	0,57	0,82	0,67
R	SA	A	SA-SR	A-SA	A
S	MS	MS	MS	WS	PS

---

Q	62,6 4,8	65,9 4,4	48,9 5,0	37,2 5,4	63,2 5,4
F	19,2 3,9	19,1 3,7	36,3 4,8	29,4 5,1	16,2 4,2
L	18,2 3,9	15,0 3,4	14,8 3,6	33,4 5,3	20,6 4,6

---

T1	RO	RO	RO	DA	RO
----	----	----	----	----	----

---

QM	43,1 4,9	43,5 4,7	27,8 4,5	29,7 5,1	42,2 5,6
LT	37,7 4,8	37,4 4,3	35,9 4,8	40,9 5,5	41,6 5,6

---

T2	M	M	TA	DA	M
----	---	---	----	----	---

---

N <sub>A</sub>	508	530	500	464	472
N <sub>B</sub>	401	444	399	320	315

---

Appendix 2 cont.

Component	P6115 E	P1853 E	P9102 E	P6108 E	P6112 E
Qm	46,1 2,3	41,2 4,9	37,0 6,4	54,2 4,5	49,6 4,5
Qp1	- -	12,0 3,3	- -	20,4 3,6	8,4 2,5
Qp2	13,3 1,5	12,8 3,3	39,0 6,5	9,6 2,6	5,8 2,1
F	- -	1,5 1,2	- -	- -	- -
L	10,2 1,4	7,0 2,6	4,0 2,6	1,2 1,0	- -
C	5,0 1,0	4,2 2,0	4,0 2,6	5,6 2,1	8,6 2,5
M	23,7 1,9	22,0 4,1	16,0 4,9	8,6 2,5	24,8 3,9
H	1,4 0,5	- -	- -	- -	2,6 1,4
Q*	0,78	0,62	0,64	0,78	0,76
R	A-SA	SA	R	R	R
S	PS	M-PS	PS	WS	WS
Q	85,3 1,9	88,6 3,7	97,0 2,5	98,6 1,1	100 -
F	- -	2,0 1,6	- -	- -	- -
L	14,7 1,9	9,4 3,7	3,0 2,5	1,4 1,1	- -
T1	RO	RO	CI/RO	CI	CI
QM	66,2 2,5	55,3 5,8	49,0 7,3	63,5 4,7	77,7 4,7
LT	33,8 2,5	42,7 5,8	51,0 7,3	36,5 4,7	22,3 4,7
T2	QR	TR	TR	QR	QR
N <sub>a</sub>	496	400	226	500	500
N <sub>b</sub>	346	398	186	427	319

Appendix 2 cont.

Component	P6120 E	P1852 E	P6852 E	P6110 E	P6501 E
Qm	59,8 4,4	36,9 6,1	46,6 4,5	55,4 3,9	53,1 4,5
Qp1	12,4 2,9	16,1 4,6	7,8 2,4	3,2 1,4	7,2 2,3
Qp2	7,0 2,4	25,0 5,5	8,4 2,5	22,4 3,3	4,0 1,8
F	- -	- -	- -	0,6 0,6	- -
L	2,2 1,3	10,3 3,8	2,6 1,4	2,0 1,1	1,6 1,1
C	14,2 3,1	2,5 2,9	9,2 2,6	8,9 2,7	12,0 2,9
M	4,0 4,4	8,3 3,5	24,4 3,8	6,7 2,0	22,2 3,7
H	- -	- -	1,0 0,9	0,6 0,6	- -
Q*	0,76	0,47	0,74	0,68	0,82
R	R	SA-SR	SA-SR	R	SA-SR
S	WS	MS	PS	MS	WS
Q	97,3 1,6	88,5 4,3	91,1 2,1	96,8 1,5	97,6 1,4
F	- -	- -	- -	0,7 0,7	- -
L	2,7 1,6	11,5 4,3	7,9 2,1	2,5 1,3	2,4 1,4
T1	RO	RO	RO	RO	CI
QM	73,5 4,4	41,4 6,6	71,2 5,0	66,2 4,1	80,5 4,4
LT	26,5 4,4	58,6 6,6	28,2 5,0	33,1 4,1	19,5 4,4
T2	QR	TR	QR	QR	QR
N <sub>a</sub>	500	252	500	639	500
N <sub>b</sub>	407	222	327	535	329

Appendix 2 cont.

Component	P1851 E	P6115a E	P9678 E	P6107 E	P6103 E
Qm	47,0 5,8	56,1 3,2	49,2 4,1	40,1 4,0	61,7 3,3
Qp1	13,3 3,9	12,9 2,1	8,5 2,3	5,3 1,9	10,9 2,1
Qp2	22,3 4,9	10,8 2,0	8,2 2,2	38,8 4,0	11,5 2,1
F	- -	- -	0,2 0,4	0,2 0,3	- -
L	0,3 0,6	6,5 1,6	3,3 1,5	2,2 1,2	3,8 1,3
C	5,6 2,7	10,8 2,0	17,2 3,1	5,3 1,8	11,9 2,2
M	11,3 3,7	2,9 1,1	11,3 2,6	7,0 2,1	- -
H	- -	- -	0,5 0,6	0,2 0,4	- -
Q*	0,57	0,70	0,75	0,48	0,74
R	SA-SR	SA-SR	SA	SA	SA
S	MS	WS	WS	WS	WS
Q	99,6 0,8	92,5 1,8	95,0 2,1	97,3 1,4	95,7 1,5
F	- -	- -	0,2 0,2	0,2 0,4	- -
L	0,4 0,8	7,5 1,8	4,8 2,1	2,5 1,3	4,3 1,5
T1	CI	RO	RO	CI-RO	RO
QM	56,6 6,3	65,0 3,3	70,9 4,4	46,4 4,4	70,2 3,3
LT	43,4 6,3	35,0 3,3	28,9 4,4	53,5 4,4	29,8 3,3
T2	QR	QR	QR	QR	QR
N <sub>A</sub>	300	1000	600	603	872
N <sub>A</sub>	249	863	416	522	766

Appendix 2 cont.

Component	P5851 E	P1382 E	P1384 E	P6104 E	P1385 E
Qm	52,2 4,5	59,4 4,4	55,2 4,0	63,6 4,3	54,6 4,5
Qp1	16,4 3,3	6,6 2,2	6,1 1,9	7,2 2,3	7,0 2,3
Qp2	16,2 3,3	8,2 2,5	8,0 2,2	11,0 2,8	10,4 2,7
F	- -	1,6 1,1	- -	- -	0,6 0,7
L	- -	2,2 1,3	5,4 1,8	1,4 1,1	- -
C	10,2 2,7	15,0 3,2	19,1 3,1	16,4 3,3	16,4 2,3
M	5,0 1,9	6,8 2,3	6,2 1,9	- -	10,8 2,8
H	- -	0,2 0,4	- -	0,4 0,6	0,2 0,4
Q*	0,62	0,80	0,79	0,78	0,76
R	SA	R	SA	R	R
S	MS	WS	WS	WS	MS
Q	100,0 -	95,1 1,9	92,7 2,4	98,3 1,3	99,2 0,9
F	- -	2,1 1,3	- -	- -	0,8 0,9
L	- -	2,8 1,5	7,3 2,4	1,7 1,3	- -
T1	CI	RO	RO	CI	CI
QM	61,6 4,4	76,2 3,8	73,9 4,1	76,4 3,8	75,2 3,9
LT	38,4 4,4	21,7 3,7	26,1 4,1	23,6 3,8	24,0 4,5
T2	QR	QR	QR	QR	QR
N <sub>a</sub>	500	500	627	500	500
N <sub>b</sub>	424	390	468	416	363

Appendix 2 cont.

Component	P1383 E	P1852 E	P1851 E	G9852 E	G6121 E
Qm	57,0 4,4	54,2 4,5	48,6 4,5	59,8 4,2	57,7 4,5
Qp1	7,4 2,3	11,2 2,8	15,8 3,3	9,1 2,5	18,8 3,6
Qp2	12,4 2,9	13,8 3,1	15,2 3,2	11,0 2,7	4,5 1,9
F	- -	- -	- -	- -	0,2 0,4
L	0,6 0,7	2,8 1,5	3,8 1,7	4,3 1,8	5,9 2,1
C	14,8 3,2	4,4 1,8	5,2 2,0	15,8 3,2	3,2 1,6
M	7,8 2,4	13,6 3,1	11,4 2,8	3,5 1,6	8,7 2,6
H	- -	- -	- -	- -	1,0 1,0
Q*	0,78	0,68	0,61	0,75	0,71
R	WR	SR	SA-SR	R	R
S	WS	MS	MS	WS	WS
Q	99,2 0,8	96,6 1,8	95,4 2,0	94,7 2,2	92,9 2,5
F	- -	- -	- -	- -	0,2 0,4
L	0,8 0,8	3,4 1,8	4,6 2,0	5,3 2,2	6,9 2,5
T1	CI	RO	RO	RO	RO
QM	73,6 3,9	66,1 4,7	58,3 4,8	74,1 4,2	66,2 4,6
LT	26,4 3,9	33,9 4,7	41,7 4,8	25,9 4,2	33,6 4,6
T2	QR	QR	QR-TR	QR	QR
N <sub>a</sub>	500	500	500	537	485
N <sub>b</sub>	387	410	417	433	423

Appendix 2 cont.

Component	G6406 E	G6403 E	G6302 E	G2385 E	G6303 E
Qm	59,6 3,9	37,0 4,3	45,9 4,1	62,1 4,3	48,0 3,0
Qp1	8,6 2,2	8,8 2,5	12,4 2,7	2,7 1,4	11,3 1,9
Qp2	8,7 2,2	22,2 3,7	6,3 2,0	2,9 1,5	15,9 2,2
F	0,9 0,7	0,1 0,6	4,8 1,8	- -	5,0 1,3
L	4,6 1,6	7,2 2,3	4,3 1,7	5,7 2,0	7,9 1,6
C	2,4 1,2	4,8 1,9	11,7 2,6	1,6 1,1	2,6 1,0
M	8,7 2,2	16,8 3,3	12,4 2,7	25,0 3,8	5,6 1,4
H	0,7 0,7	2,8 1,4	2,2 1,2	- -	2,6 1,0
Q*	0,78	0,54	0,71	0,92	0,64
R	R	R	SA	SR	R
S	WS	WS	WS	WS	WS(Polym)
Q	90,6 2,5	88,3 3,3	87,6 3,1	92,3 2,8	85,4 2,3
F	1,1 0,9	0,5 0,7	6,6 2,4	- -	5,7 1,5
L	8,3 2,3	11,2 3,2	5,8 2,2	7,7 2,8	8,9 1,8
T1	RO	RO	RO	RO	RO
QM	70,2 3,9	48,1 5,1	62,2 4,6	84,6 3,7	54,5 3,2
LT	28,7 3,8	51,4 5,1	31,2 4,4	15,4 3,7	39,8 3,2
T2	QR	TR	QR	QR	QR
N <sub>a</sub>	650	500	599	512	1095
N <sub>b</sub>	553	385	442	376	965

Appendix 2 cont.

Component	G6304 E	G6114 E	G1390 E	G1389 E	G1391 E
Qm	64,9 4,3	53,8 4,0	51,0 4,0	54,2 3,8	51,0 4,5
Qp1	3,5 1,6	4,3 1,6	3,6 1,5	5,0 1,7	4,2 1,8
Qp2	7,9 2,4	16,1 2,9	9,0 2,3	7,3 2,0	5,8 2,1
F	1,0 0,9	- -	4,7 1,7	3,4 1,4	4,2 1,8
L	2,6 1,4	6,7 2,0	- -	2,6 1,2	4,4 1,9
C	18,1 3,5	15,0 2,9	23,0 3,3	22,3 3,1	19,8 3,6
M	1,8 1,2	6,9 2,0	2,2 1,2	1,1 0,8	9,4 2,6
H	- -	- -	0,8 0,7	4,0 1,6	0,2 0,4
Q*	0,85	0,77	0,80	0,82	0,84
R	SR	R	SR	SR	WR
S	WS	WS (bi)	MS	WS	WS
Q	95,4 2,3	89,6 2,8	86,8 3,1	91,2 2,5	87,6 3,5
F	1,3 1,2	0,4 0,6	6,4 2,3	4,7 1,9	6,0 2,5
L	3,3 1,9	8,7 2,6	6,8 2,3	4,1 1,8	6,4 2,6
T1	RO	RO	RO	RO	RO
QM	81,2 4,1	69,9 4,8	69,5 4,3	74,8 3,9	73,3 4,7
LT	17,6 3,9	29,7 1,6	24,1 3,9	20,5 3,6	20,7 4,3
T2	QR	QR	QR	QR	QR
N <sub>a</sub>	493	626	641	699	500
N <sub>b</sub>	394	482	470	507	348

Appendix 2 cont.

Component	G1386 E	G1387 E	G1388 E	G6402 E	G6307 E
Qm	42,2 3,7	59,8 3,2	50,9 3,3	22,5 4,2	66,8 4,2
Qp1	8,1 2,0	3,6 1,2	7,1 1,7	10,0 3,0	9,0 2,6
Qp2	8,4 2,0	10,7 2,0	8,4 1,9	36,7 4,8	1,6 1,1
F	6,0 1,8	1,0 0,7	1,0 0,7	0,5 0,7	0,8 0,8
L	8,9 2,1	7,0 1,7	3,1 1,2	22,7 4,2	1,2 1,0
C	19,2 3,0	15,9 2,4	26,5 2,9	1,7 1,3	4,2 1,8
M	1,1 0,8	1,9 0,9	2,1 0,9	5,5 2,3	16,2 3,3
H	1,9 1,1	0,2 0,3	0,7 0,6	0,4 0,6	0,4 0,6
Q*	0,74	0,80	0,82	0,86	0,86
R	R	R	R	SR	A-R
S	WS	MS	WS	WS(poly)	P
Q	80,7 3,4	90,3 2,1	94,2 1,2	74,5 4,5	98,2 1,3
F	7,7 2,3	1,2 0,7	1,4 0,9	0,5 0,7	1,0 1,0
L	11,6 2,7	8,5 1,9	4,4 1,6	24,6 4,5	0,8 0,9
T1	RO	RO	RO	RO	RO
QM	59,5 4,2	72,9 2,9	72,2 3,6	24,3 4,5	84,7 3,6
LT	32,8 4,0	25,9 2,9	26,4 3,5	75,2 4,5	14,3 3,5
T2	QR	QR	QR	LR	QR
N <sub>a</sub>	714	915	901	400	500
N <sub>b</sub>	555	751	636	370	394

Appendix 2 cont.

Component	G6308 E	G6305 E	G6304 E	G6407 E	G6409 E
Qm	65,5 3,9	59,8 4,0	64,6 5,5	62,8 4,3	63,4 4,3
Qp1	5,3 1,8	4,6 1,7	4,3 2,3	4,2 1,8	9,0 2,4
Qp2	5,6 1,9	4,0 1,6	1,0 1,1	8,6 2,5	6,8 2,3
F	0,5 0,6	- -	- -	- -	1,4 1,1
L	4,3 1,7	3,0 1,4	1,6 1,4	1,8 1,2	2,4 1,4
C	15,7 3,0	11,1 2,6	6,3 2,8	15,4 3,2	10,4 2,7
M	2,8 1,3	17,2 3,1	20,3 4,6	5,8 2,1	6,6 2,2
H	- -	- -	1,6 1,4	1,4 1,1	- -
Q*	0,86	0,87	0,92	0,83	0,81
R	R	R	SR	WR	WR
S	WS	WS	WS	WS	WS(poly)
Q	94,1 2,1	95,8 1,9	97,7 2,0	97,7 1,5	95,4 2,1
F	0,6 0,7	- -	- -	- -	1,7 1,3
L	5,3 2,0	4,2 1,9	2,3 2,0	2,3 1,5	2,9 1,5
T1	RO	RO	CI	CI	RO
QM	80,5 3,6	83,7 3,6	90,2 4,0	81,1 4,0	76,4 4,2
LT	18,9 3,5	16,3 3,6	9,8 4,0	18,9 4,0	21,9 4,1
T2	QR	QR	QR	QR	QR
N <sub>a</sub>	600	600	300	500	500
N <sub>b</sub>	488	429	215	387	415

Appendix 2 cont.

Component	G6400 E	G6401 E
Qm	44,8 4,4	30,4 4,1
Qp1	5,6 2,1	6,6 2,2
Qp2	15,4 3,2	45,6 4,5
F	0,4 0,6	- -
L	6,2 2,2	4,4 1,8
C	9,0 2,6	4,8 1,9
M	17,8 3,4	8,2 2,5
H	0,8 0,8	- -
Q*	0,68	0,34
R	SR	SA
S	WS(poly)	PS(poly)
Q	90,8 3,0	94,9 2,1
F	0,6 0,8	- -
L	8,6 2,9	5,1 2,1
T1	RO	RO
QM	61,9 5,1	34,9 4,6
LT	37,5 5,1	65,1 4,6
T2	QR	LR
N <sub>a</sub>	500	500
N <sub>b</sub>	362	435

(poly = poly-modal grain size distribution)

(bi=bi-modal grain size distribution, based on visual compactor)

APPENDIX 3

SUMMARY OF TEXTURAL CHARACTERISTICS

Field sample number	* authigenic * primary pore * fill *	* authigenic * oversized/ * elongate * pore fill	* qtz framework/ * cement dissol. * pore fill *
K 204a	* X	* X	* X
K 205	* X	* X	* X
K 202	* X	* X	* X
K 206	* X	* X	* X
K 204b	* X	* X	* X
K 105	* X	* X	* X
K 107	* X	* X	* X
K 207a	* X	* X	* X
K 208	* X	* X	* X
K 207b	* X	* X	* X
P 6115a			* Y
P 1853			* Y
P 6120	* X	* X	* X
P 6108			* Y
P 6112			* Y
P 9102			* Y
P 6852			* Y
P 6110			* Y
P 6501			* Y
P 1851			* Y
P 6115b			* Y
P 9678		* X	* X
P 6107	* X	* X	* X
P 6104		* X	* X
P 5851			* X
P 1382		* X	* X
P 1384		* X	* X
P 6103			* Z
P 1385	* X	* X	* X
P 1383		* X	* X
P 1852	* X	* X	* X
P 1851			* Y
G 9852			* Z
G 6121			* Z
G 6406	* X	* X	* X
G 6403	* X	* X	* X
G 6302	* X		* X
G 2385			* Z
G 6303		* X	* X

G 6309	*	X	*	X	*		*
G 6114	*		*	X	*	X	*
G 1390	*	X	*	X	*		*
G 1389	*		*	X	*		*
G 1391	*	X	*	X	*	X	*
G 1386	*		*		*	Z	*
G 1387	*		*		*	Z	*
G 1388	*		*		*	X	*
G 6402	*		*	X	*	X	*
G 6307	*	X	*	X	*	X	*
G 6308	*	X	*	X	*		*
G 6305	*		*	X	*	X	*
G 6304	*	X	*		*		*
G 6407	*	X	*	X	*		*
G 6409	*	X	*		*		*
G 6400	*		*	X	*		*
G 6401	*	X	*	X	*	X	*

.....

X : textural feature present in sample  
Y : sandstones containing pyrophyllite  
Z : sandstones cemented by quartz only

Primary pore fill : authigenic clay occludes primary porosity.

Oversized/elongate pore fill : authigenic clay occludes pores of similar size to grains.

Cement/framework dissolution pore fill : authigenic clay occludes pores which have dissolution pits, notches and depressions at the clay cement/framework contact.